

ผลของส่วนประกอบในไมโครอิมัลชันต่อการซึมผ่านนอกร่างและผลทางเภสัชวิทยาในร่างกาย
ของเบนโซเคน



เรือโทหญิง อรวดี พงษ์วุฒิจรรณ

วิทยานิพนธ์นี้เป็นส่วนหนึ่งของการศึกษาตามหลักสูตรปริญญาเภสัชศาสตรมหาบัณฑิต

สาขาวิชาเภสัชกรรม ภาควิชาเภสัชกรรม

คณะเภสัชศาสตร์ จุฬาลงกรณ์มหาวิทยาลัย

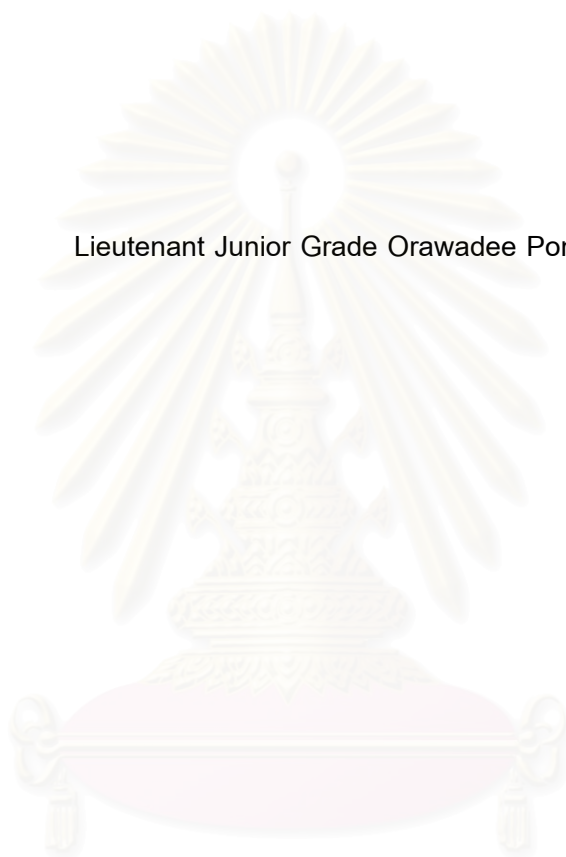
ปีการศึกษา 2544

ISBN 974-03-1038-9

ลิขสิทธิ์ของจุฬาลงกรณ์มหาวิทยาลัย

EFFECT OF MICROEMULSIONS COMPONENTS ON *IN VITRO* PERMEATION AND
IN VIVO ACTIVITY OF BENZOCAINE

Lieutenant Junior Grade Orawadee Pongvutitham



A Thesis Submitted in Partial Fulfillment of the Requirements

for the Degree of Master of Science in Pharmacy

Department of Pharmacy

Faculty of Pharmaceutical Sciences

Chulalongkorn University

Academic Year 2001

ISBN 974-03-1038-9

Thesis Title Effect of Microemulsions Components on *In Vitro* Permeation and
In Vivo Activity of Benzocaine
By Lieutenant Junior Grade Orawadee Pongvutitham
Field of Study Pharmacy
Thesis Advisor Associate Professor Ubonthip Nimmannit, Ph.D.
Thesis Co-advisor Lieutenant Pasarapa Chaiyakul, Ph.D.

Accepted by the Faculty of Pharmaceutical Sciences, Chulalongkorn
University in Partial Fulfillment of the Requirements for the Master's Degree

..... Dean of Faculty of
Pharmaceutical Sciences
(Associate Professor Boonyong Tantisira, Ph.D.)

Thesis Committee

..... Chairman
(Associate Professor Pranom Pothiyant, M.Sc. in Pharm.)

..... Thesis Advisor
(Associate Professor Ubonthip Nimmannit, Ph.D.)

..... Thesis Co-advisor
(Lieutenant Pasarapa Chaiyakul, Ph.D.)

..... Member
(Assistant Professor Panida Vayumhasuwan, Ph.D.)

..... Member
(Warangkana Warisnoicharoen, Ph.D.)

รท.หญิง อรวดี พงษ์วุฒิจรรณ รน. : ผลของส่วนประกอบในไมโครอิมัลชันต่อการซึมผ่านนอกร่างกายและผลทางเภสัชวิทยาในกายของเบนโซเคน (EFFECT OF MICROEMULSIONS COMPONENTS ON *IN VITRO* PREMEATION AND *IN VIVO* ACTIVITY OF BENZOCAINE) อ. ที่ปรึกษา : รศ. ดร. อุบลทิพย์ นิมมานนิตย์, อ. ที่ปรึกษาร่วม : อ. ดร.รท.หญิง ภัศราภา ชัยกุล, 127 หน้า. ISBN

การศึกษาการเกิดไมโครอิมัลชันโดยใช้คาบรีค/คาโปรลิก ไตรกลีเซอไรด์เป็นน้ำมัน ซอร์บิแทน สเตียเรท (และ) เมทิลกลูโคสเสตควิสเตียเรท, พอลิออกซีเอทิลีน ซอร์บิแทน โมโนโอเลเอต และพอลิออกซีเอทิลีน (10) โอลีอิลอีเทอร์ เป็นสารลดแรงตึงผิว ใช้กลีเซอริน และ บิวทานอลเป็นสารลดแรงตึงผิวร่วม พบว่าการใช้บิวทานอลเป็นสารลดแรงตึงผิวร่วมจะช่วยเพิ่มพื้นที่การเกิดไมโครอิมัลชัน ในขณะที่การใช้กลีเซอรินเป็นสารลดแรงตึงผิวร่วมจะทำให้บริเวณการเกิดไมโครอิมัลชันต่ำลง การใช้พอลิออกซีเอทิลีน (10) โอลีอิลอีเทอร์ผสมกับบิวทานอลในอัตราส่วนโดยน้ำหนักเท่ากับ 1:1 เป็นสารลดแรงตึงผิวจะทำให้เกิดบริเวณของไมโครอิมัลชันในแผนภูมิวิภูภาคมากที่สุด สำหรับการศึกษาผลของส่วนประกอบในไมโครอิมัลชันต่อการซึมผ่านนอกร่างกาย และในกายใช้เบนโซเคน 7.5 เปอร์เซ็นต์ โดยน้ำหนักเป็นยาต้นแบบผสมในไมโครอิมัลชันซึ่งประกอบด้วย คาบรีค/คาโปรลิก ไตรกลีเซอไรด์, น้ำ และพอลิออกซีเอทิลีน (10) โอลีอิลอีเทอร์ การศึกษาการซึมผ่านนอกร่างกายทดสอบโดยใช้ฟรานซ์ เซลล์ ใช้คราบงูเห่าเป็นเมมเบรน และการศึกษาฤทธิ์การเป็นยาชาเฉพาะที่ในกายทดสอบโดยใช้วิธีวัดการกระดกหางหนีของหนูจากแหล่งที่ให้ความร้อน ผลการทดลองพบว่าเมื่อปริมาณน้ำในไมโครอิมัลชันเพิ่มขึ้นจะทำให้การซึมผ่านของเบนโซเคนเพิ่มขึ้น ในขณะที่เมื่อเพิ่มความเข้มข้นของสารลดแรงตึงผิวในไมโครอิมัลชันจะทำให้การซึมผ่านของเบนโซเคนลดลง จากผลการทดลองพบว่าผลของการทดสอบการซึมผ่านนอกร่างกายมีความสัมพันธ์อย่างมีนัยสำคัญกับการออกฤทธิ์เป็นยาชาเฉพาะที่ในกายของเบนโซเคน ($p < 0.01$)

ภาควิชา	เภสัชกรรม	ลายมือชื่อนิสิต.....
สาขาวิชา	เภสัชกรรม	ลายมือชื่ออาจารย์ที่ปรึกษา.....
ปีการศึกษา	2544	ลายมือชื่ออาจารย์ที่ปรึกษาร่วม.....

4376644133 : MAJOR PHARMACY

KEY WORD: MICROEMULSION/ BENZOCAINE/ PERMEATION/ TAIL FLICK TEST

Lt.J.G. ORAWADEE PONGVUTITHAM RTN. : EFFECT OF MICROEMULSIONS COMPONENTS ON *IN VITRO* PERMEATION AND *IN VIVO* ACTIVITY OF BENZOCAINE. THESIS ADVISOR : ASSOCIATE PROFESSOR UBONTHIP NIMMANNIT, Ph.D., THESIS COADVISOR : Lt. PASARAPA CHAIYAKUL, Ph.D., 127 pp. ISBN

To investigate microemulsion formation, capric/caprylic triglyceride was used as oil component. Sorbitan stearate (and) methylglucose sesquistearate, polyoxyethylene sorbitan monooleate and polyoxyethylene (10) oleyl ether were used as surfactants, *n*-butanol and glycerin were used as co-surfactants. The area of microemulsion was increased by using the *n*-butanol as co-surfactant while the area of microemulsion was lowered by using glycerin as co-surfactant. Using polyoxyethylene (10) oleyl ether:*n*-butanol in the ratio of 1:1 by weight produced the largest region of microemulsion in phase diagram. To investigate the effect of microemulsions components on *in vitro* permeation and *in vivo* activity, 7.5% by weight benzocaine as a model drug were incorporated in microemulsion consisted of capric/caprylic triglyceride, water and polyoxyethylene (10) oleyl ether. The *in vitro* permeation studies were determined by Franz cell using shed cobra skin as membrane, and *in vivo* activities were measured using mouse tail flick test. The results indicated that benzocaine permeation was increased as water content in the microemulsion increased, but was decreased as surfactant concentration in the microemulsion increased. The *in vitro* permeation results were significantly correlated with *in vivo* local anesthetic activity ($p < 0.01$).

Department	Pharmacy	Student's signature.....
Field of study	Pharmacy	Advisor's signature.....
Academic year	2001	Co-advisor's signature.....

ACKNOWLEDGEMENTS

This thesis entitled “Effects of microemulsions components on *in vitro* permeation and *in vivo* activity of benzocaine” was succeeded with strong supports and encouragement from several persons.

Among those core persons, associate professor Ubonthip Nimmannit, Ph.D. as an advisor of this thesis, who provided many beneficial suggestion, comment, guidance and also helped evaluate the results to reach the objectives.

Moreover, Lt. Pasarapa Chaiyakul, Ph.D., co-advisor of the thesis, who supported a lot of technical information, instruments and advice. She gave me some special experiences which I have never seen before.

A few companies included Chemico Supply Co Ltd who supplied some concerned chemicals such as sorbitan stearate (and) methylglucose sesquistearate and East Asiatic (Thailand) Co Ltd for the support of polyoxyethylene (10) oleyl ether.

Snake Farm, Thai Red Cross Society, to support shed Cobra skin, an important material, to complete the experiment.

I could not ignore all of the faculty members as well as master-degree students in pharmaceutic department of Chulalongkorn University for their encouragement.

Finally, my Dad and Mom who always sacrifice for my successful.

I would like to express my deeply thanks to whom I have mentioned for all of their kindness and assistance.

สถาบันวิทยบริการ
จุฬาลงกรณ์มหาวิทยาลัย

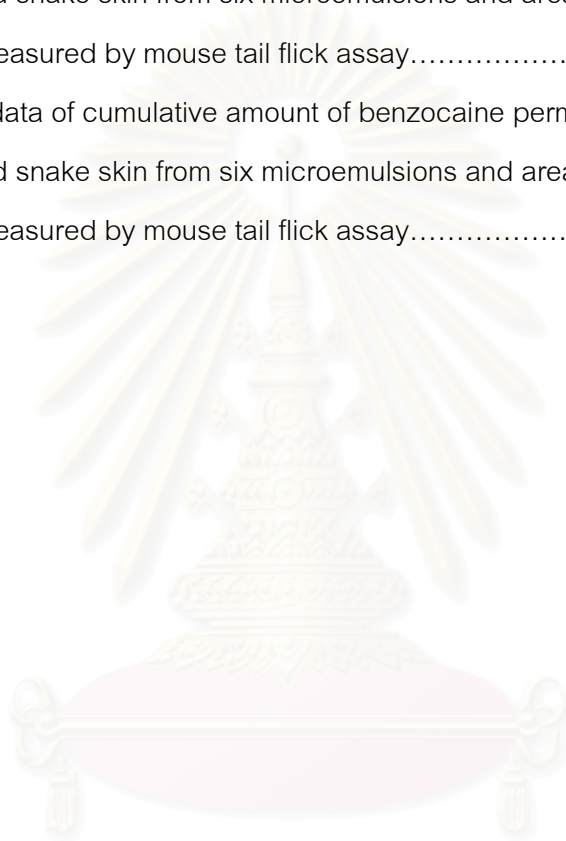
CONTENTS

THAI ABSTRACT.....	iv
ENGLISH ABSTRACT.....	v
ACKNOWLEDGEMENTS.....	vi
CONTENTS.....	vii
LIST OF TABLES.....	viii
LIST OF FIGURES.....	x
LIST OF ABBREVIATIONS.....	xiv
CHAPTER	
I. INTRODUCTION.....	1
II. LITERATURE REVIEW.....	3
III. MATERIALS AND METHODS.....	20
Materials.....	20
Equipments.....	21
Methods.....	22
IV. RESULTS AND DISCUSSION.....	33
Preparation of Microemulsions and Benzocaine Microemulsions.....	33
<i>In Vitro</i> Evaluation of Benzocaine Microemulsions.....	52
<i>In Vivo</i> Evaluation of Analgesic Effect Using Mouse Tail-Flick Test.....	62
V. CONCLUSION.....	71
REFERENCES.....	73
APPENDICES.....	77
VITA.....	127

LIST OF TABLES

Table	Page
1 Compositions of microemulsions containing 7.5% by weight benzocaine.....	25
2 Percent labeled amount of benzocaine microemulsions.....	52
3 Compositions of microemulsion base with varied water content in microemulsion.....	53
4 Permeation data of benzocaine through shed snake skin from microemulsion formulas A, B and C.....	55
5 Compositions of microemulsion base with varied surfactant concentration in microemulsion.....	57
6 Permeation data of benzocaine through shed snake skin from microemulsion formulas D, E, B and F.....	58
7 Comparison of average cumulative amount and steady state flux of benzocaine permeation from six formula microemulsions through shed snake skin.....	60
8 Solubility of benzocaine at 20 ^o C	79
9 Solubility of polyoxyethylene (10) oleyl ether.....	84
10 Data of calibration curve of benzocaine, detecting by UV/vis spectrophotometer at 286 nm.....	89
11 Data of percent labeled amount of benzocaine in microemulsions, detecting by UV/vis spectrophotometer at 286 nm.....	95
12 Data of benzocaine solubility in phosphate buffer pH 7.4, detecting by UV/vis spectrophotometer at 286 nm.....	97
13 Permeation data of benzocaine through shed snake skin from microemulsion formula A.....	99
14 Permeation data of benzocaine through shed snake skin from microemulsion formula B.....	101
15 Permeation data of benzocaine through shed snake skin from microemulsion formula C.....	103
16 Permeation data of benzocaine through shed snake skin from microemulsion formula D.....	105

Table	Page
17 Permeation data of benzocaine through shed snake skin from microemulsion formula E.....	107
18 Permeation data of benzocaine through shed snake skin from microemulsion formula F.....	108
19 Correlation data of steady state flux of benzocaine permeate through shed snake skin from six microemulsions and area of analgesia measured by mouse tail flick assay.....	125
20 Correlation data of cumulative amount of benzocaine permeate through shed snake skin from six microemulsions and area of analgesia measured by mouse tail flick assay.....	126



สถาบันวิทยบริการ
จุฬาลงกรณ์มหาวิทยาลัย

LIST OF FIGURES

Figure	Page
1 Schematic representation of the most commonly encountered self-association structures in water, oil or a combination thereof.....	5
2 Schematic representation of the three most commonly encountered microemulsion microstructures.....	5
3 Effect of molecular moieties and solution condition on the CPP of a surfactant and the resulting range of possible surfactant aggregates in water or aqueous solution.....	9
4 A diagrammatic representation of the proposed mechanism of action of local anesthetics.....	14
5 Photograph of Franz diffusion cell.....	29
6 Diagrammatic of Franz diffusion cell.....	29
7 Photograph of a mouse on the device showing the focus of light beam.....	31
8 Photograph of a Harvard Tail Flick Analgesia Meter.....	31
9 Phase diagram of sorbitan stearate (and) methylglucose sesquistearate(A)-water(B)-capric/caprylic triglyceride(C).....	34
10 Phase diagram of sorbitan stearate (and) methylglucose sesquistearate: <i>n</i> -butanol; 1:1(A)-water(B)-capric/caprylic triglyceride(C).....	35
11 Phase diagram of sorbitan stearate (and) methylglucose sesquistearate:glycerin; 1:1(A)-water(B)-capric/caprylic triglyceride(C).....	36
12 Phase diagram of polyoxyethylene sorbitan monooleate(A)-water(B)-capric/caprylic triglyceride(C).....	37
13 Phase diagram of polyoxyethylene sorbitan monooleate: <i>n</i> -butanol; 1:1(A)-water(B)-capric/caprylic triglyceride(C).....	38
14 Phase diagram of polyoxyethylene sorbitan monooleate:glycerin; 1:1(A)-water(B)-capric/caprylic triglyceride(C).....	40
15 Phase diagram of polyoxyethylene (10) oleyl ether(A)-water(B)-capric/caprylic triglyceride(C).....	41
16 Phase diagram of polyoxyethylene (10) oleyl ether: <i>n</i> -butanol; 1:1(A)-water(B)-capric/caprylic triglyceride(C).....	42

Figure	Page
17 Phase diagram of polyoxyethylene (10) oleyl ether:glycerin; 1:1(A)- water(B)-capric/caprylic triglyceride(C).....	43
18 Phase diagram of 7.5% by weight benzocaine in polyoxyethylene (10) oleyl ether(A)-water(B)-capric/caprylic triglyceride(C).....	47
19 Photograph of 7.5% benzocaine microemulsion using JEOL JEM-200 CX, microemulsion base consisted with 70%, 10% and 20% w/w of polyoxyethylene (10) oleyl ether, water and capric/caprylic triglyceride, respectively.....	48
20 Photograph of 7.5% benzocaine microemulsion using JEOL JEM-200 CX, microemulsion base consisted with 60%, 10% and 30% w/w of polyoxyethylene (10) oleyl ether, water and capric/caprylic triglyceride, respectively.....	49
21 Photograph of 7.5% benzocaine microemulsion using JEOL JEM-200 CX, microemulsion base consisted with 50%, 10% and 40% w/w of polyoxyethylene (10) oleyl ether, water and capric/caprylic triglyceride, respectively.....	50
22 Photograph of 7.5% benzocaine microemulsion using JEOL JEM-200 CX, microemulsion base consisted with 40%, 10% and 50% w/w of polyoxyethylene (10) oleyl ether, water and capric/caprylic triglyceride, respectively.....	51
23 Comparison of permeation profiles of benzocaine through shed snake skin from microemulsion formulas A, B and C.....	56
24 Comparison of permeation profiles of benzocaine through shed snake skin from microemulsion formulas D, E, B and F.....	59
25 Comparison of area of analgesia provided by microemulsion formulas A, B and C.....	63
26 Comparison of area of analgesia provided by microemulsion formulas D, E, B and F.....	64

Figure	Page
27 Comparison of area of analgesia provided by benzocaine microemulsions and microemulsion bases.....	65
28 Correlation between the area of analgesia provided by mouse tail flick test and the steady state flux of benzocaine permeated through shed snake skin from microemulsions.....	69
29 Correlation between the area of analgesia provided by mouse tail flick test and the cumulative amount of benzocaine permeated through shed snake skin from microemulsions.....	70
30 Calibration curve of benzocaine in phosphate buffer pH 7.4 with 30% methanol solution.....	89
31 UV spectrum of phosphate buffer pH 7.4 with 30% methanol solution.....	90
32 UV spectrum of benzocaine in phosphate buffer pH 7.4 with 30% methanol solution.....	91
33 UV spectrum of microemulsion base in phosphate buffer pH 7.4 with 30% methanol solution.....	92
34 UV spectrum of benzocaine microemulsion in phosphate buffer pH 7.4 with 30% methanol solution.....	93
35 Permeation profile of benzocaine through shed snake skin from microemulsion formula A.....	100
36 Permeation profile of benzocaine through shed snake skin from microemulsion formula B.....	102
37 Permeation profile of benzocaine through shed snake skin from microemulsion formula C.....	104
38 Permeation profile of benzocaine through shed snake skin from microemulsion formula D.....	106
39 Permeation profile of benzocaine through shed snake skin from microemulsion formula E.....	108
40 Permeation profile of benzocaine through shed snake skin from microemulsion formula F.....	110

Figure	Page
41 Profile of the analgesic responses provided by microemulsion base formula A.....	112
42 Profile of the analgesic responses provided by microemulsion base formula B.....	113
43 Profile of the analgesic responses provided by microemulsion base formula C.....	114
44 Profile of the analgesic responses provided by microemulsion base formula D.....	115
45 Profile of the analgesic responses provided by microemulsion base formula E.....	116
46 Profile of the analgesic responses provided by microemulsion base formula F.....	117
47 Profile of the analgesic responses provided by benzocaine microemulsion formula A.....	118
48 Profile of the analgesic responses provided by benzocaine microemulsion formula B.....	119
49 Profile of the analgesic responses provided by benzocaine microemulsion formula C.....	120
50 Profile of the analgesic responses provided by benzocaine microemulsion formula D.....	121
51 Profile of the analgesic responses provided by benzocaine microemulsion formula E.....	122
52 Profile of the analgesic responses provided by benzocaine microemulsion formula F.....	123

LIST OF ABBREVIATIONS

A	=	Ampere
Abs	=	Absorbance
ANOVA	=	Analysis of variance
° C	=	Degree Celsius
cm	=	Centimeter
cm ²	=	Square centimeter
CV	=	Coefficient of variation
gm	=	Gram
HLB	=	Hydrophilic-lipophilic balance
hr	=	Hour
J _{ss}	=	Steady state flux
μm	=	Micrometer
M	=	Molar
mcg	=	Microgram
mg	=	Milligram
min	=	Minute
ml	=	Milliliter
mm	=	Millimeter
mPas	=	Millipascal
MPE	=	Maximum possible effect
nm	=	Nanometer
P	=	Partition coefficient
r ²	=	Correlation coefficient
S	=	Surface area
SD	=	Standard deviation
sec	=	Second
V	=	Voltage
w/w	=	Weight by weight

Chapter I

Introduction

Transdermal and topical delivery of drugs may provide advantages over conventional oral administration. The advantages of transdermal system include convenience, improved patient compliance and elimination of hepatic first-pass effect. Although transdermal systems have many advantages, most drugs are not applicable to this mode of administration because of the excellent barrier properties of the skin. Molecules must first penetrate the stratum corneum, the outer horny layer of the skin. The molecule then penetrates the viable epidermis before passing into the papillary dermis and through the capillary walls into systemic circulation. It is the stratum corneum, a complex structure of compact keratinized cell layers, presenting the greatest barrier to absorption of topically or transdermally administered drugs (Walters, 1989). The success of all transdermal system depends on the ability of the drug to permeate skin in sufficient quantities to achieve its desired therapeutic effect. Many of the drugs do not intrinsically possess any great ability to cross the skin, and way must be found to modify the diffusional barrier such as use of penetration enhancer or development of a the vehicle system to improved drugs penetration into the skin such as microemulsions.

Microemulsions are the vehicle systems consisted of an aqueous component, a lipophilic component and a surfactant or a surfactant/co-surfactant mixture. They are transparent, low viscosity, isotropic and thermodynamically stable. The mean diameter of the droplets is in the range between 10-100 nanometers. Microemulsions exhibit several properties that are of particular interest for transdermal vehicle. a) They act as supersolvents of drugs, including drugs that are relatively insoluble in both aqueous and hydrophobic solvents. b) The dispersed phase can be lipophilic or hydrophilic drugs. When the system comes into contact with skin, the drug can be transported through the barrier. Drug release with pseudo-zero-order kinetics can be obtained. c) The use of microemulsions as delivery system can improve the efficacy of a drug, allowing the total dose to be reduced and thus minimizing side effect (Gasco, 1997). Drug transport from microemulsions is usually better than that from conventional topical vehicle, for example,

ointment, solutions or cream (Baroli et al., 2000; Kemken, Ziegler and Muller, 1992; Linn, Pohland and Bryd, 1990).

To use microemulsions as the vehicle for transdermal delivery, many factors are concerned to achieve desirable delivery of drugs, for example, the components of microemulsion. Many studies have shown that deliveries of hydrophilic drugs were dependent on amount of water and surfactant in microemulsions; delivery of drugs increased as the amount of water and surfactant in microemulsions increased up to a certain concentration (Osborn, Ward and O'Neill, 1991; Changez and Varshney, 2000). However, a few studies have investigated effects of microemulsion components on their ability to deliver the lipophilic drugs (Ktistis and Niopas, 1998).

As previously stated, benzocaine, a local anesthetic of the ester type with low systemic toxicity drug, was selected as the lipophilic model drug to investigate effects of microemulsion components on delivery of the drug by transdermal route. To evaluate the ability of delivering benzocaine, *in vitro* permeation through vertical diffusion cell and *in vivo* pharmacological activity test were used.

Objectives

The purposes of this study were as follows:

1. To investigate the appropriate weight percentage of oil, water and surfactant to produce microemulsions and benzocaine microemulsions.
2. To study the effect of microemulsion components on benzocaine permeation and local anaesthetic effect.
3. To study the correlation between *in vitro* permeation and *in vivo* local anaesthetic effect.

Chapter II

Literature Review

During recent years there has been interest in the development of new effective vehicle systems to modify drug penetration into the human skin. These studies started using liposomes. In recent years colloidal vehicle systems such as microemulsions have been included in the investigated spectrum of potential dermal therapeutics in order to obtain enhanced penetration.

Microemulsions are isotropic, transparent, low-viscosity, and thermodynamically stable systems usually consisting of water, oil, surfactant and co-surfactant. The diameter of the disperse phase of microemulsions is in the range between 10-100 nm. These systems show structural similarity to micelles and inverse micelles, respectively. According to the content of water and oil, microemulsions can be classified into water-in-oil and oil-in-water types. They are highly dynamic systems showing fluctuated surfaces caused by formation and deforming processes.

Microemulsions have been shown to exert a high capacity for incorporating both lipophilic or hydrophilic substances, depending on the composition of the formulation. Therefore, they have been considered as vehicle systems for drugs. Recently, research and commercial interest in microemulsions has increased (Neubert and Schmalfub, 1999)

The microemulsion concept was introduced in 1940s by Hoar and Schulman who generated a clear single-phase solution by titrating a milky emulsion with hexanol. Schulman and coworkers subsequently coined the term microemulsion, and it has since been defined and indeed redefined on many occasions. However, the definition of microemulsions provided by Danielsson and Lindman in 1981 is a system of water, oil and amphiphile having is a single optically isotropic and thermodynamically stable liquid solution.

However, the above broad definition does not require a microemulsion to contain any microstructure, in other words it includes systems that are co-solvents, that is, systems in which the constituent components are molecularly dispersed. Most researchers in the field agree however that for a microemulsion to be formed it is important

that the system contains some definite microstructure, in other words there is a definite boundary between the oil and water phases at which the surfactant is located. In order to gain an understanding of the reasons for microemulsion formation, it is first useful to consider the properties of amphiphiles, such as surfactants, in solution.

Conventional surfactant molecules comprise a polar head group region and an apolar tail region, the latter having the larger molecular volume particularly in the case of ionic surfactants. On dispersal in water, surfactants self-associate into a variety of equilibrium phases, the nature of which stems directly from the interplay of the various intra and inter-molecular forces as well as entropy considerations. Surfactants also self-associate in non-aqueous solvents, particularly apolar liquids such as alkanes. In this case the orientation of the surfactant molecules are reversed compared to those adopted in aqueous solution. This reorientation serves to optimize the solvation requirements of the surfactant and minimizes the free energy of the system overall. When surfactants are incorporated into immiscible mixtures of oil and water, the surfactant molecules can locate at the oil/water interface that is thermodynamically very favorable. A number of phases may be structured on the microscopic or macroscopic scale, one example of a phase structured on the microscopic scale is an optically isotropic microemulsion phase. The schematic given in figure 1 gives an indication of a few of the wide variety of possible self-association structures that surfactants can form in the presence of water, oil or combination of all three.

Figure 2 shows schematic representations of the three types of microemulsions which are most likely to be formed depending on their components. It can be seen while the three structures shown are quite different, in each there is an interfacial surfactant monolayer separating the oil and water domains. The presence of oil-in-water microemulsions droplets is likely to be a feature in microemulsions where the volume fraction of oil is low. Conversely, water-in-oil droplets are likely when the volume fraction of water is low, and in systems where the amounts of water and oil are similar, a bicontinuous microemulsion may result. In the latter case, both oil and water exist as a continuous phase in the presence of a continuously fluctuating surfactant-stabilized interface with a net curvature of zero (Lawrence and Rees, 2000).

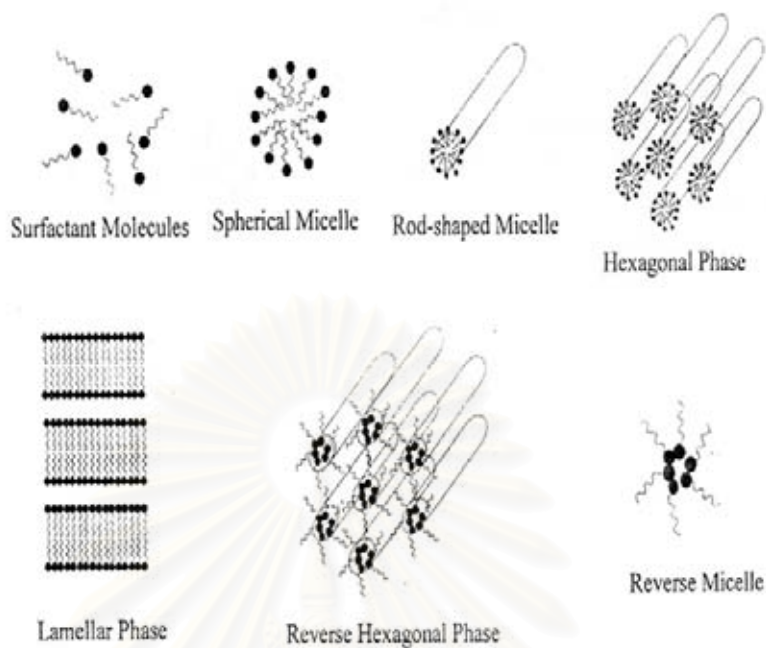


Figure 1. Schematic representation of the most commonly encountered self-association structures in water, oil or a combination thereof (from Lawrence and Rees, 2000).

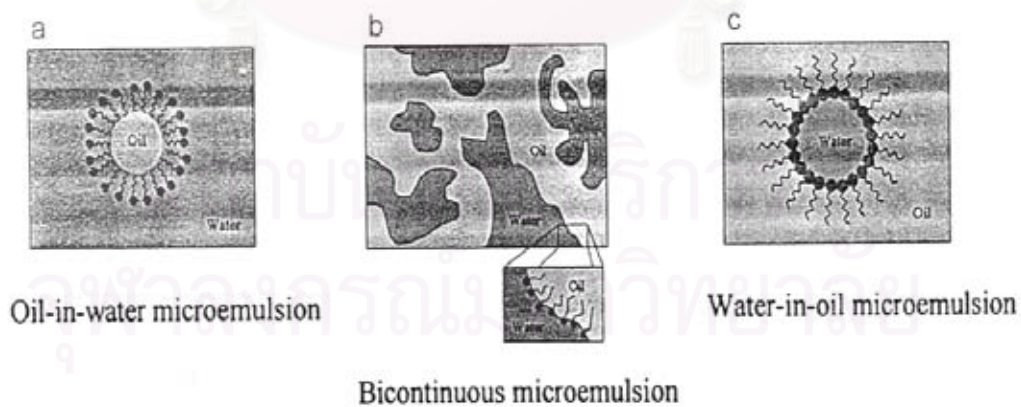


Figure 2. Schematic representation of the three most commonly encountered microemulsion microstructure: a) oil-in-water, b) bicontinuous and c) water-in-oil microemulsion (from Lawrence and Rees, 2000).

The difference between emulsions and microemulsions are their appearance; emulsions are cloudy while microemulsions are clear or translucent. Nevertheless there are distinct differences in their method of preparation, since emulsions require a large input of energy while microemulsions do not. The structure of emulsions depends on their history and they are thermodynamically unstable and will eventually phase separate, whereas microemulsions are thermodynamically stable and their structure is independent of their preparation. Other differences arise from other aspects. Emulsion droplets are spherical or nearly spherical; this form minimizes the interface, which gives a highly energetic term because of the interfacial tension. In microemulsions, because of the very low interfacial tension, the energetic term related to the interfacial tension and total surface is of less importance and therefore nonspherical droplets can be present without a large energy contribution. However the similarity of emulsions and microemulsions is the two systems consisted of two immiscible phases, for discrete or spherical microemulsion (Solans, Pons and Kunieda, 1997).

Theories of Microemulsion Formation

Historical, three approaches have been used to explain microemulsion formation and stability. These are: i) interfacial or mixed film theories, ii) solubilisation theories and iii) thermodynamic treatments. An admittedly simplified thermodynamic rationalization is presented below. The free energy of microemulsion formation can be considered to depend on the extent to which surfactant lowers the surface tension of the oil-water interface and the change in entropy of the system such that,

$$\Delta G_f = \gamma \Delta A - T \Delta S \quad (1)$$

where ΔG_f is the free energy of formation, γ is the surface tension of the oil-water interface, ΔA is the change in interfacial area on microemulsification, ΔS is the change in entropy of the system which is effectively the dispersion entropy, and T is the temperature. It should be noted that when a microemulsion is formed the change in ΔA is very large due to the large number of very small droplets formed. Originally workers proposed that in order for a microemulsion to be formed a (transient) negative value of γ was required, it is now recognized that while value of γ is positive at all times, it is very small (of the order of fractions of mN/m), and is offset by the entropic component. The dominant favorable

entropic contribution is the very large dispersion entropy arising from the mixing of one phase in the other, in the form of large numbers of small droplets. However, there are also expected to be favorable entropic contributions arising from other dynamic processes such as surfactant diffusion in the interfacial layer and monomer-micelle surfactant exchange. Thus a negative free energy of formation is achieved when large reduction in surface tension are accompanied by significant favorable entropic change. In such cases, microemulsification is spontaneous and the resulting dispersion is thermodynamically stable.

Phase Behavior

The phase behavior of simple microemulsion systems comprising oil, water and surfactant can be studied with the aid of ternary phase diagram in which each corner of the diagram represents 100% of that particular component. More commonly, and almost always in the case of microemulsion in pharmaceutical applications, the microemulsion will contain additional components such as a co-surfactant and/or drug. The co-surfactant is also amphiphilic with an affinity for both the oil and aqueous phases and partitions to an appreciable extent into the surfactant interfacial monolayer at the oil-water interface. The co-surfactant need not necessarily be capable of forming association structures in its own right. A wide variety of molecules can function as co-surfactant including non-ionic surfactant, alcohol, alkanolic acids, alkanediol and alkyl amines.

In the case where four or more components are investigated, pseudo-ternary phase diagrams are used where a corner will typically represent a binary mixture of two components such as surfactant/co-surfactant, water/drug or oil/drug. The number of different phases present for a particular mixture can be visually assessed. Microstructural features can also be investigated with the aid of a wide variety of techniques. It should be noted that not every combination of components produce microemulsions over the whole range of possible compositions, in some instances the extent of microemulsion formation may be very limited.

The Role of Surfactant

Attempts have been made to rationalize surfactant behavior in terms of the hydrophile-lipophile balance (HLB), as well as the critical packing parameter (CPP). Both approaches are fairly empirical but can be a useful guide to surfactant selection. The HLB takes into account the relative contribution of hydrophilic and hydrophobic fragments of the surfactant molecule. It is generally accepted that low HLB (3-6) surfactants are favored for the formation of water-in-oil microemulsions whereas surfactants with high HLB (8-18) are preferred for the formation of oil-in-water microemulsion systems.

In contrast, the CPP relates the ability of surfactants to form particular aggregates to the geometry of the molecule itself. The CPP can be calculated using the following equation:

$$\text{CPP} = v / a \cdot l \quad (2)$$

where v is the partial molar volume of the hydrophobic portion of the surfactant, a is the optimal head group area and l is the length of the surfactant tail. The latter parameter is often expressed as l_c , that is the critical length of the hydrophobic chain, generally assumed to be 70-80% of its fully extended length. The CPP is a measure of the preferred geometry adopted by the surfactant, and as a consequence is predictive of the type of aggregate that is likely to form. The effect of changing CPP is illustrated in figure 3 but put simply, cone-shaped surfactants will pack at curved interface whereas surfactants whose geometry can be represented by truncated cones or rectangular blocks prefer to form worm-like micelles or lamellar structures.

The presence of hydrophilic molecules such as glycerol and sorbitol in the aqueous phase will also influence optimal head group area by altering the solubility of the head group in the aqueous phase. Because of these effects, water-soluble hydrophilic materials have been used as to aid microemulsion formation. For medium chain length alcohols, which are usually added as co-surfactants, its have the effect of further reducing the interfacial tension, whilst increasing the fluidity of the interface thereby increasing the entropy of the system. Furthermore medium chain length alcohols also increase the mobility of the hydrocarbon tail and also allow greater penetration of the oil into this region. Alcohols may also influence the solubility properties of the aqueous and oily phases due to its partitioning between these phases.

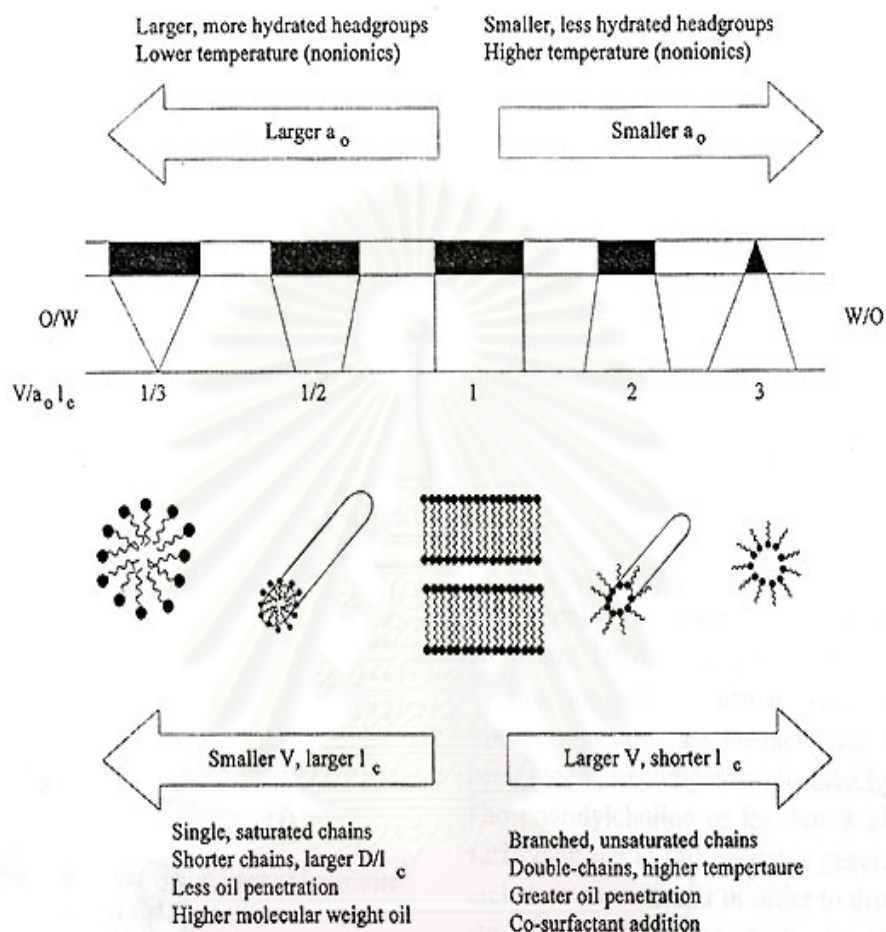


Figure 3. Effect of molecular moieties and solution condition on the CPP of a surfactant and the resulting range of possible surfactant aggregates in water or aqueous solution (from Lawrence and Rees, 2000).

Microemulsion Characterization

A. Phase Behavior

Phase diagram determinations, are essential in the study of surfactant systems to study the phase behavior. They provide information on the boundaries of the different phases as a function of composition and temperature, so structural organization can be also inferred. In addition, phase behavior studies allow comparison of the efficiency of different surfactants for a given application. It is important to note that simple measurements and equipment are required in this type of study. The boundaries of one-phase regions can be assessed easily by visual observation of samples of known composition. However, long equilibration times in multiphase regions, especially when liquid crystalline phase is involved, can make these determinations long and difficult.

B. Scattering Techniques

Scattering methods have been widely applied in the study of microemulsions. These include small-angle X-ray scattering (SAXS), small-angle neutron scattering (SANS) and static as well as dynamic light scattering.

Dynamic light scattering, also referred to as photon correlation spectroscopy (PCS), is used to analyze the fluctuations in the intensity of scattering by the droplets due to Brownian motion. The self-correlation function is measured and gives information on the dynamics of the system. Although dynamic light scattering measurements are relatively easy and fast, extrapolation of results to infinite dilution is not possible in most microemulsion systems.

C. Nuclear Magnetic Resonance

Nuclear magnetic resonance techniques have been used to study the structure and dynamics of microemulsions. Self-diffusion measurements using different tracer techniques, generally radioactive labeling, supply information on the mobility of the components (self-diffusion coefficient). A limitation of this technique is that experiments are time-consuming and the use of labeled molecules in multicomponent systems such as microemulsions is not practical.

D. Electron Microscopy

Several electron microscopic techniques have been attempted for the characterization of microemulsions. Because of the high lability of the samples and danger of artifacts, electron microscopy used to be considered a misleading technique in microemulsion studies. However, images showing clear evidence of the microstructure have been obtained.

However, using microemulsions for dermal and transdermal drug delivery are influenced by composition in microemulsion. Osborne, Ward and O'Neill (1991) investigated the dependence of glucose transport on the water content in microemulsion. Its was found that topical delivery from the microemulsions studied was highly variable and extremely dependent upon composition. While each of microemulsion evaluated had the same ratio of surfactant to co-surfactant, differences in water content caused the *in vitro* percutaneous transport of water and glucose to vary fifteen fold and greater than thirty fold, respectively. Changez and Varshney (2000) investigated that the local analgesic response time of tetracaine hydrochloride was dependent on the composition of microemulsion. The local analgesic responses increased as the weight percentage of surfactant and water increased up to a certain concentration in the microemulsion. Thus, while microemulsion may provide topical formulations with increased drug transportation and superior drug solubilization, microemulsion component must be carefully optimized to achieve maximum percutaneous transport.

To date, few studies have investigated the influenced of microemulsions components on lipophilic drug delivery. Hence in this study benzocaine was selected as model lipophilic drug to examine effect of water and surfactant amounts on lipophilic drug deliver, including *in vitro* permeation and *in vivo* activity test.

Benzocaine

Benzocaine is a surface anaesthetic of the ester type with low systemic toxicity. Its low aqueous solubility allows the drug to stay at the site of application for long periods. Its minimal rate of absorption after topical administration. It is used, often in combination with other drugs such as analgesics, antiseptics, antibacterial, antifungal agents and antipruritics, for the temporary local relief of pain associated with dental conditions, sore throats, haemorrhoids, anal pruritus, and ear pain. It has also been used for pain relief in minor cuts, scrapes, burns, muscular pains, strains and sprains. Benzocaine is used in creams, ointments, lotions, solutions, gels and suppositories in concentration up to 20% for topical analgesia and anesthesia. Benzocaine is contraindicated in patients with known sensitivity to ester-linked anesthetics or PABA-containing compounds.

Mechanism of Action

The application of a local anesthetic to a nerve that is actively conducting impulses will inhibit the inward migration of Na^+ ions. This results in elevation of the threshold for electrical excitation, reduction in the rate of rise of the action potential, slowing of the propagation of the impulse, and, if the drug concentration is sufficiently high, complete block of conduction. The local anesthetics interfere with the process fundamental to the generation of the action potential, namely, the large transient, voltage-dependent rise in the permeability of the membrane to Na^+ ions.

While the physiological basis for the local anesthetic action is known, the precise molecular nature of the process is not completely clear. At present, two theories enjoy considerable experimental support.

One proposal, the membrane expansion theory, is that the local anesthetics, by virtue of their lipophilic nature, become incorporated into the nerve cell membrane and disrupt the normal integrity of the membrane. This theory suggests that either a conformational change occurs in a critical macromolecule associated with the Na^+ conducting channels or that the lateral pressure in the membrane is increased because of the presence of the drug, or both. If lateral pressure is increased, the channels become constricted and, therefore, unable to accommodate the passage of ions.

Another hypothesis of local anesthetic action, the specific receptor theory, arises from knowledge that almost all local anesthetics can exist as either the uncharged base or as an ionized cation. The uncharged base is important for adequate penetration to the site of action, and the charged form of the molecule is required at the site of action.

The cation forms of local anesthetics appear to be required for binding to specific site in or near the Na^+ channels. The presence of the local anesthetic at these sites interferes with the normal passage of Na^+ through the cell membrane. In a sense, the local anesthetic plugs the Na^+ channel.

Studies suggest that the receptor for the local anesthetic is near the inner (axoplasmic) surface of the cell membrane, because quaternary analogues of local anesthetics are quite effective when applied to the inside, but are inactive when placed on the outside, of the membrane. These permanently charged molecules cannot penetrate to the receptor sites. A schematic model incorporates elements of both the membrane expansion theory and the specific receptor theory to explain local anesthetic action. The model is shown in figure 4.

Pharmacokinetic Properties

Absorption and Distribution

The rate of absorption of a local anesthetic into the bloodstream is affected by the dose administered, the vascularity at the site of injection, and the specific physicochemical properties of the drug itself. All tissues will be exposed to local anesthetics after their absorption, but the concentration achieved will vary among the different organs. Although the highest concentrations appear to occur in the more highly perfused organs (i.e. brain, kidney and lung), factors such as degree of protein binding and lipid solubility also affect drug distribution. The lung can absorb as much as 90 percent of a local anesthetic drug during the first pass. Consequently, it acts as a buffer to prevent toxic concentrations than would occur otherwise. Placental transfer of local anesthetics is known to occur rapidly, the fetal blood concentrations generally reflect those found in the mother.

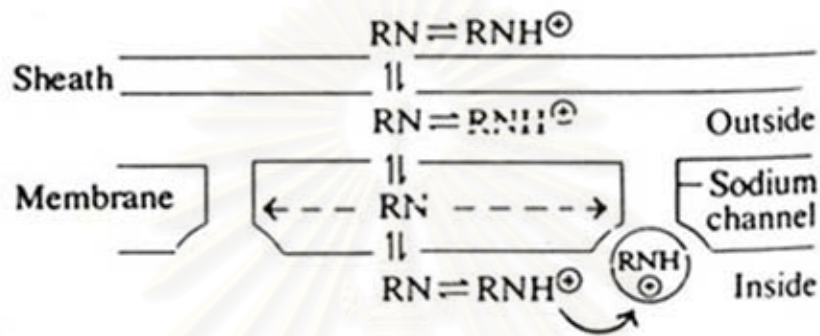


Figure 4. A diagrammatic representation of the proposed mechanism of action of local anesthetics. The ionized form (RNH^+) is required for binding to sites on sodium channels (solid arrow), while the unionized form (RN) is necessary for the drug to reach its intracellular site of action and to cause membrane expansion, dashed arrows. (From Haddox and Baumann, 1997).

สถาบันวิทยบริการ
จุฬาลงกรณ์มหาวิทยาลัย

However, the quantity of drug crossing to the fetus is also related to the time of exposure, that is, from the time of injection to delivery.

Metabolism

The metabolic degradation of ester local anesthetics is extensively and rapidly metabolized in plasma by pseudocholinesterase. The rate of local anesthetic hydrolysis is important, since a slow biotransformation may lead to drug accumulation and toxicity. In patients with atypical plasma cholinesterase, the use of ester-linked compound such as benzocaine has an increased potential for toxicity. The hydrolysis of all ester-linked local anesthetics leads to the formation of para-aminobenzoic acid (PABA), which is known to be allergenic in nature. Therefore, some people experience allergic reactions to the ester class of local anesthetics.

Adverse Effects

The central nervous and cardiopulmonary systems are most commonly affected by high plasma levels of local anesthetics. Local anesthetics given in initially high doses produce CNS stimulation characterized by restlessness, disorientation, tremors and, at times, clonic convulsions. Continued exposure to high concentrations results in generalized CNS depression; death occurs from respiratory failure secondary to medullary depression. Cardiac toxicity is generally the result of a drug induced depression of cardiac conduction (e.g. atrioventricular block, intraventricular conduction block) and systemic vasodilation. These effects may progress to severe hypotension and cardiac arrest. Allergic reactions, such as a red and itchy eczematoid dermatitis or vesiculation, are of concern when administering the ester-type local anesthetic (Haddox and Baumann, 1997).

In this study, *in vitro* permeation studies and *in vivo* activity test were selected to investigate the effect of surfactant and water content in microemulsions on drug delivery by microemulsion, which used as transdermal carrier.

Methods to Evaluate Percutaneous Drug Absorption and Topical Bioavailability

Typical methods for evaluating the percutaneous absorption of drug are the *in vitro* permeation studies and *in vivo* pharmacological activity test in an animal or humans.

A. In Vitro Permeation Studies.

Most common methods for *in vitro* percutaneous permeation use skin membranes mounted in a diffusion cell and investigate amount of drug through the skin membranes. The results from *in vitro permeation* studies are expected to reflect the percutaneous absorption of drug that actually occurs *in vivo*. The major advantage of *in vitro* investigations is that the experimental conditions can be controlled precisely and the simplicity of the experiments. The data obtained are usually more reproducible. Nevertheless, their predictive value of the *in vivo* result may not be reliable, depending on the skin model and experimental conditions employed.

In general, an excised human skin is often used in *in vitro* permeation study to predict the *in vivo* absorption. A variety of model membranes have been used for transdermal research for example human cadaver skin, hairless mouse skin and synthetic membranes. However, human skin is the best model membrane, the cost and limited availability put a limitation on its use. Moreover, the permeability through human skin varies up to ten folds and depending on the body site. On the other hand, it is easy to obtain animal skins of the same species with the same line and age. However, the time for experimental use of some animal skins in *in vitro* penetration studies is limited because of deterioration of membrane integrity after prolonged use. Furthermore, most animal skins are more permeable than human skin partly because of a larger number of hair follicles. The use of artificial membranes in transdermal research is limited because they lack keratinized proteins and lipids which are primary components in the stratum corneum of human skins (Itoh et al., 1990).

Shed skin snake is an another interested skin model, It is a nonliving pure stratum corneum with no hair follicle. Snake shed their skins periodically, leaving their old stratum corneum behind, so it is possible to obtain multiple shed skins from the same individual snake. Unlike human stratum corneum, which consisted of 10-20 layers of as alpha-keratin-rich intracellular layer and a lipid-rich intercellular layer, shed snake skin consists of three distinctive layers. These are the beta-keratin-rich outermost beta layer, alpha-keratin- and lipid-rich intermediate mesos layer, and alpha-keratin-rich innermost alpha layer. Further, the mesos layer shows three to five layers of multilayer structure with cornified cells surrounded by intercellular lipids, which is similar to human stratum corneum. This mesos layer is also a major depot of lipids, and the mesos layer and alpha layer are considered to be the main barrier to water penetration through the skin.

Pongjanyakul, Prakongpan and Priprem (2000) comparing the permeation of nicotine through cobra skin with human skin. It was found that human skin and cobra skin had a good correlation between both specimens. Moreover, the value of permeation fluxes obtained with the cobra skin gave lower %CV of permeation parameters than those obtained with the human skin. Thus, cobra skin could be used as a potential membrane to evaluate drug permeation since it demonstrates low intra- and interspecimen variation.

Hence, in this study cobra skin (*Naja naja* Khaotia), which a snake that available in Thailand, was selected as a model membrane.

Theoretical Background of *In Vitro* Permeation

The process of percutaneous absorption is usually a passive diffusion. In which the process that the matter moves from the higher concentration to the lower concentration. And the diffusion of drugs may be expressed by Fick's first law (Martin, Bustamante and Chun, 1993).

Fick's first law

The amount M of material flowing through a unit cross-section, S , of a barrier in unit time, t , is known as the flux, J

$$J = dM / S.dt \quad (3)$$

The flux in turn is proportional to the concentration gradient, dC/dx

$$J = -D \cdot \frac{dC}{dx} \quad (4)$$

D is the diffusion coefficient of a penetrant, cm²/hr

C is concentration in mcg/cm³ and x is the distance in cm of the movement perpendicular to the surface of the barrier

S is cross section area, cm²

An important condition in diffusion is that of the steady state. Fick's first law equation give the flux in the steady state of flow. And in the separated two compartments of a diffusion cell of cross-sectional area (S) and thickness, (h) and if the concentrations in the donor and the receptor sides are C₁ and C₂, respectively. The first law of Fick may be written as

$$J = \frac{DK(C_1 - C_2)}{h} \quad (5)$$

K is distribution or partition coefficient

At the steady state in diffusion experiments, the solution in the receptor compartment is constantly removed and replace with fresh solvent to keep the concentration at low level (or as sink condition), therefore C₁ >> C₂ and C₂ is approximately 0 the steady state flux (J_{ss}) are described as below

$$J_{ss} = PC_{ss} \quad (6)$$

J_{ss} is steady state flux of permeation, mcg/hr.cm²

P is permeability coefficient, cm/hr

C_{ss} is concentration gradient across the membrane barrier at steady state,

mcg/cm³

Since the equation was derived from Fick's first law, the permeation of drug can be expressed in term of flux.

B. In Vivo Pharmacological Activity Test

The quantitative measuring of pain threshold in mice against thermal radiation was used to investigate the local analgesic effect of benzocaine microemulsion. The procedure has been used by many authors to evaluate analgesic activity in animal experiments by measuring drug induced changes in the sensitivity of mice to heat stress

applied to their tails. Briefly, mice are placed into the restrainers leaving the tail exposed. A light beam is focus to the proximal third of the tail. Within a few seconds the animal flicks the tail aside or tries to escape. The time until this reaction occurs is measured. This procedure was introduced in tail-flick assay.

The method was described by Ther, Lindner and Vogel in 1963 as a modification of earlier publications by D'Armour and Smith in 1941. Group of 10 mice with weight between 18 and 22 gm are used for each dose. Before administration of the test compound or the standard, the reaction time is determined as a baseline latency. The animal is put into a restrainer with an opening for the tail at the rear wall and the tail lies flat on a surface device. By opening of a shutter, a light beam exerting radiant heat is directed to the proximal third of the tail. For about 4 seconds the reaction of the animal is observed. Moreover, to prevent tissue damage the heat source is terminated after 4 second also. The mouse tries to pull the tail away and turns the head. The escape reaction, which is the endpoint of this test, can be regarded as a complex phenomenon mediated by brain. In contrast, the simple tail flick as an endpoint of this test may be mediated as a spinal reflex. Therefore the observation of the escape reaction can be regarded as a true assessment of the influence of the drug on brain (Vogel, 1997).

The degree of reflex inhibition can be expressed as a percentage of the maximum possible effect (%MPE) according to the formula:

$$\% \text{ MPE} = \frac{\text{drug latency} - \text{predrug latency}}{(\text{cut-off time}) - \text{predrug latency}} \times 100 \quad (7)$$

Note: cut-off time is 4 seconds

สถาบันวิทยบริการ
จุฬาลงกรณ์มหาวิทยาลัย

Chapter III

Materials and Methods

Materials

Chemicals :

Sorbitan stearate (and) methylglucose sesquistearate (Sympatens-O/2500G[®]), Kolb, Switzerland.

Polyoxyethylene sorbitan monooleate (Tween 80[®]), Nof Co., Ltd, Japan.

Polyoxyethylene (10) oleyl ether (Brij 97[®]), Uniquema, USA.

n- butanol AR grade, APS, Australia.

Glycerin, Soci, Indonesia.

Capric/caprylic triglyceride (Captex 300[®]), Abitec Co., Ltd, USA.

Ethyl *p*- aminobenzoate (Benzocaine), Wujin, China.

Potassium dihydrogen phosphate, Merck, USA.

Sodium hydroxide, Merck, USA.

Methanol AR grade, Lab-Scan, Thailand.

Distilled water

Mice feed, CP, Thailand.

All chemical were analytical or pharmaceutical grades and were used as received.

สถาบันวิทยบริการ
จุฬาลงกรณ์มหาวิทยาลัย

Membranes :

Shed cobra skin (*Naja Naja Khoatia*) was donated by Thai Red Cross Society, Bangkok, Thailand.

Equipments :

Vortex mixer, Scientific Industries Inc., USA.

Analytical balance, Sartorius 1615 MP, range 300 gm/0.1 mg, Germany.

Hot plate, EGO, Germany.

Polarized light microscope, Leica ATC 2000, USA.

Transmission electron microscope, JEOL JEM-200 CX, Japan.

Thermostatted shaker bath, HetoFRIG CB 60, Scandinavia.

pH Meter, Orion model 420A, USA.

UV/vis spectrophotometer, Jasco model 7800, USA.

Modified franz diffusion cells, Crown glass, USA.

Harvard tail-flick analgesia meter, USA.

Subjects :

Male ICR mice (weighing 15-18 gm. upon arrival; National Laboratory Animal Centre, Mahidol University) were served as experimental subjects. Mice were maintained on a 12 hr. light/dark cycle with food and tap water available ad libitum and housed in groups of 20 until testing. Animals were allowed to acclimate to the facility for at least 3 days prior to experimentation.

สถาบันวิทยบริการ
จุฬาลงกรณ์มหาวิทยาลัย

Methods

Experiments were separated into three parts:

1. Preparation of microemulsions and benzocaine microemulsions.
 - 1.1. Determination of phase diagram of surfactant-water-oil and surfactant:co-surfactant-water-oil.
 - 1.2. Preparation of benzocaine microemulsions.
2. *In vitro* evaluation of benzocaine microemulsions with respect to benzocaine solubility, percent labelled amount and drug permeation through shed snake skin.
3. *In vivo* evaluation of analgesic effect using mouse tail-flick test.

1. Preparation of Microemulsions and Benzocaine Microemulsions

- 1.1. Determination of Phase Diagrams of Surfactant-water-oil and Surfactant:co-surfactant-water-oil.

Capric/caprylic triglyceride was used as an oil phase in phase diagram of surfactant-water-oil and surfactant:co-surfactant-water-oil. Samples were prepared individually by weighing the required amounts of surfactant, co-surfactant (if required), water and oil in each closed test tube, the total weight was 3 grams. The compositions of these three components were varying from 10 to 90 percent by weight. Approximately 45 points on the triangular diagram were chosen for investigation. The mixtures were heated at 50-60^o C for 10 min and then mixing with vortex mixer about 5 min. Then mixtures were stored at ambient temperature for 24 hours and the types of region were examined visually. After that, the ternary or pseudoternary phase diagram was constructed, which each corner of the diagram represents 100% of that particular component.

Surfactants were varied as following:

- Sorbitan stearate (and) methylglucose sesquisterate (Sympatens-O/2500G[®])
- Polyoxyethylene (20) sorbitan monooleate (Tween 80[®])
- Polyoxyethylene (10) oleyl ether (Brij 97[®])

Co-surfactants were varied as following:

- Glycerin
- *n*-butanol

Surfactant and co-surfactant were combined in the ratio of 1: 1 by weight.

Phase diagram 1. Sorbitan stearate (and) methylglucose sesquistearate-water-capric/caprylic triglyceride

Phase diagram 2. Sorbitan stearate (and) methylglucose sesquistearate:*n*-butanol (1:1)-water-capric/caprylic triglyceride

Phase diagram 3. Sorbitan stearate (and) methylglucose sesquistearate:glycerin(1:1)-water-capric/caprylic triglyceride

Phase diagram 4. Polyoxyethylene sorbitan monooleate-water-capric/caprylic triglyceride

Phase diagram 5. Polyoxyethylene sorbitan monooleate:*n*-butanol(1:1)-water-capric/caprylic triglyceride

Phase diagram 6. Polyoxyethylene sorbitan monooleate:glycerin(1:1)-water-capric/caprylic triglyceride

Phase diagram 7. Polyoxyethylene (10) oleyl ether-water-capric/caprylic triglyceride

Phase diagram 8. Polyoxyethylene (10) oleyl ether:*n*-butanol(1:1)-water-capric/caprylic triglyceride

Phase diagram 9. Polyoxyethylene (10) oleyl ether:glycerin(1:1)-water-capric/caprylic triglyceride

Regions in ternary phase diagram were identified under following definitions (Alany et al., 2001)

Cloudy systems with separated two or more phases were classified as unstable emulsion.

Cloudy systems with one phases and showing no birefringence under a cross polarizer were classified as coarse emulsion.

Opaque systems showing birefringence when viewed by cross-polarized light microscopy were classified as liquid crystal.

Clear, one-phase systems with low viscosity were classified as microemulsion.

Clear, one-phase systems which did not allowed a change in meniscus after tilling the test tube to an angle of 90° were classified as microemulsion gel (Malcolmson et al., 1998)

1.2. Determination of Phase Diagram of Benzocaine Micromulsions

Phase diagram of polyoxyethylene (10) oleyl ether-water-capric/caprylic triglyceride which produce the second larger region of microemulsion in 1.1, was selected to prepare benzocaine microemulsions. The concentration of benzocaine in commercial product for topical analgesia was varied from 7.5 to 20 %. Concentration of benzocaine in this investigation was fixed at 7.5 percent by weight. Then the series of benzocaine, polyoxyethylene (10) oleyl ether, water and capric/caprylic triglyceride were prepared by fixed benzocaine at 7.5 percent by weight in each sample. Poxyoxyethylene (10) oleyl ether, water and capric/caprylic triglyceride were varied from 10 to 90 percent by weight of total weight of 3 grams. Approximately 45 points on the ternary phase diagram were chosen for investigation, the same procedure was conducted as in 1.1. The pseudoternary phase diagram and regions in phase diagram were classified as in 1.1

The pseudoternary phase diagram of benzocaine, polyoxyethylene (10) oleyl ether -water-capric/caprylic triglyceride was observed. The effect of benzocaine on microemulsion region in phase diagram was also investigated. Six formulas of benzocaine in various amount of water and surfactant were selected for further studies as shown in table 1.

สถาบันวิทยบริการ
จุฬาลงกรณ์มหาวิทยาลัย

Table 1 Compositions of microemulsions containing 7.5% by weight benzocaine

Formula	Surfactant ^a (%w/w)	Water (%w/w)	Oil ^b (%w/w)
A	60	15	25
B	60	10	30
C	60	5	35
D	40	10	50
E	50	10	40
F	70	10	20

^a Surfactant is polyoxyethylene (10) oleyl ether.

^b Oil is capric/caprylic triglyceride.

1.3. Benzocaine Microemulsions Characterization.

Benzocaine microemulsions were characterized by transmission electron microscope (TEM) technique. The benzocaine microemulsion was dropped into formvar coated copper grid size 300 mesh and left for 3-5 min. The sample was spread off with filter paper. Then 1% phosphotungstic acid was added into the sample and left for 30 seconds. The excess of sample was absorbed with filter paper and the sample was allowed to dry. Photographs of the samples were taken with JEOL JEM-200 CX.

2. *In Vitro* Evaluation of Benzocaine Microemulsions.

2.1. Assay of Percent Labelled Amount.

2.1.1. Preparation of Standard Solution.

Standard solution was prepared by accurately weighing about 12.5 mg of benzocaine in a 25 ml volumetric flask. The solution was then adjusted to volume with phosphate buffer pH 7.4 mixed with 30% methanol solution. The concentration of benzocaine stock solution was 0.5 mg/ml. Two and half ml of this solution was pipetted

into another 25 ml volumetric flask and adjusted to volume with phosphate buffer pH 7.4 mixed with 30% methanol solution, the final concentration of the benzocaine standard solution was 50 mcg/ml. Each of 0.4, 0.6, 0.8, 1.0, 1.2, 1.4, 1.6 and 1.8 ml of the standard benzocaine solution were pipetted and transferred into eight 10 ml volumetric flasks, then solutions subsequently were diluted to volume with phosphate buffer pH 7.4 mixed with 30% methanol solution so that the final drug concentrations were 2.0, 3.0, 4.0, 5.0, 6.0, 7.0, 8.0 and 9.0 mcg/ml, respectively.

2.1.2. Preparation of Sample Solutions.

Approximately 0.1 gm of benzocaine microemulsion was accurately weighted in a 10 ml volumetric flask and adjust to volume with phosphate buffer pH 7.4 mixed with 30% methanol solution. 0.1 ml of this solution was pipetted to another 10 ml volumetric flask and adjust to volume with phosphate buffer pH 7.4 mixed with 30% methanol solution. Each sample was prepared in duplicate. The solutions were analyzed with UV/vis spectrophotometer at a wavelength of 286 nm using phosphate buffer pH 7.4 mixed with 30% methanol solution as a blank. By comparing the absorbance with that of the standard solution, the percent labelled amount of benzocaine in each microemulsion was calculated.

2.2. Benzocaine Solubility Studies

The solubility of benzocaine in phosphate buffer pH 7.4 was determined by equilibrating excess benzocaine with phosphate buffer pH 7.4. The solution was left to shake overnight at 37^o C in shaker bath. In previous study, it was found that equilibrium of benzocaine was obtained after 4 hr (Lalor, Flynn and Weiner, 1994). However in this study excess benzocaine was left for 36 hr to allow equilibrate. Upon equilibration, excess benzocaine was allowed to sediment and clear supernatant part of solution was separated. Then the supernatant solution was diluted and assayed for benzocaine solubility with UV/vis spectrophotometer at wavelength 286 nm. Benzocaine solubility assay was performed in triplicate.

2.3. *In Vitro* Permeation Studies of Benzocaine Through Shed Cobra Skin.

2.3.1. Pretreatment of Shed Snake Skin.

Shed snake skin specimens from *Naja Naja khaotia* were selected as representatives of stratum corneum, the major barrier to percutaneous drug absorption. It was kept in a freezer refrigerator. Before use, it was thawed at room temperature and dorsal part of the specimen was cut about the same size as the diffusion cell and then immersed in phosphate buffer pH 7.4 for 30 min prior to use (Pongjanyakul, Prakongpan and Priprem, 2000)

2.3.2. Preparation of Phosphate Buffer pH 7.4.

Phosphate buffer pH 7.4 was prepared as described in USP. 24 (2000). First 1.6 gm of sodium hydroxide was accurately weighed and transferred into 200 ml volumetric flask then adjusted to volume with distilled water and the flask was shaken until sodium hydroxide was completely dissolved, then 195.5 ml of this solution was measured and transferred into 1000 ml volumetric flask. And 6.805 gm of monobasic potassium phosphate was dissolved in 250 ml of distilled water, then added into sodium hydroxide solution. The final volume was adjusted to 1000 ml with distilled water. The pH was adjusted to 7.4 ± 0.02 with either 1 M phosphoric acid or 1 N sodium hydroxide.

2.3.3. Permeation Studies.

The contents of benzocaine in six microemulsions were determined prior to study the *in vitro* permeation study using a modified franz diffusion apparatus. The apparatus consisted of 6 water-jacketed cell holders fixed on the same mounting case with built-in magnetic stirrer (Figure 5). Each cell consisted of two parts, namely the donor and the receiver compartments vertically attached to each other via a metal clamp. The inside diameter was approximately 1.6 cm, equivalent to the area of 2.01 cm^2 . The receptor volume in each cell ranged from 13.81 to 14.24 ml. The diagram of the apparatus was shown in Figure 6. The two compartments were separated by a shed cobra skin.

Briefly, 3 gm of each microemulsion was placed in the donor chamber on the top of the receiver compartment which contained phosphate buffer pH 7.4. The preparation of

the buffer is described in 2.3.2. The system was maintained at 37° C throughout the study by means of circulating water bath.

Phosphate buffer pH 7.4 was filled into the receiver compartment, the volume varying from 13.81 to 14.21 ml depending on the calibrated volume of each diffusion cell. A small magnetic bar was placed in the receptor compartment for stirring the receiver fluid allowed to achieve homogeneous. A piece of shed cobra skin, which had previously hydrated was mounted between the donor and receiver compartments by means of a clamp. The skin was placed in such a way that faced the stratum corneum surface to the donor compartment that allowed to contact with the preparation and the other side contacted with the receiver fluid. After assembling, the diffusion cell was pre-warmed at 37° C for at least 20 min prior to the experiment started. Excess amount of benzocaine microemulsions (3 gm) were applied over the skin surface in the donor chamber, the experiment was then started when the microemulsions were applied. Each sample was prepared in triplicate. The amount of permeated benzocaine was detected by collecting 3 ml of samples at 1, 2, 3, 4, 5, 6, 7 and 8 hours. The volume of withdrawn fluid was replaced with fresh phosphate buffer pH 7.4. The temperature of the assembled diffusion cell was maintained at 37° C by means of circulating water jacket connected to a constant temperature water bath. During the cell assembly it should be no bubble underneath the cobra skin.

All the sampled receptor fluids were analyzed using the UV/vis spectrophotometer technique. The benzocaine concentrations in the receptor compartment were determined from the calibration curve. The amount permeating through the membrane was calculated by multiplying the drug concentration with the respective receptor volume. The cumulative amount of the drug found in the receptor compartment at various time intervals was then plotted as a function of the sampling time. The steady state flux for the permeation was subsequently calculated from the slope of the linear portion of each plot. Analysis of variance (ANOVA) was then applied at 5% significant level to see if there were any significant differences in cumulative amount and steady state flux among the six microemulsions. If such difference existed, further statistical analysis was performed in order to rank the microemulsions using tests such as Newman-keuls's test.



Figure 5 Photograph of Franz diffusion cell.

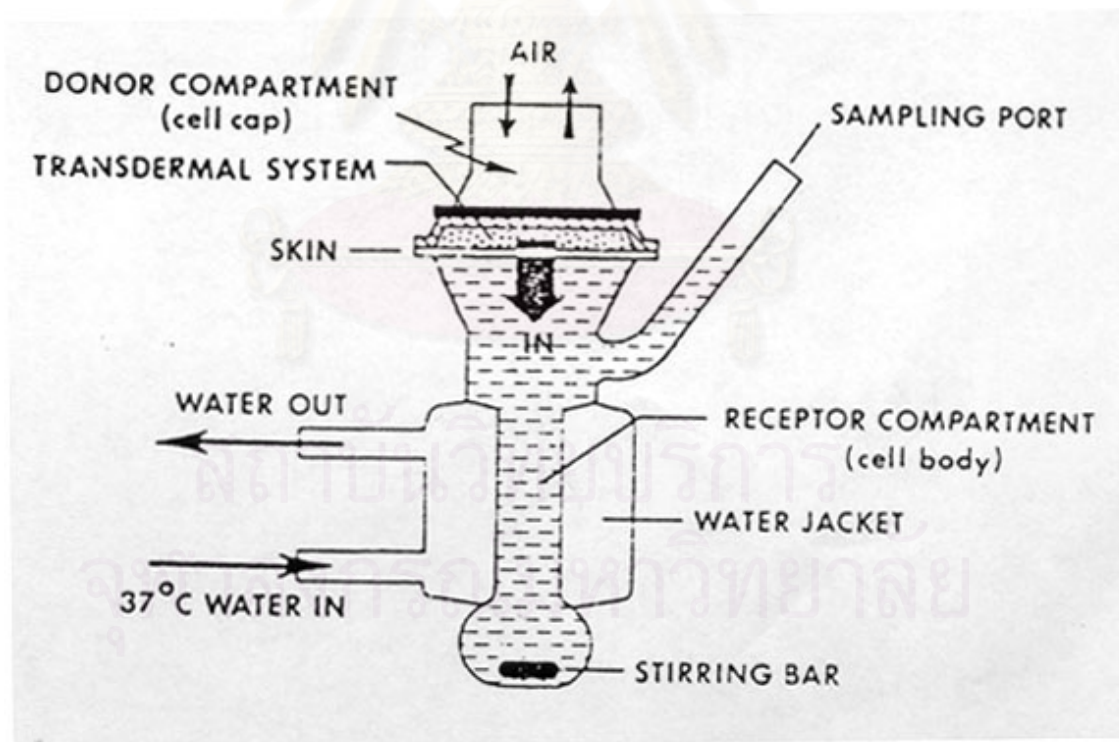


Figure 6 Diagrammatic of Franz diffusion cell. (From Chien, 1987)

3. *In Vivo* Evaluation of Analgesic Effect Using Mouse Tail-Flick Test.

3.1. Mouse Tail-Flick Test.

To investigate the effect of microemulsion components on *in vivo* activity of benzocaine, six formulas of microemulsions, with various amount of water and surfactant, as in *in vitro* evaluation were selected to investigate local analgesic effect using mouse tail-flick test. Six formulas of microemulsions without benzocaine, which had the same compositions as benzocaine microemulsions, were selected as control for each sample. The number of mice used in each experiment was ten.

This study employed the tail-flick assay described by D' Amour and Smith in 1941, with minor modifications. Male ICR mice weighing 18-22 gm were used. Mice were placed in individual restrainers with an opening to allow the tail to protrude. Each tail rested in a shallow groove housing a light sensitive sensor. A beam of radiant heat (24-V, high amperage 150-watt light bulb situated 8 cm above the tail) was aimed at the middle of the marked dorsal portion of the distal part of each subject's tail as shown in figure 7. The device (Harvard Tail Flick Analgesia Meter, Figure 8) automatically recorded (in 0.1 sec) the latency between the onset of the light beam stimulus and the response to heat, at which point the light beam was terminated. The maximum duration of each test was set at 4.0 sec to minimize the potential for thermal injury. The stimulus intensity was set so that the baseline tail-flick latencies were approximately 0.8-1.7 sec (intensity \cong 3.7 A). The intensity was not changed for any animal within any given experiments.

On the day of testing, all subjects underwent 3 pre-drug tail-flick baseline trials conducted at 10-15 min intervals. The score from the third trial served as the baseline measure for each subject. The distal portion of the tail (about 3 cm from tip) was immersed in benzocaine microemulsion for 1 min (Kolesnikov and Pasternak, 1999). Then testing was performed on the portion of the tail immersed in the treatment microemulsions, because the analgesic actions of agents administered in this manner are restricted to the exposed portions of the tail (Kolesnikov, Chereshevnev and Pasternak, 2000). Testing was performed immediately after termination of topical administration into the tail. Tail-flick latencies were recorded every 10 min for 180 min after topical administration (0, 10, 20, 30, 40, 50, 60, 70, 80, 90, 100, 110, 120, 130, 140, 150, 160, 170 and 180 min).



Figure 7 Photograph of a mouse on the device showing the focus of light beam.



Figure 8 Photograph of a Harvard Tail Flick Analgesia Meter.

3.1.1. Data Treatment and Statistical Analyse

Tail-flick latencies are expressed as the mean percent maximum possible effect (%MPE) according to the following formula:

$$\%MPE = \frac{\text{drug latency} - \text{predrug latency}}{(\text{cut-off time}) - \text{predrug latency}} \times 100 \quad (7)$$

Note: cut-off time is 4 seconds

Potential of local analgesia of each treatment was expressed in term of area of analgesia that were derived by computing the cumulative area under the corresponding 0-180 min time course-% MPE curves, area was calculated using the trapezoidal rule.

Statistical analysis were performed on area of analgesia by analysis of variance (ANOVA) and, where appropriate, were followed by Newman-Keuls' *post hoc* testing. The minimum level of statistical significance was set at $p < 0.05$.

3.2. Correlation between *In Vitro* Permeation and *In Vivo* Activity

Attempt was made to find any correlations between the *in vitro* permeation study results and the *in vivo* tail-flick test data. First, the ranking relationship obtained from post-ANOVA multiple range test stated in 3.1.1 after the *in vitro* tests of the six formulas of microemulsions (i. e. steady state flux and cumulative amount) were compared with those of the *in vivo* result (i.e. area of analgesia) to initially determine if there were any similarities in the ranking order among the six formulas of microemulsions. Second, the correlation test was applied at 5% significant level to determine if there was any significant correlations between these *in vitro* and *in vivo* parameters.

สถาบันวิทยบริการ
จุฬาลงกรณ์มหาวิทยาลัย

Chapter IV

Results and Discussion

1. Preparation of Microemulsions and Benzocaine Microemulsions

1.1. Determination of Phase Diagram of Surfactant-water-oil and Surfactant:co-surfactant-water-oil

Phase diagram of sorbitan stearate (and) methylglucose sesquistearate-water-capric/caprylic triglyceride was shown in figure 9. The emulsion was form at low surfactant concentration, 5-10% w/w surfactant and 35-90% w/w water, and at high surfactant concentration, 50-90% w/w surfactant and 5-60% w/w water. The liquid crystalline phase was formed at 10-50% w/w surfactant and 5-90% w/w water. The microemulsions were not found by using this surfactant.

The *n*-butanol was then select as a co-surfactant to study the phase boundaries. The surfactant and co-surfactant was used in the ratio of 1:1 by weight. Phase diagram of sorbitan stearate (and) methylglucose sesquistearate:*n*-butanol (1:1)-water-capric/caprylic triglyceride was shown in figure 10. Emulsion was formed at 5-20% w/w surfactant:co-surfactant and 20-90% w/w water. Microemulsion and liquid crystalline regions were not found in this diagram.

In figure 11, glycerin was used as a co-surfactant in the ratio of 1:1 by weight. The liquid crystalline was formed at 30-80% w/w surfactant:co-surfactant and 10-60%w/w water. Glycerin was also failed to produce clear area of microemulsion.

In figure 12, the surfactant was changed to polyoxyethylene sorbitan monooleate. Microemulsion was formed at 55-90%w/w surfactant and 5-30% water. Microemulsion gel was formed at 50-70% w/w surfactant and 25-50%w/w water. The liquid crystalline region was formed at 40-50% w/w surfactant and 20-55% w/w water.

In figure 13, *n*-butanol was used as co-surfactant in the ratio of 1:1 by weight. Microemulsion was formed at 45-90% w/w surfactant:co-surfactant and 5-55% w/w water. Emulsion and liquid crystalline regions were not appeared, only microemulsion and unstable emulsion regions were found in this diagram.

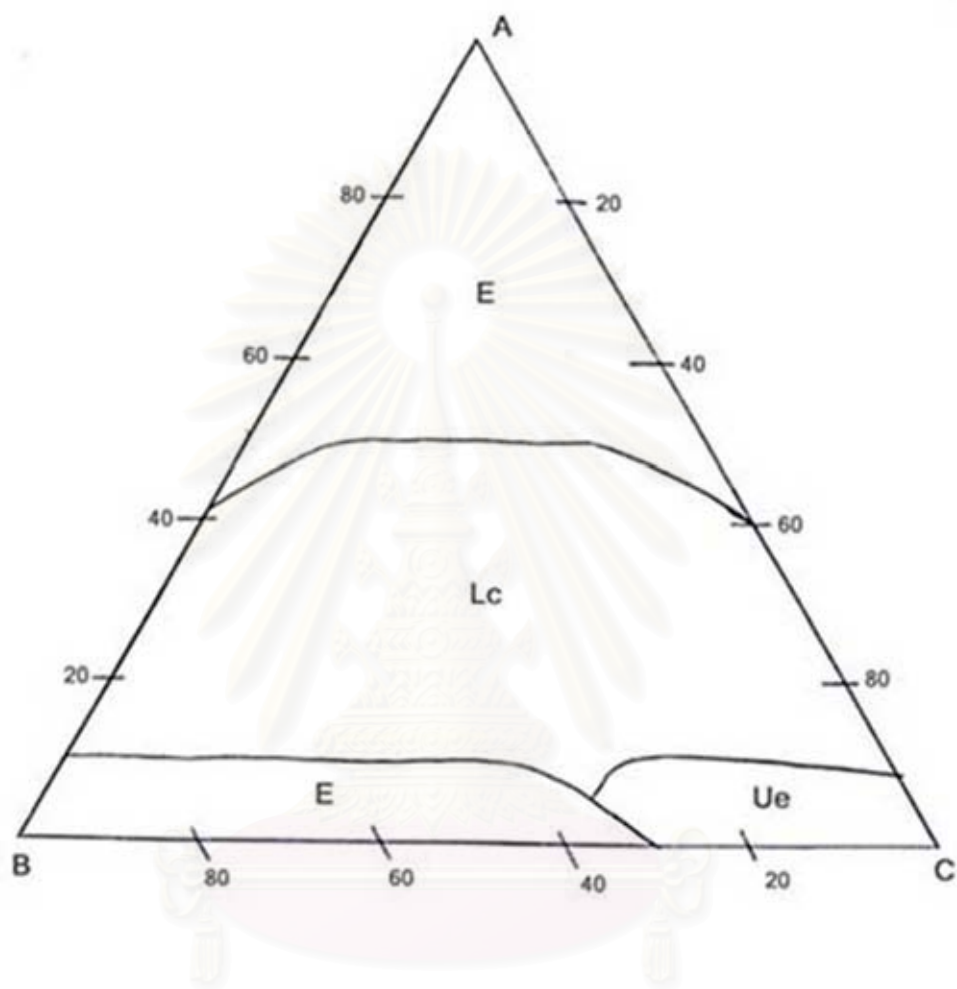


Figure 9 Phase diagram of sorbitan stearate (and) methylglucose sesquistearate (A)-water(B)-capric/caprylic triglyceride(C), Ue: unstable emulsion, E: emulsion, Lc: liquid crystalline.

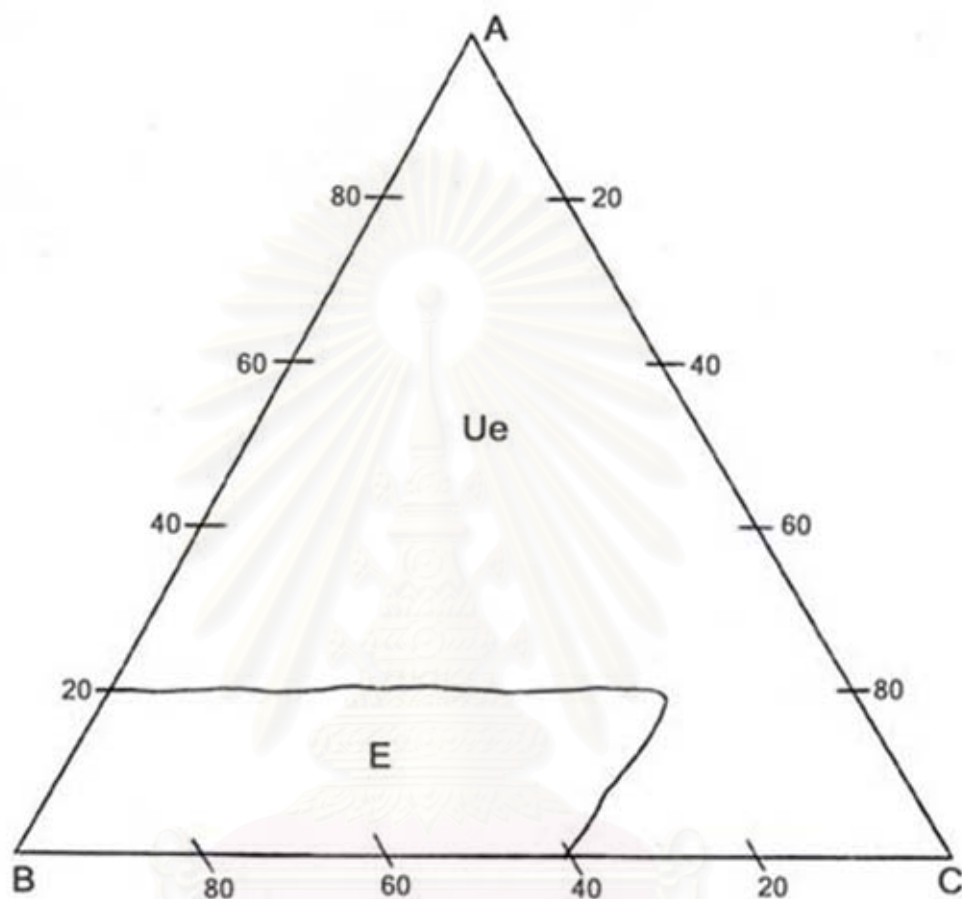


Figure 10 Phase diagram of sorbitan stearate (and) methylglucose sesquistearate:*n*-butanol; 1:1(A)-water(B)-capric/caprylic triglyceride(C), Ue: unstable emulsion, E: emulsion.

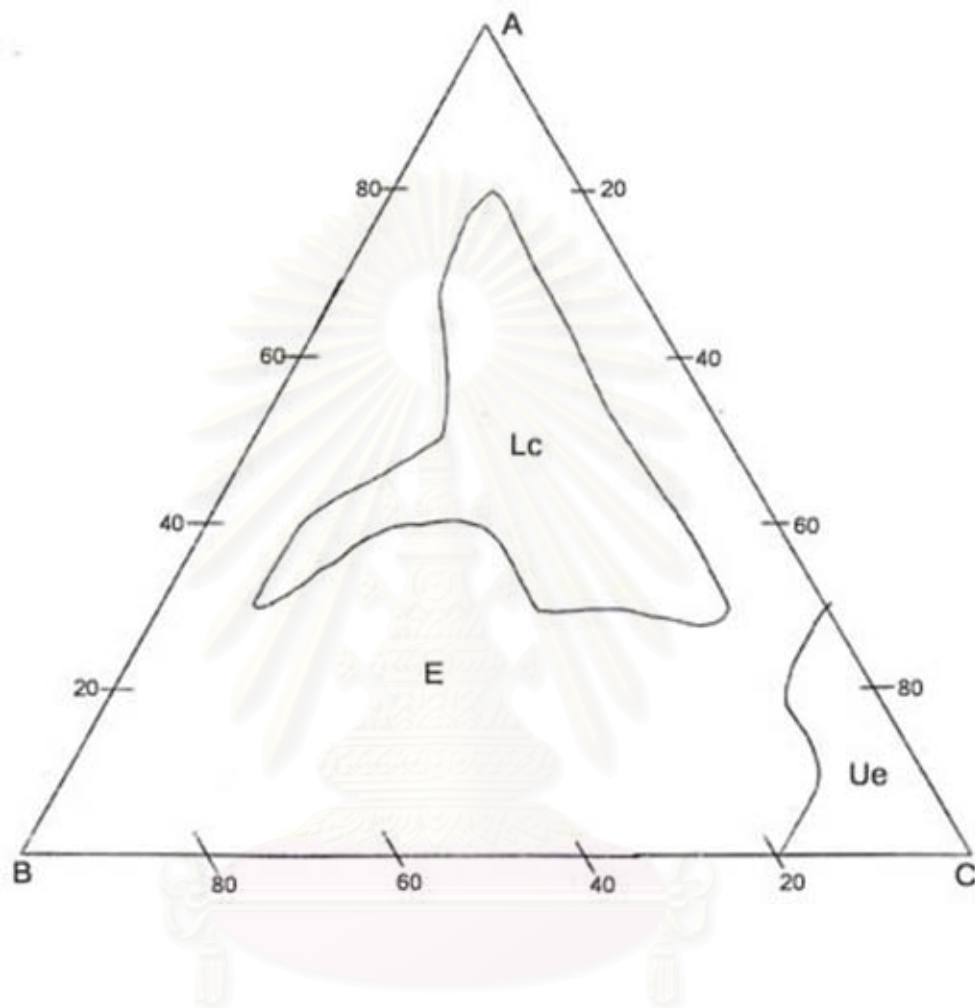


Figure 11 Phase diagram of sorbitan stearate (and) methylglucose sesquistearate:glycerin; 1:1(A)-water(B)-capric/caprylic triglyceride(C), Ue: unstable emulsion, E: emulsion, Lc: liquid crystalline.

จุฬาลงกรณ์มหาวิทยาลัย

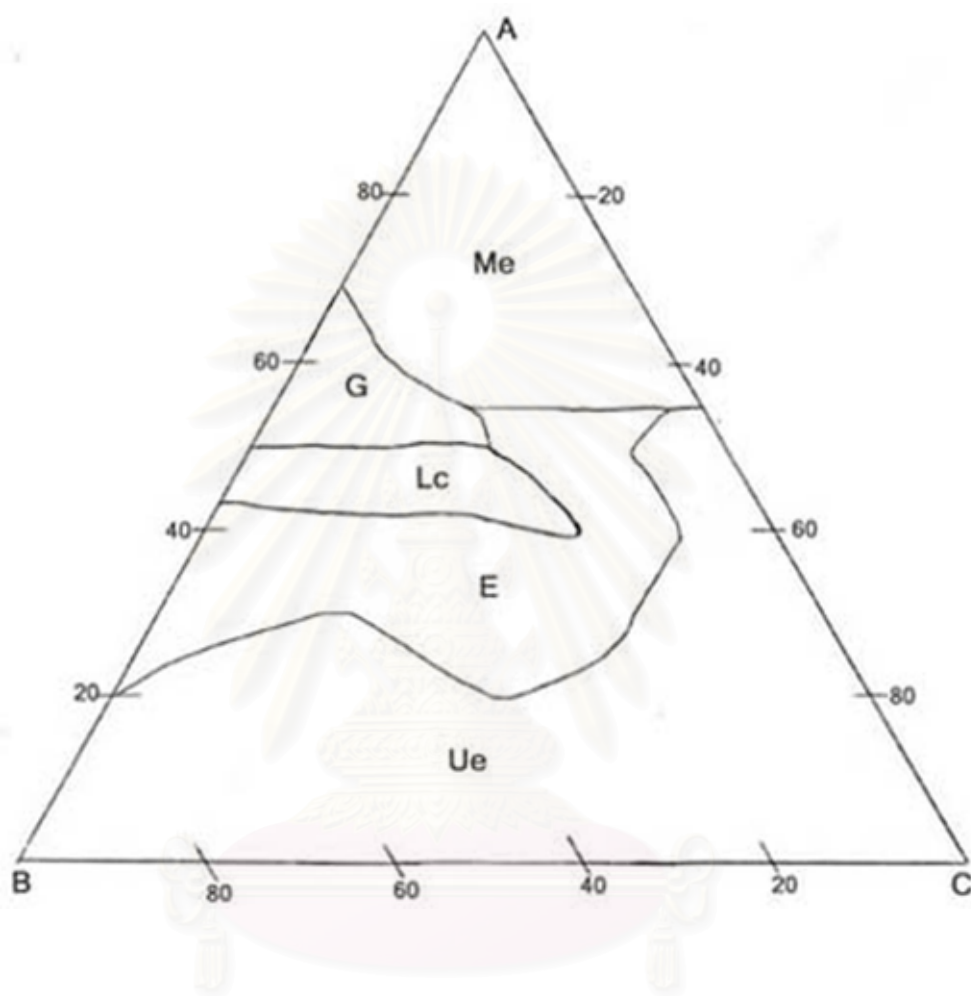


Figure 12 Phase diagram of polyoxyethylene sorbitan monooleate(A)-water(B)-capric/caprylic triglyceride(C), Ue: unstable emulsion, E: emulsion, Lc: liquid crystalline, G: microemulsion gel, Me: microemulsion.

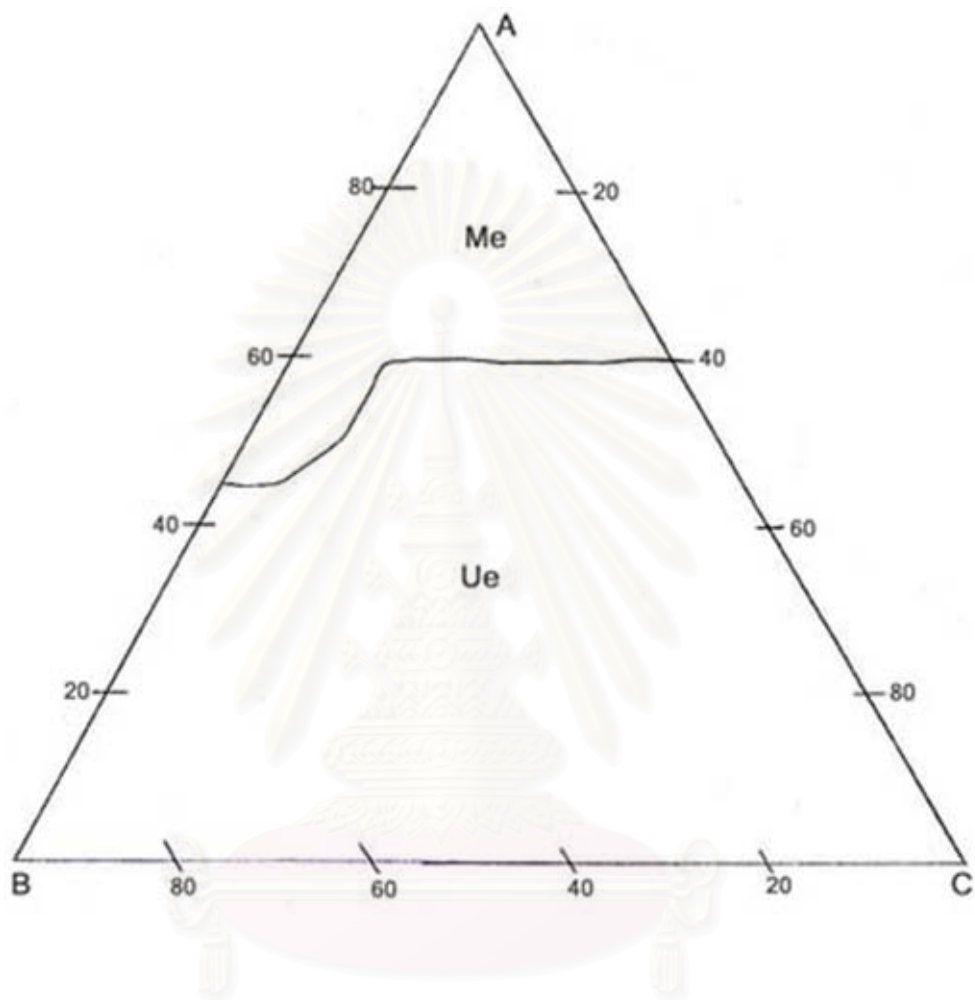


Figure 13 Phase diagram of polyoxyethylene sorbitan monooleate:*n*-butanol; 1:1
 (A)-water(B)-capric/caprylic triglyceride(C), Ue: unstable emulsion, Me: microemulsion.

จุฬาลงกรณ์มหาวิทยาลัย

In figure 14, glycerin was used as co-surfactant instead of *n*-butanol. The surfactant and co-surfactant were combined in the ratio of 1:1 by weight. Microemulsion area was lower when using the glycerin as co-surfactant, it was formed at 50-80% w/w surfactant:co-surfactant and 5-40% w/w water. The liquid crystalline region was formed at 30-50% w/w surfactant:co-surfactant and 30-60% w/w water. Microemulsion gel was not appeared in this diagram.

In figure 15, polyoxyethylene (10) oleyl ether was selected as surfactant. The microemulsion could form at low concentration of surfactant to produce oil-in-water microemulsion, it was formed at 15-25% w/w surfactant and 60-80% w/w water. And at higher surfactant concentration, microemulsion region was formed at 40-90% w/w surfactant and 5-15% w/w water. The microemulsion gel region was formed at 30-85% w/w surfactant and 15-70% w/w water.

In figure 16, *n*-butanol was used as co-surfactant in the ratio of 1:1 by weight. The microemulsion area was increased comparing with using polyoxyethylene (10) oleyl ether alone. Microemulsion region was formed at 35-90% w/w surfactant:co-surfactant and 5-35% w/w water. Only microemulsion and unstable emulsion regions were found in this diagram.

In figure 17, glycerin as co-surfactant was combined with surfactant in the ratio of 1:1 by weight. The microemulsion region was formed at 50-70% w/w surfactant:co-surfactant and 10-40% w/w water. Microemulsion gel region was formed at 70-90% w/w surfactant: co-surfactant and 5-10% w/w water.

Sorbitan stearate (and) methylglucose sesquistearate was failed to produce the microemulsion either by using surfactant alone or with co-surfactant such as *n*-butanol or glycerin. It is probable that capric/caprylic triglyceride is the medium chain triglyceride which has three hydrophobic chain with hydrocarbon chain length of C_8 - C_{10} while sorbitan stearate (and) methylglucose sesquistearate has hydrocarbon chain length $R_1 = C_8$, $R_2 = C_{17}$ and $R_3 = C_{33}$. According to the critical packing parameter, sorbitan stearate (and) methylglucose sesquistearate has high steric effect and the hydrophobic tail of oil and surfactant did not suitable. So the phase bounded behavior showed only liquid crystalline region. And in sense of HLB value, sorbitan stearate (and) methylglucose sesquistearate has low HLB (6). It is not suitable for capric/caprylic triglyceride to form

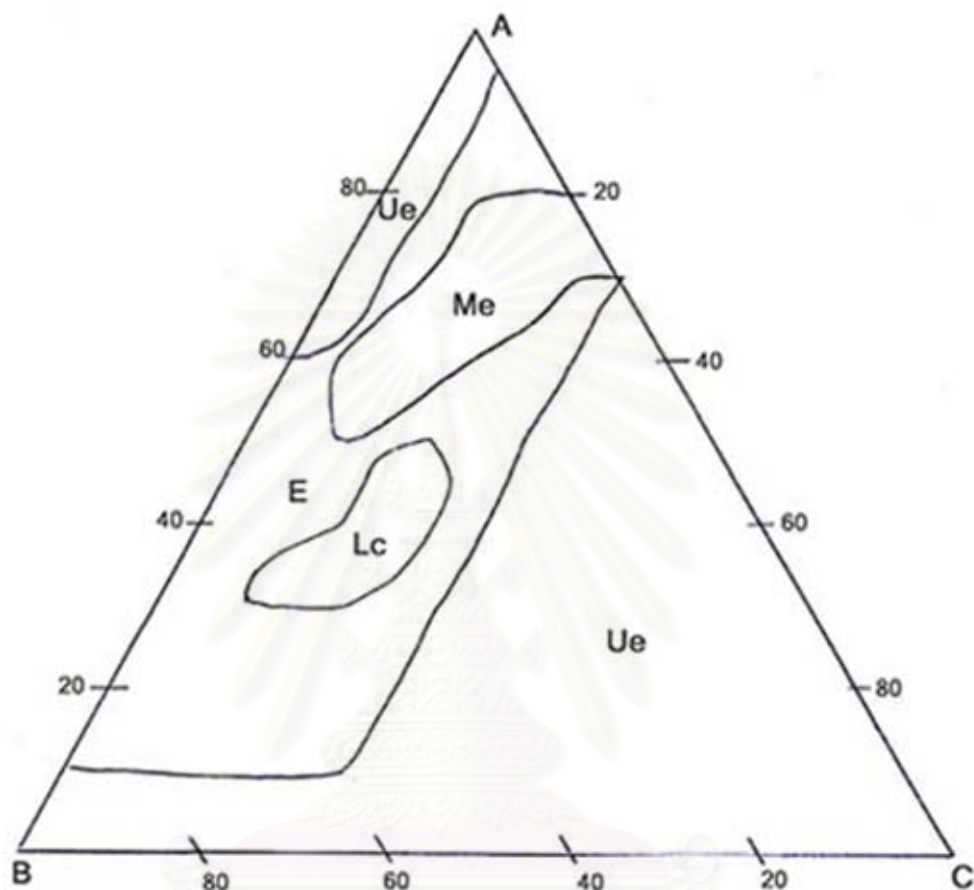


Figure 14 Phase diagram of polyoxyethylene sorbitan monooleate:glycerin; 1:1(A)-water(B)-capric/caprylic triglyceride(C), Ue: unstable emulsion, E: emulsion, Lc: liquid crystalline, Me: microemulsion.

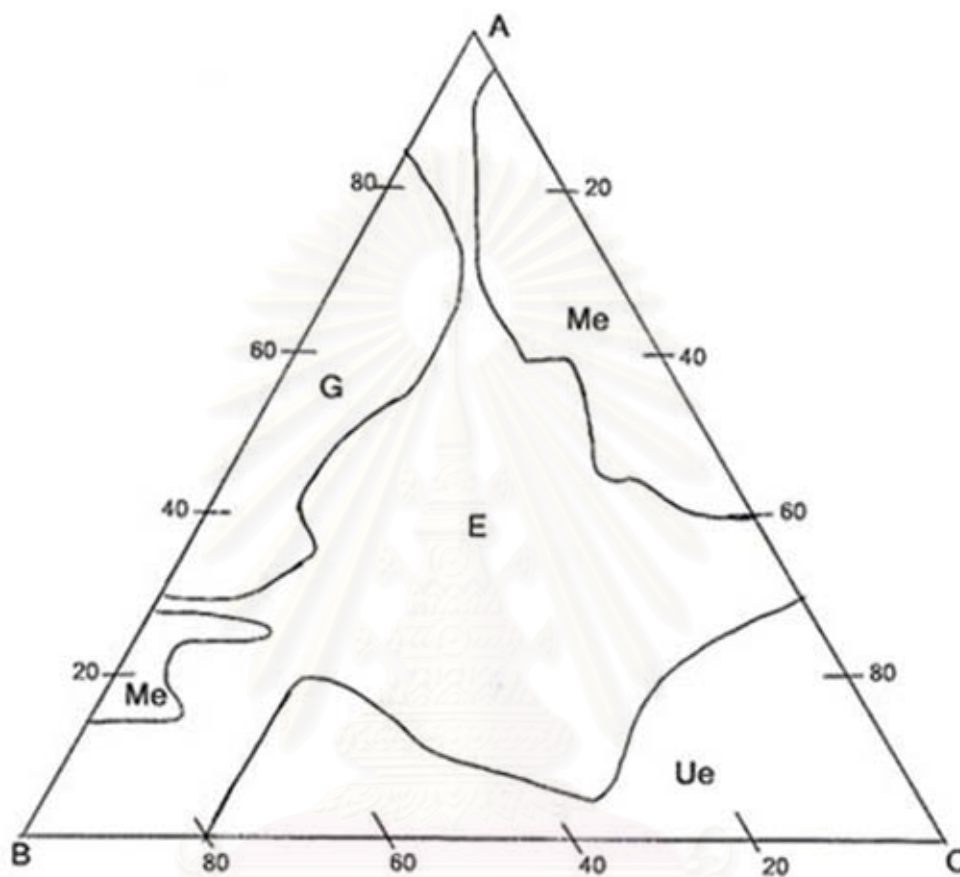


Figure 15 Phase diagram of polyoxyethylene (10) oleyl ether(A)-water(B)-capric/caprylic triglyceride(C), Ue: unstable emulsion, E: emulsion, Lc: liquid crystalline, G: microemulsion gel, Me: microemulsion.

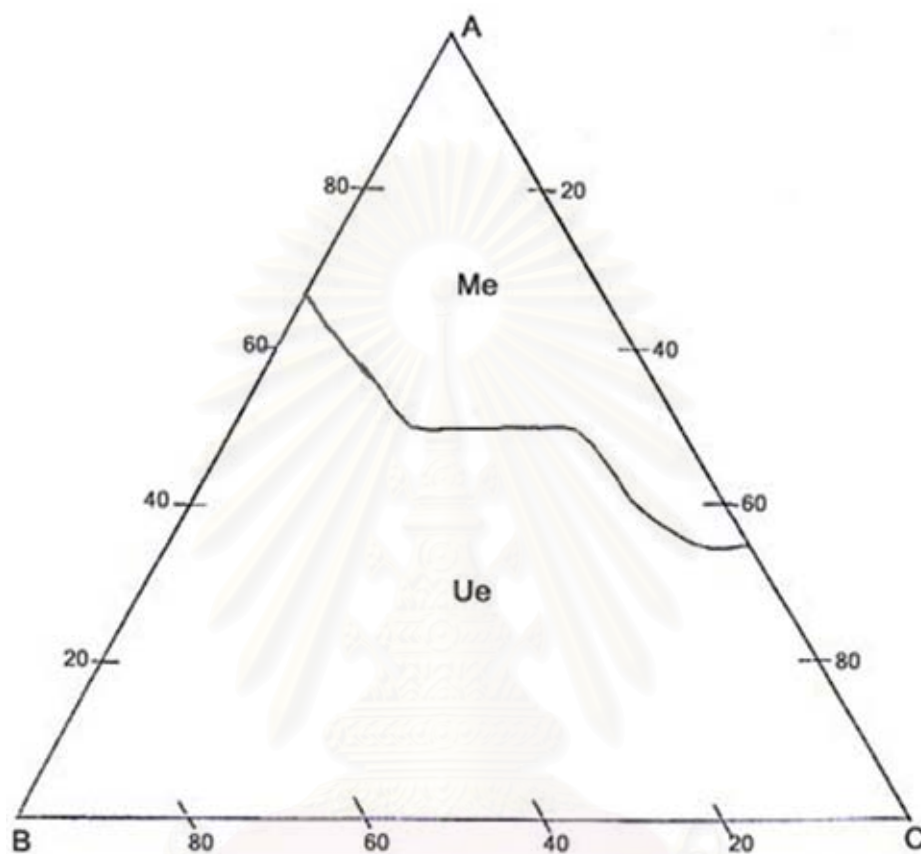


Figure 16 Phase diagram of polyoxyethylene (10) oleyl ether:*n*-butanol; 1:1(A)-water(B)-capric/caprylic triglyceride(C), Ue: unstable emulsion, Me: microemulsion.

จุฬาลงกรณ์มหาวิทยาลัย

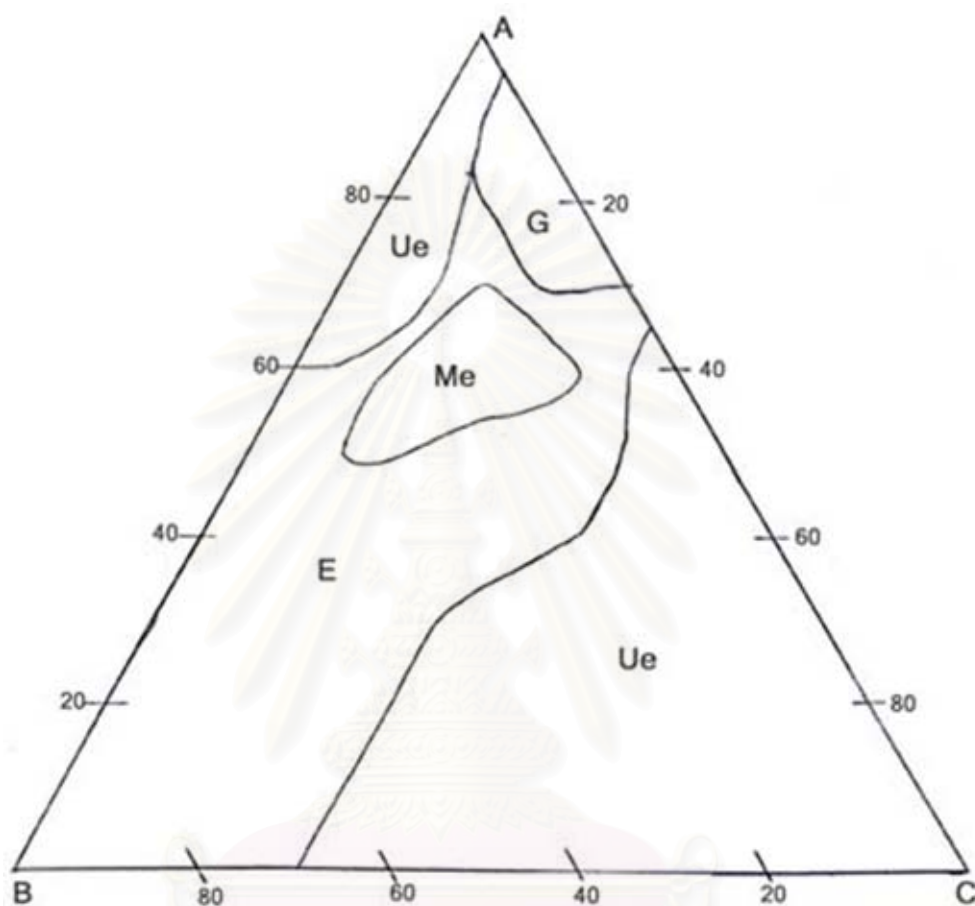


Figure 17 Phase diagram of polyoxyethylene (10) oleyl ether:glycerin; 1:1(A)-water (B)-capric/caprylic triglyceride(C), Ue: unstable emulsion, E: emulsion, G: microemulsion gel, Me: microemulsion.

microemulsion, it might be that sorbitan stearate (and) methylglucose sesquistearate cannot reduce the interfacial tension to the values required for microemulsion formation. Ho, Hsiao and Sheu (1996) have reported that using capric/caprylic triglyceride as oil component, microemulsion was only formed when HLB value of surfactant was between 8 and 13. Actually the HLB value describes the relative polarity of the surfactant. The HLB value may also indicate the extent of favorable for surfactant migrating into the interface between water and oil phases. It seems to be important for surfactant being able to migrate into the interface to reduce interfacial tension to a lower level of 0 to form microemulsion. Those surfactants having HLB within a certain range would show higher preference of migrating into the interface. This is the reason that microemulsions could only be formed using surfactant having HLB within a certain range.

When *n*-butanol and glycerin were used as co-surfactant to modify the HLB value of the surfactant to an optimal value suitable for microemulsion formation, it was also failed to produce microemulsion. It might be because of co-surfactants cannot penetrate to the oil-in-water interface for reduce free surface energy to zero in order to form microemulsion.

Polyoxyethylene sorbitan monooleate and polyoxyethylene (10) oleyl ether as surfactants were succeeded to produce clear area of microemulsion. It was noted that polyoxyethylene (10) oleyl ether, which has smaller hydrophilic head group, larger microemulsion area was produced. Polyoxyethylene sorbitan monooleate has higher HLB value (15) than suggestion in previous study(Ho et al., 1996), but it can still produce microemulsion. It might be due to difference of surfactant, polyglycerol fatty acid esters were served as surfactant in that study. Besides the HLB value, geometric packing parameter of surfactant in the interface may be another influencing factor to be considered in terms of its effect on the curvature and the fluidity of interface. The hydrophobic tail of oil and surfactant might be suitable and polyoxyethylene sorbitan monooleate can reduce free surface energy to zero to form microemulsion. In general, Aboofazeli et al. (1995) considered that oils readily formed microemulsion when the hydrophobic chains of the surfactant stabilizing the system are longer than those of the oil being incorporated.

When *n*-butanol was used as co-surfactant, the microemulsion area was expanded in both surfactants. This is consistent with a previous study that *n*-butanol is an effective co-surfactant to blend with surfactant for the formation of microemulsion (Trotta, Pattarino

and Grosa, 1998). A short chain alcohol can act to reduce the effective critical packing parameter in two ways, firstly by its incorporation into the interfacial film and/or secondly by dissolving in the aqueous phase thereby making it less hydrophilic. The short chain alcohol can also have a third effect, in that it can reduce the tendency of long hydrophobic chain surfactant to form highly rigid films, thus allowing the interfacial film sufficient flexibility to take up the different curvatures required to form microemulsion (Aboofazeli et al., 1994). Butanol is expected to interact with the head region of the surfactant and increased the optimal head group area resulted in reduce the critical packing parameter of the surfactant. Thus the molecules at the interface were better packing and increased the area of existence of microemulsion systems (Alany et al., 2001). Unsurprisingly, the formation of liquid crystalline phase was vanished when butanol was used as co-surfactant, it might be because butanol perturbed the long range ordered packing of the surfactant so it was not appropriate to form liquid crystalline (Alany et al., 2000). Since butanol increases the fluidity of the surfactant film to form microemulsion, in general an elastic or flexible surfactant film favors to form microemulsion, whereas a liquid crystalline phase is formed with more rigid film.

Glycerin is a polyhydroxy compound used widely in pharmaceutical field. Kale and Allen, Jr. (1989) reported that using glycerin as co-surfactant in the ratio of 1:1 by weight provided a larger microemulsion region than the other polyhydroxy compounds such as propylene glycol and ethylene glycol. In this study, using glycerin as co-surfactant in the ratio of 1:1 by weight could lower the microemulsion region in phase diagram provided by polyoxyethylene sorbitan monooleate, resulted in decreasing the concentration of surfactant and co-surfactant in forming microemulsion. Kale and Allen, Jr. explained the effect of using glycerin on changing the microemulsion region in terms of glycerin inserted in the interfacial film. But Lawrence and Rees (2000) suggested that the presence of glycerin in the aqueous phase will influence optimal surfactant head group area by altering the solubility of the head group in the aqueous phase. In these sense, glycerin might change the surfactant characteristic to appropriate critical packing parameter thus they can reduce the concentration of surfactant to form microemulsion structure.

From the data obtained it was found that polyoxyethylene (10) oleyl ether blended with *n*-butanol in the ratio of 1:1 by weight was produced the largest area of microemulsion, the polyoxyethylene (10) oleyl ether without co-surfactant produced the second larger area of microemulsion. Nevertheless, concentration of *n*-butanol contained in microemulsion was not suitable for using with human skin because exposure limit of butanol is 50 ppm (Reynold, 1989); it can induce skin irritation and dermal toxicity. Hence, polyoxyethylene (10) oleyl ether without co-surfactant, the second best, was selected as surfactant for further investigation.

1.2. Determination of Phase Diagram of Benzocaine Microemulsions

Benzocaine 7.5% by weight was incorporated into each composition of capric/caprylic triglyceride-water-polyoxyethylene (10) oleyl ether, and pseudoternary phase diagram was constructed as shown in figure 18. The microemulsion region was form at 35-90% w/w surfactant and 10-15%w/w water, and microemulsion gel was formed at 35-90% w/w surfactant and 10-60% w/w water. The microemulsion area at low surfactant concentration was vanished. Malcolmson et al. (1998) suggested from studies of the solubilization of testosterone propionate into nonionic oil-in-water microemulsions, that most drugs were solubilized predominately in the relatively concentrated polyoxyethylene region close to the core of micelle. Only very lipophilic drug (i.e. those with $\log P > 5-6$) have in addition a significant solubility in the hydrophobic core of the aggregates. Thus benzocaine may be considered to be predominately solubilized in the polyoxyethylene region close to the micelle core, it can perturb the interfacial film of surfactant. At low surfactant concentration the interfacial film might be loosely packing and sensitive structure, while benzocaine was incorporated into this region it might be alter structural and destructive the interfacial film.

1.3. Benzocaine Microemulsions Characterization

Benzocaine microemulsions were characterized by transmission electron microscope (TEM) technique as shown in figures 19-22. In microemulsion consisted of 70% surfactant concentration, the diameter of droplets were between 22-66 nm.

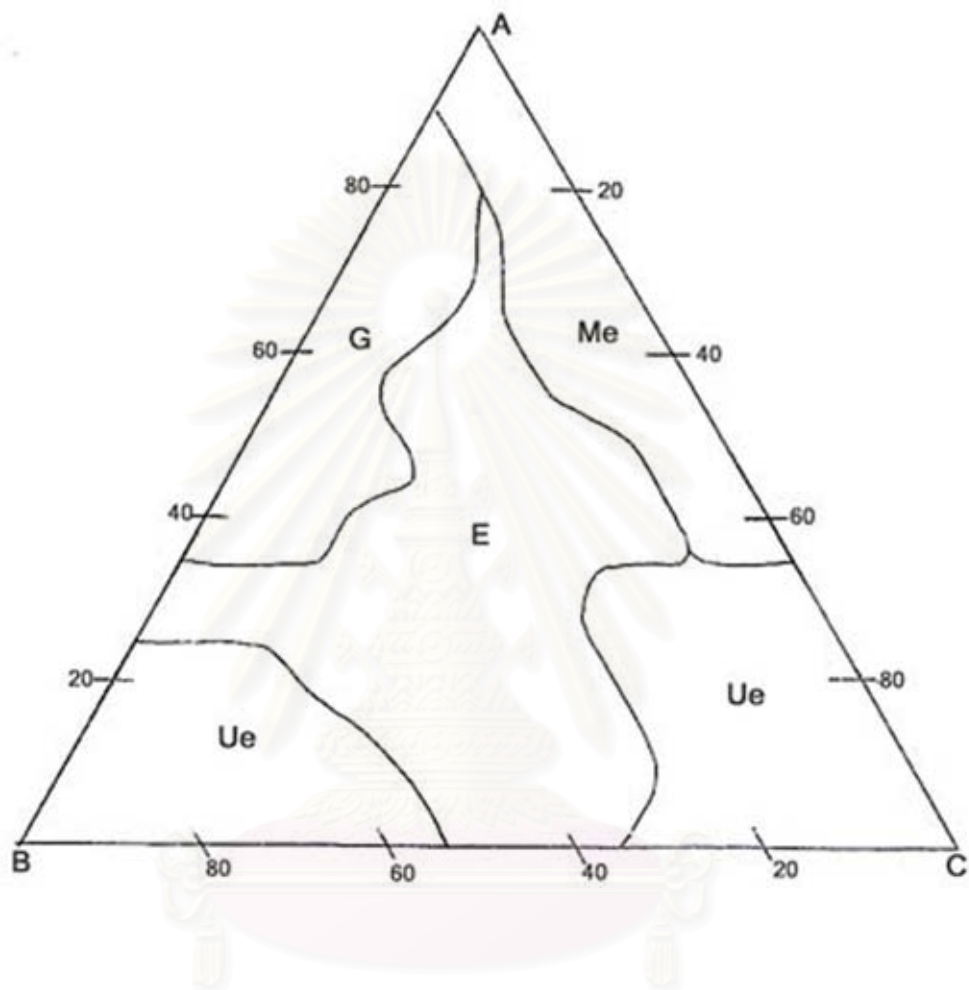


Figure 18 Phase diagram of 7.5% by weight benzocaine in polyoxyethylene (10) oleyl ether(A)-water(B)-capric/caprylic triglyceride(C), Ue: unstable emulsion, E: emulsion, G: microemulsion gel, Me: microemulsion.

จุฬาลงกรณ์มหาวิทยาลัย

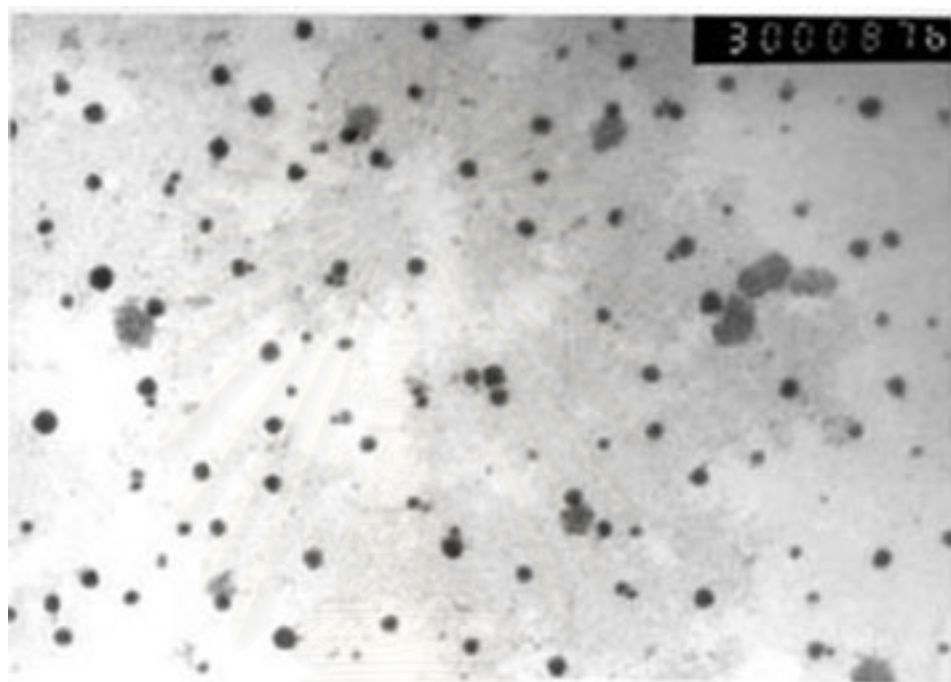


Figure 19 Photograph of 7.5% benzocaine microemulsion using JEOL JEM-200 CX, microemulsion base consisted with 70%, 10% and 20%w/w of polyoxyethylene (10) oleyl ether, water and capric/caprylic triglyceride, respectively. The magnification is 45000 folds.

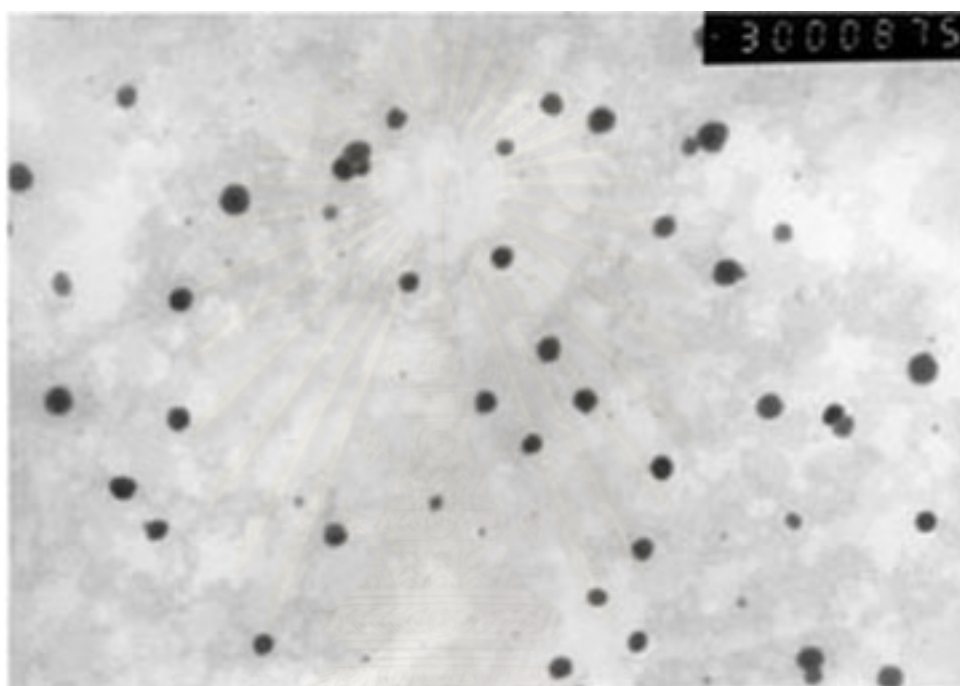


Figure 20 Photograph of 7.5% benzocaine microemulsion using JEOL JEM-200 CX, microemulsion base consisted with 60%, 10% and 30%w/w of polyoxyethylene (10) oleyl ether, water and capric/caprylic triglyceride, respectively. The magnification is 45000 folds.

จุฬาลงกรณ์มหาวิทยาลัย

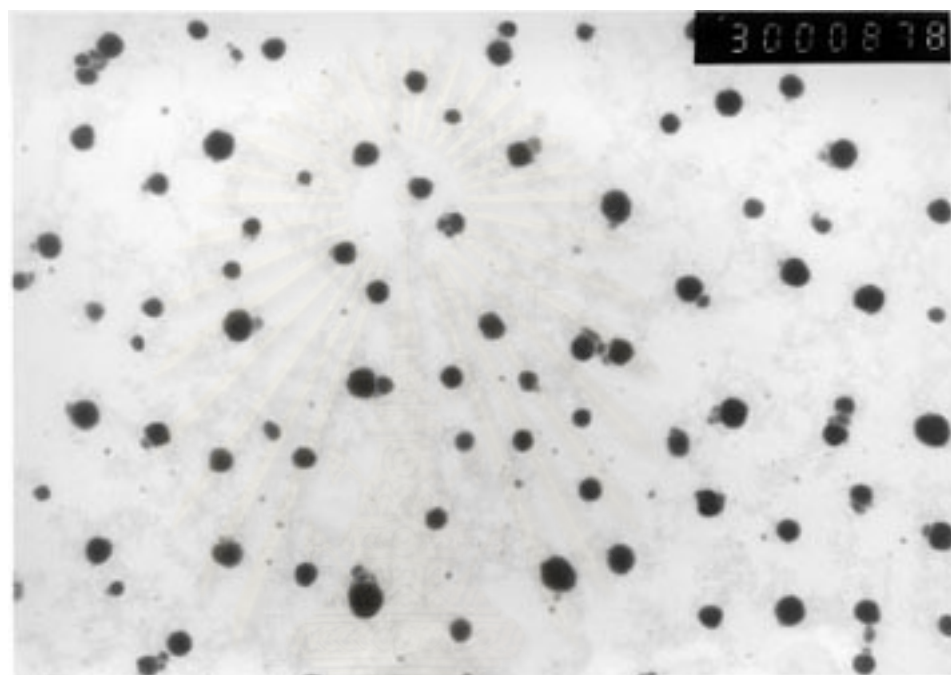


Figure 21 Photograph of 7.5% benzocaine microemulsion using JEOL JEM-200 CX, microemulsion base consisted with 50%, 10% and 40%w/w of polyoxyethylene (10) oleyl ether, water and capric/caprylic triglyceride, respectively. The magnification is 45000 folds.

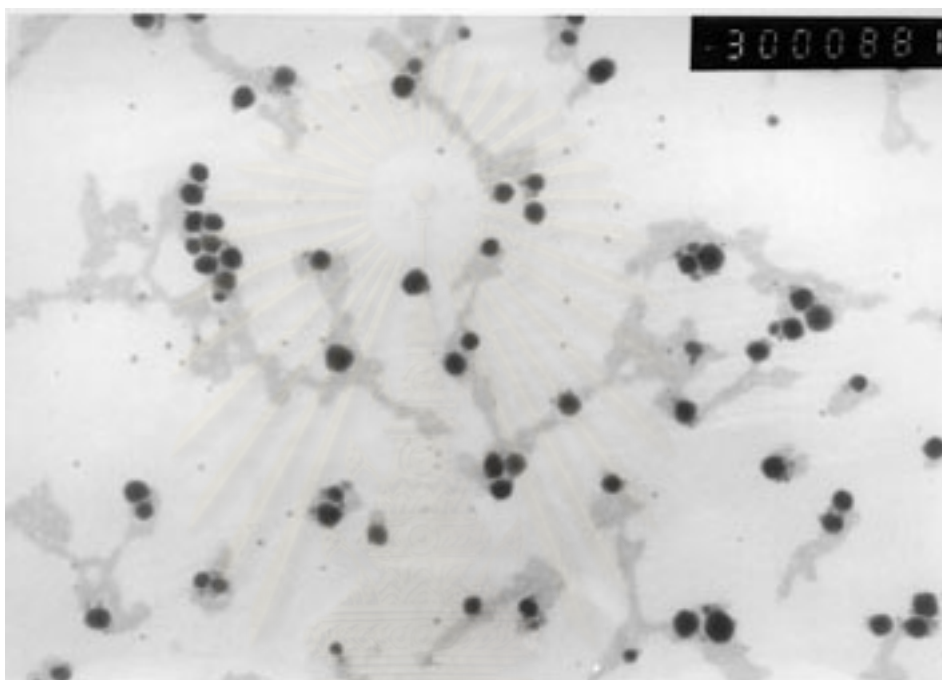


Figure 22 Photograph of 7.5% benzocaine microemulsion using JEOL JEM-200 CX, microemulsion base consisted with 40%, 10% and 50%w/w of polyoxyethylene (10) oleyl ether, water and capric/caprylic triglyceride, respectively. The magnification is 45000 folds.

And the diameter of the droplets in microemulsions consisted of 60%, 50% and 40% surfactant concentration were between 22-88 nm. The droplet sizes were below than 100 nm. It is confirmed that capric/caprylic triglyceride-water-polyoxyethylene (10) oleyl ether containing benzocaine 7.5% by weight can form microemulsion system. The type of microemulsion should be oil-in-water microemulsion considered from HLB value of polyoxyethylene (10) oleyl ether (12.4), it has a trend to form oil-in-water microemulsion.

2. *In Vitro* Evaluation of Benzocaine Microemulsions

2.1. Assay of Percent Labeled Amount

Six microemulsions with varied water and surfactant concentrations were selected to explore in permeation studies, the reasons to select and details of components in each microemulsion were stated in 2.3. The purpose of this part of study was to standardize the benzocaine microemulsions with respect to the percent labeled amount prior to further *in vitro* permeation studies. Table 2 shows the assay result. The method to calculate the percent labeled amount and individual data is shown in appendix III.

Table 2 Percent labeled amount of benzocaine microemulsions

Formula	Percent labeled amount
A	98.14
B	96.86
C	96.12
D	97.30
E	95.10
F	97.38

From this data, percent labeled amount of each microemulsion was in an acceptable range (90-105%) and close to 100%. Hence, they could be used for further

investigation, since any differences found in the permeation characteristics of these products would not be due to the difference in their initial amount of benzocaine.

2.2. Benzocaine Solubility Studies

Benzocaine solubility in phosphate buffer pH 7.4 is 1.021 mg/ml. The details of solubility studies are shown in appendix IV. The solubility of benzocaine in phosphate buffer is low and about the same as that in water. In previous study, Lalor, Flynn and Weiner (1994) reported that the solubility of benzocaine in water was 1.04 mg/ml.

2.3. *In Vitro* Permeation Studies of Benzocaine Through Shed Cobra Skin

Initially, three benzocaine microemulsions with varied amount of water but fixed surfactant concentration were selected to examine the effect of water content in microemulsion on permeation of benzocaine through shed cobra skin. Surfactant concentration was fixed at 60% by weight because this concentration provided the wide range of water content to form microemulsions. The compositions of each microemulsion base were presented in table 3. The benzocaine concentration was 7.5% by weight.

Table 3 Compositions of microemulsion base with varied water content in microemulsion

Formula	Surfactant ^a (%w/w)	Water (%w/w)	Oil ^b (%w/w)
A	60	15	25
B	60	10	30
C	60	5	35

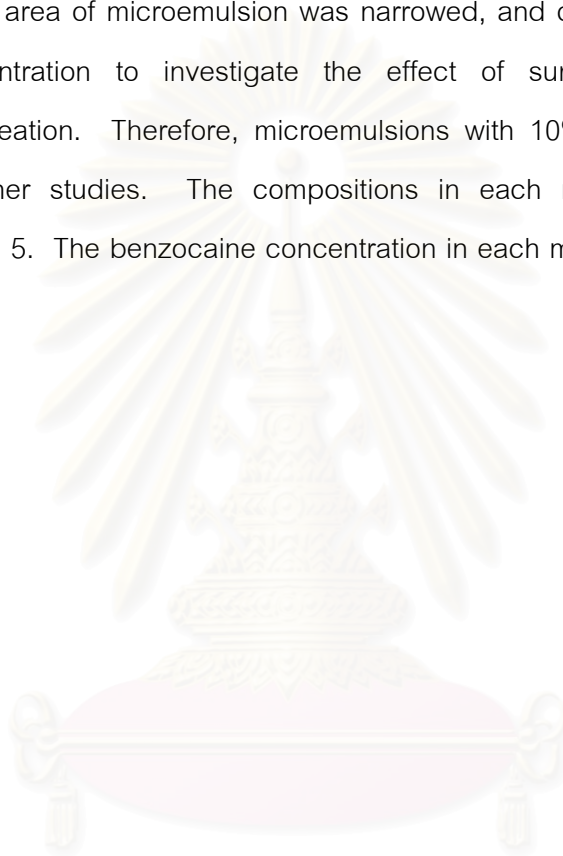
^a Surfactant is polyoxyethylene (10) oleyl ether.

^b Oil is capric/caprylic triglyceride.

The cumulative amounts of benzocaine from three microemulsions penetrating through the shed snake skin at various times during the 8 hours experiment are presented

in table 4. The amount of benzocaine permeated through shed snake skin also depend on their ability to penetrate through membrane and solubility in receiving solution in the experiment. Comparison of permeation profile of benzocaine through shed snake skin from three microemulsions is shown in figure 23.

From this result, the permeation of benzocaine from 15% water content microemulsion was higher than the other two microemulsions. However, at 15% by weight water content the area of microemulsion was narrowed, and cannot allow to varying the surfactant concentration to investigate the effect of surfactant concentration on benzocaine permeation. Therefore, microemulsions with 10% w/w water content was selected for further studies. The compositions in each microemulsion base were presented in table 5. The benzocaine concentration in each microemulsion was 7.5% by weight.



สถาบันวิทยบริการ
จุฬาลงกรณ์มหาวิทยาลัย

Table 4 Permeation data of benzocaine through shed snake skin from microemulsion formulas A, B and C

Time (hours)	Cumulative Amount of Benzocaine* (mcg)		
	A	B	C
1	49.12 ± 2.16	29.64 ± 0.46	31.07 ± 0.81
2	93.08 ± 4.40	66.50 ± 10.34	48.76 ± 1.00
3	127.32 ± 7.64	92.85 ± 5.67	68.31 ± 3.6
4	160.37 ± 4.83	120.95 ± 0.51	93.57 ± 5.33
5	198.23 ± 6.42	149.70 ± 1.99	114.95 ± 5.68
6	231.81 ± 8.18	173.75 ± 0.88	137.13 ± 6.65
7	265.52 ± 7.17	202.20 ± 1.22	157.36 ± 5.52
8	300.20 ± 7.47	235.44 ± 2.86	181.57 ± 5.42

* n= 3, mean ± SD

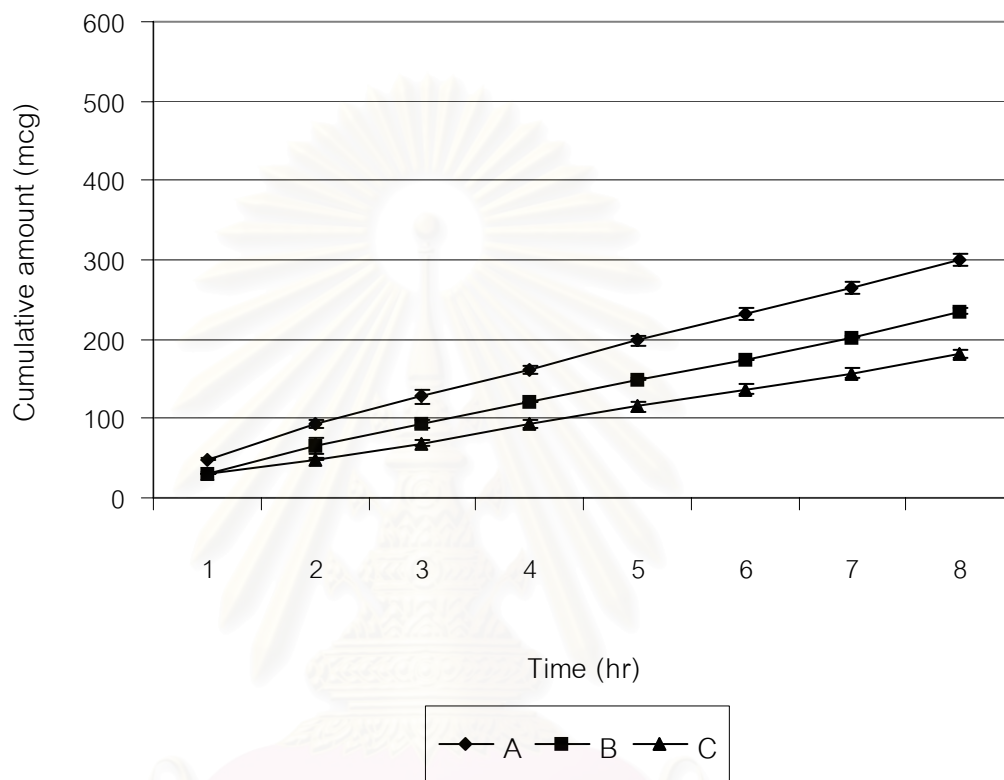


Figure 23 Comparison of permeation profiles of benzocaine through shed snake skin from microemulsion formulas A, B and C. (n = 3)

สถาบันวิจัยบริการ
จุฬาลงกรณ์มหาวิทยาลัย

Table 5 Compositions of microemulsion base with varied surfactant concentration in microemulsion

Microemulsion	Surfactant ^a (%w/w)	Water (%w/w)	Oil ^b (%w/w)
D	40	10	50
E	50	10	40
B	60	10	30
F	70	10	20

^aSurfactant is polyoxyethylene (10) oleyl ether.

^bOil is capric/caprylic triglyceride.

Table 6 presents the cumulative amounts of benzocaine from four formulas of microemulsions penetrate through shed snake skin at various time during 8 hours. The permeation profiles of benzocaine through shed snake skin from microemulsion containing equal amount of water but the concentrations of surfactant were varied from 40%, 50%, 60% and 70% w/w as shown in figure 24.

The summary of the cumulative amounts of drug permeated in 8 hr and the steady state fluxes of each microemulsion are presented in table 7. The steady state flux was obtained from the slope after linear regression of the terminal portion of the plot of the cumulative amount permeated versus time. Individual diffusion data, determination of the fluxes and permeation profiles for each microemulsion are presented in appendix V. From these data, the calculated regression analysis gave r^2 values which were greater than 0.99 in most of the experiments, indicating the establishment of steady state diffusion through this skin model.

Table 6 Permeation data of benzocaine through shed snake skin from microemulsion formulas D, E, B and F

Time (hours)	Cumulative Amount of Benzocaine* (mcg)			
	D	E	B	F
1	47.95 ± 2.36	43.50 ± 2.59	29.64 ± 0.46	38.30 ± 3.78
2	105.50 ± 3.69	81.11 ± 1.73	66.50 ± 10.34	50.64 ± 2.77
3	167.90 ± 8.96	139.22 ± 3.58	92.85 ± 5.67	65.91 ± 2.76
4	234.24 ± 6.42	185.01 ± 2.91	120.95 ± 0.51	82.22 ± 4.70
5	304.44 ± 8.85	226.97 ± 3.09	149.70 ± 1.99	103.10 ± 4.47
6	379.52 ± 11.01	270.58 ± 4.82	173.75 ± 0.88	120.72 ± 5.91
7	455.20 ± 11.39	324.40 ± 4.68	202.20 ± 1.22	140.37 ± 5.59
8	537.55 ± 7.13	373.88 ± 3.93	235.44 ± 2.86	158.77 ± 1.58

* n= 3, mean ± SD

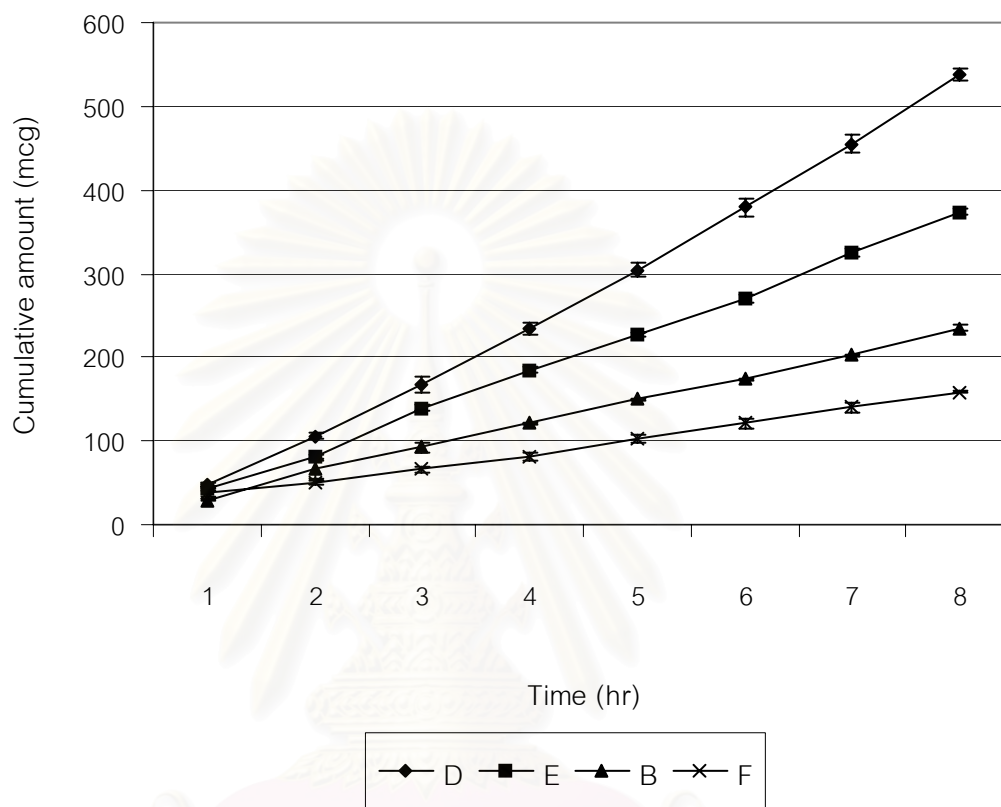


Figure 24 Comparison of permeation profile of benzocaine through shed snake skin from microemulsion formulas D, E, B and F. (n =3)

จุฬาลงกรณ์มหาวิทยาลัย

Table 7 Comparison of average cumulative amount and steady state flux of benzocaine permeation from six formula microemulsions through shed snake skin

Formula	Surfactant ^a (%w/w)	Water (%w/w)	Cumulative Amount* (mcg)	Steady State Flux* (mcg/hr/cm ²)
A	60	15	300.20 ± 7.47	16.09 ± 0.32
B	60	10	235.44 ± 2.85	13.28 ± 1.06
C	60	5	181.57 ± 5.41	10.54 ± 0.16
D	40	10	537.55 ± 7.15	34.40 ± 0.65
E	50	10	373.87 ± 3.93	21.83 ± 0.58
F	70	10	158.77 ± 1.57	8.64 ± 0.14

^a Surfactant is polyoxyethylene (10) oleyl ether.

^b Oil is capric/caprylic triglyceride.

* n = 3, mean ± SD

From the permeation results, analysis of variance (ANOVA) was applied for statistical analysis, the minimum level of statistical significance was set at 95% ($p < 0.05$). If ANOVA shows statistical significance, Newman-keuls test was further performed to these data.

The steady state fluxes of benzocaine from six formulas of microemulsions were significant difference as well as the cumulative amounts ($p < 0.01$). So, the Newman-keuls test was then applied. To investigate the effect of water amount in microemulsion on benzocaine permeation, three benzocaine microemulsions consisted with various water content were compared. The steady state fluxes of benzocaine were significantly increased as increasing the water content in microemulsion (15%, 10% and 5% w/w), there were significant differences between the steady state fluxes of benzocaine from 15%, 10% and 5% w/w water content microemulsion ($p < 0.01$).

The steady state flux of benzocaine in 15% water microemulsion (A) was 16.09 mcg/hr/cm² while the steady state flux of benzocaine in 10% water microemulsion (B) was

13.28 mcg/hr/cm². The steady state flux of benzocaine permeate through the shed snake skin was increased 1.2 fold while the difference of water content was 5%. The steady state flux of benzocaine in 5% water microemulsion (C) was 10.54 mcg/hr/cm² the differences amount of water content in B and C was the same as in B and A. Whilst the differences in the steady state flux of benzocaine permeate through the shed snake skin was also 1.2 fold increased.

To investigate the effect of surfactant concentration in microemulsion on permeation of benzocaine, the various surfactant concentration microemulsions (40%, 50%, 60% and 70% w/w) with 10% water were studied. In contrast with water content studies, the steady state fluxes of benzocaine were significantly decreased as surfactant concentration were increase (40%, 50%, 60% and 70% w/w). There were significant differences between the steady state fluxes of benzocaine from four microemulsions ($p < 0.01$).

The steady state flux of benzocaine from 70% surfactant microemulsion was the lowest. The steady state flux of benzocaine in 70% surfactant microemulsion (F) was 8.64 mcg/hr/cm² while the steady state flux of benzocaine in 60% surfactant microemulsion (B) was 13.28 mcg/hr/cm². The steady state flux of benzocaine through shed snake skin was 1.6 fold decreased while the difference of surfactant concentration was 10%. The steady state flux of benzocaine in 50% surfactant microemulsion (E) was 21.83 mcg/hr/cm², compared with 60% surfactant microemulsion (B), it was 1.6 fold decreased as in F and B. The steady state flux of benzocaine in 40% surfactant microemulsion (D) was 34.40 mcg/hr/cm², the difference of surfactant concentration in D and E was the same as that in B and E, thus the steady state flux of benzocaine permeate through the shed snake skin was 1.6 fold decreased.

Moreover, the cumulative amounts of benzocaine from microemulsions with 15%, 10% and 5% water content were compared. The cumulative amounts of benzocaine were increased as increasing the water content in microemulsion. There was a significant difference between the cumulative amount of benzocaine from 15%, 10% and 5% water content microemulsion ($p < 0.01$). And the cumulative amounts of benzocaine from 40%, 50%, 60% and 70% surfactant concentration microemulsion were significantly decreased as a result of increasing surfactant concentration. There were significant differences

between the cumulative amount of benzocaine from four microemulsions ($p < 0.01$). The results of cumulative amount of benzocaine agree with the steady state flux results.

3. *In Vivo* Evaluation of Analgesic Effect Using Mouse Tail-Flick Test

3.1. Mouse Tail-Flick Test

To investigate the effect of water and surfactant concentrations in microemulsion on drug delivery from microemulsion, six microemulsions as same as in the *in vitro* permeation studies were applied on distal portion of mouse's tail (about 3 cm from tip). The analgesic activity was exhibited in terms of area of analgesia calculated from the area under the corresponding 0-180 min time course-%MPE curves, using the trapezoidal rule.

Initially, area of analgesia produced by the three microemulsions containing the same concentration of surfactant and various water content (15%, 10% and 5% w/w) were compared, the results were shown in figure 25. Then the area of analgesia of four microemulsions with the same amount of water and various surfactant concentration (40%, 50%, 60% and 70% w/w) were compared as illustrated in figure 26.

To assure that the microemulsion base (without benzocaine) did not exhibit any analgesic effects, all six microemulsion bases were tested utilizing the mouse tail-flick test and served as controls. The comparisons of area of analgesia provided by benzocaine microemulsions and microemulsion bases were shown in figure 27. The plots of %MPE versus time during 180 minutes curves of each experiment were illustrated in appendix VI. The area of analgesia of all benzocaine microemulsions were significantly higher than microemulsion base controls ($p < 0.01$). Microemulsion bases exhibited no or less analgesic activity compared with benzocaine microemulsions, hence the analgesic responses were due to benzocaine activity.

From statistical analysis by ANOVA the area of analgesia provided by six benzocaine microemulsions were significantly different ($p < 0.01$). In terms of effect of water content (5%, 10% and 15% by weight), the analgesic response increased as the water content in microemulsion increased. There were significant difference between 5%, 15%; 10%, 15% ($p < 0.01$) and 5%, 10% water content microemulsion ($p < 0.05$).

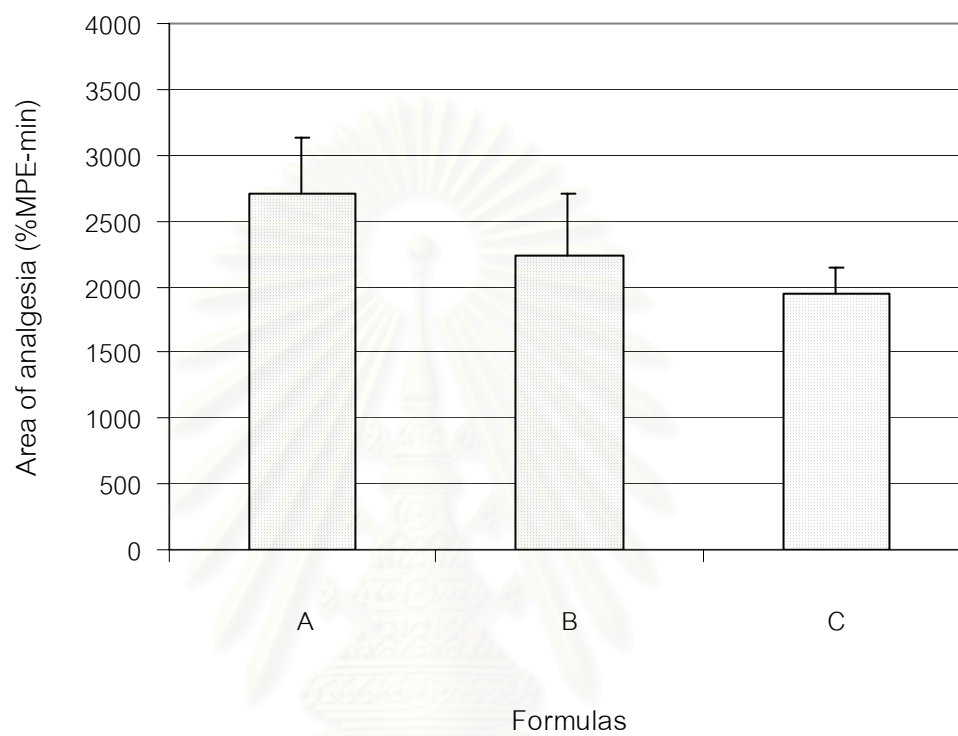


Figure 25 Comparison of area of analgesia provided by microemulsion formulas A, B and C. (n = 10)

สถาบันวิทยบริการ
จุฬาลงกรณ์มหาวิทยาลัย

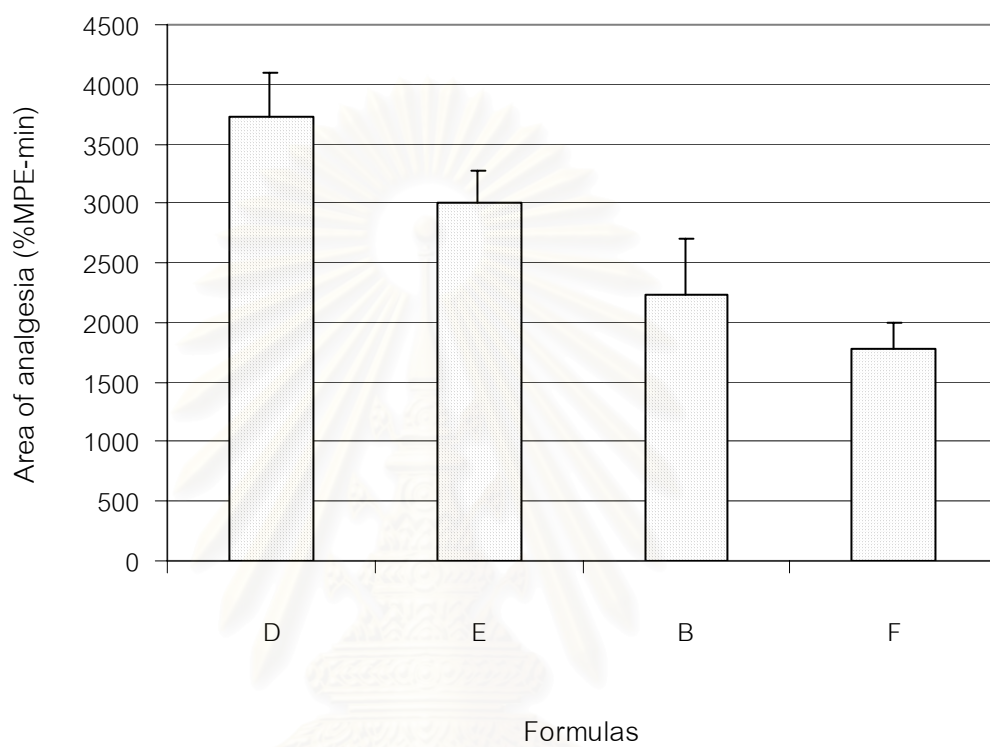


Figure 26 Comparison of area of analgesia provided by microemulsion formulas D, E, B and F. (n = 10)

สถาบันวิทยบริการ
จุฬาลงกรณ์มหาวิทยาลัย

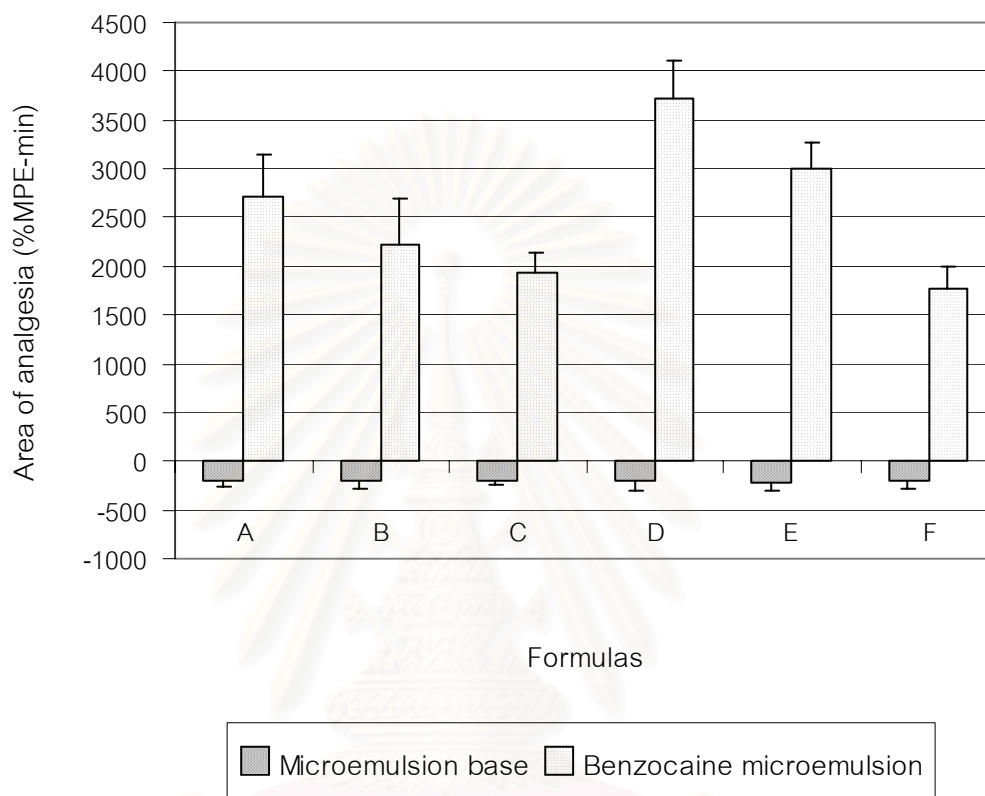


Figure 27 Comparison of area of analgesia provided by benzocaine microemulsions and microemulsion bases. (n = 10)

สถาบันวิทยบริการ
จุฬาลงกรณ์มหาวิทยาลัย

In the other hand, comparing the area of analgesia of four different surfactant concentration microemulsions, it was indicated that the analgesic responses were significantly decreased as the surfactant concentrations in microemulsions increased ($p < 0.01$). There were no significant differences between six microemulsion bases.

It has been recognized for many years, that the major source of resistance to penetration or permeation of the drug from transdermal route is the stratum corneum. As the water content in microemulsion increased benzocaine permeation through the skin was increased. It might be due to an increase in hydration of the stratum corneum, as the water content in the benzocaine microemulsion is increased, hydration of the stratum corneum will result in a decrease in barrier function. There are no firm theories on the mechanism underlying the enhancement effect, however, one possible theory that the action is mediated by aqueous solvation of the polar regions of glycosphingolipids and ceramides in intercellular lipid of stratum corneum (Walter, 1989).

In biological systems the effect of surfactants is complex, particularly their effect on cell membranes which can lead to alterations in permeability patterns. The common theme of many publications on the biological effects of surfactants is the existence of a concentration-dependent biphasic action such that an enhancement of membrane transport occurs at low concentrations of surfactant, but this decreases at higher concentrations, generally above the critical micelle concentration (CMC) of the surfactant. Increase in membrane transport at low surfactant concentrations is normally attributed to the ability of molecule to penetrate and eventually disrupt the cell membrane structure. Reduction of transport of a permeant in surfactant system is attributed to the ability of the surfactant to form micelle, and is normally only observed if interaction between micelle and permeant occurs. It can be considered, therefore, that the overall effect of the surfactant is the result of two opposing effects-interaction with the membrane and that of the permeant with the micelle.

Ktistis and Niopas (1998) investigated the permeation of propranolol from microemulsions consisted of isopropyl myristate-polysorbate 80-sorbitol-water, it was found that permeation of propranolol was decreased as surfactant concentration in microemulsion increased similar with this study. It might be because of the reduction of the concentration of the monomolecular form of the drug in the continuous phase.

Because the volume fraction of dispersed phase is increased, the amount of benzocaine in all the microemulsions used in the study is the same, the distribution of drug between continuous and disperse phases is instantaneous at any moment and only the monomolecular form of drug in the continuous phase permeates through the skin. Under these conditions an increase in surfactant concentration reduces the concentration of the monomolecular form of the drug in the continuous phase, with a resulting decrease in the rate of diffusion of drug. The other possible mechanism was suggested from Changez and Varshney (2000), who investigated the permeation of tetracaine hydrochloride from isopropyl myristate-aerosol OT-water microemulsions, explained on the basis of random motion of the droplets in microemulsions. The droplets of microemulsions collide each other and are subjected to interactions among themselves. In the case of a benzocaine microemulsion having higher surfactant concentration it could be assumed that the inter-droplet collisions initially are inelastic because of the rigid structure of the interface of droplets, resulted in that benzocaine could not come out from the droplets.

Using microemulsion as transdermal carrier, the important factor to be concerned is the concentration of the composition in microemulsion. The ability of the composition of microemulsion to obtain the maximum delivering of drug should be investigated. The results in this study should be used as a trend to develop the microemulsion formulation used as transdermal carrier for lipophilic drugs. However, delivery of the drugs from microemulsion are dependent on their characteristics such as the partition of the drug among interphase, continuous phase and dispersed phase. Therefore, in order to develop the microemulsion formulation the effect of microemulsion components on delivery ability in individual drug should be investigated.

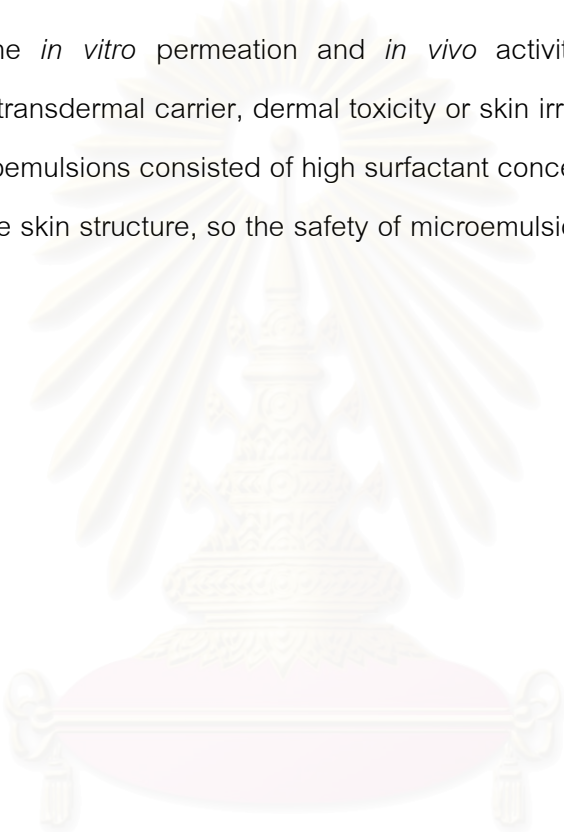
3.2. Correlation between *In Vitro* Permeation and *In Vivo* Activity

The *in vitro* permeation results such as the steady state flux and cumulative amount were consistent with the *in vivo* activity results, both showed the same ranking order. Correlation coefficient test was then applied to confirm the correlation between area of analgesia produce by mouse tail flick test and either the steady state flux or the cumulative amount of benzocaine through shed snake skin. From a statistical point of view, there were significant correlations between the area of analgesia and both the

steady state flux and the cumulative amount ($p < 0.01$) as shown in figures 28 and 29, respectively. The calculations of correlation coefficient tests were provided in appendix VII.

Therefore the *in vitro* parameters such as the steady state flux and the cumulative amount permeated may be used as an indicator in predicting the *in vivo* analgesic activity of benzocaine or to be used in the screening test during development of a formulation, with a consequent reduction of the use of animal.

Besides the *in vitro* permeation and *in vivo* activity data, in order to use microemulsion as transdermal carrier, dermal toxicity or skin irritation data should also be investigated. Microemulsions consisted of high surfactant concentration might induce skin irritation or alter the skin structure, so the safety of microemulsion should be evaluated on the human skin.



สถาบันวิทยบริการ
จุฬาลงกรณ์มหาวิทยาลัย

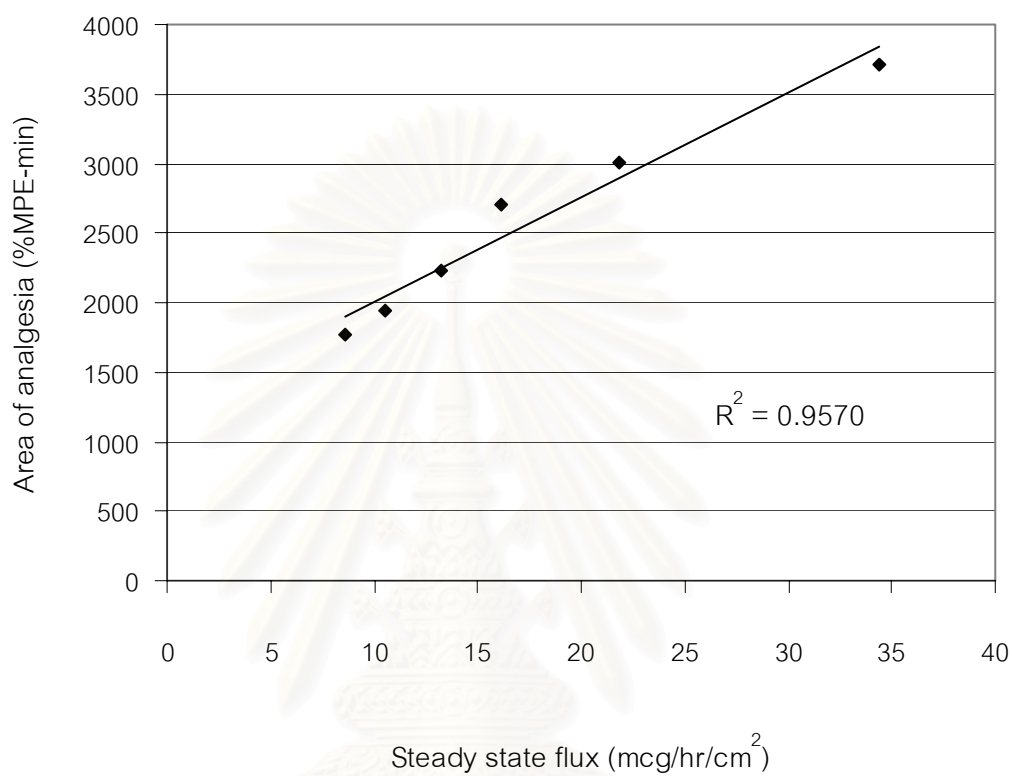


Figure 28 Correlation between the area of analgesia provided by mouse tail flick test and the steady state flux of benzocaine permeated through shed snake skin from microemulsions.

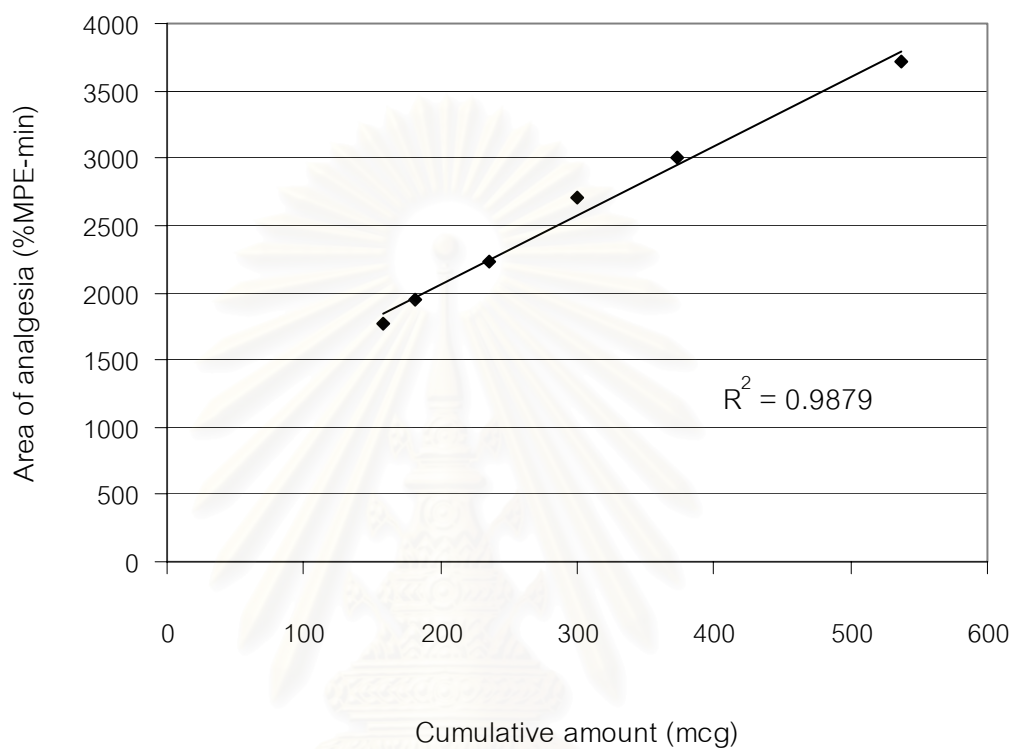


Figure 29 Correlation between the area of analgesia provided by mouse tail flick test and the cumulative amount of benzocaine permeated through shed snake skin from microemulsions.

Chapter V

Conclusion

The results from this experiment can be concluded as follows:

1. Sorbitan stearate (and) methylglucose sesquistearate as surfactant is failed to produce clear area of microemulsion using capric/caprylic triglyceride as oil component either with or without co-surfactant.

2. Capric/caprylic triglyceride, a medium chain triglyceride, as oil component can produce microemulsion area by using either polyoxyethylene sorbitan monooleate or polyoxyethylene (10) oleyl ether as surfactant, with or without co-surfactant.

3. In pseudoternary phase diagram provided by either polyoxyethylene sorbitan monooleate or polyoxyethylene (10) oleyl ether using *n*-butanol as a co-surfactant in the weight ratio of 1:1, the region of microemulsion was increased as compared to without co-surfactant.

4. In pseudoternary phase diagram provided by polyoxyethylene sorbitan monooleate using glycerin as a co-surfactant in the weight ratio of 1:1, the region of microemulsion was lower as compared to without co-surfactant.

5. Microemulsion consisted of capric/caprylic triglyceride–water-polyoxyethylene (10) oleyl ether completely solubilized 7.5 percents by weight benzocaine with isotropic and transparent characteristic of microemulsion.

6. *In vitro* permeation and *in vivo* analgesic activity of benzocaine are significantly increased as water content in microemulsion increased.

7. *In vitro* permeation and *in vivo* analgesic activity of benzocaine are significantly decreased as surfactant concentration in microemulsion increased.

8. Shed cobra (*Naja Naja Khaotia*) skin can served as model membrane in the *in vitro* permeation studies to predict the *in vivo* analgesic activity of benzocaine.

9. *In vitro* permeation results such as the steady state flux and the cumulative amount of benzocaine, using shed cobra skin as a barrier, significantly correlate with *in vivo* activity results, presented in term of area of analgesia provided by mouse tail flick assay.



สถาบันวิทยบริการ
จุฬาลงกรณ์มหาวิทยาลัย

References

- Aboofazeli, R.; Lawrence, C. B.; Wicks, S. R. and Lawrence, M. J. 1994. Investigations into the formation and characterization of phospholipid microemulsions. III. Pseudo-ternary phase diagrams of systems containing water-lecithin-isopropyl myristate and either an alkanolic acid, amine, alkanediol, polyethylene glycol alkyl ether or alcohol as cosurfactant. Int. J. Pharm. 111: 63-72.
- Aboofazeli, R.; Patel, N.; Thomas, M. and Lawrence, M. J. 1995. Investigations into the formation and characterization of phospholipid microemulsions. IV. Pseudo-ternary phase diagrams of systems containing water-lecithin-alcohol and oil; the influence of oil. Int. J. Pharm. 125: 107-116.
- Alany, R. G.; Rades, T.; Agatonovic-Kustrin, S.; Davies, N. M. and Tucker, I. G. 2000. Effects of alcohols and diols on the phase behaviour of quaternary systems. Int. J. Pharm. 196: 141-145.
- Alany, R. G.; Tucker, I. G.; Davies, N. M. and Rades, T. 2001. Characterizing colloidal structures of pseudoternary phase diagrams formed by oil/water/amphiphile systems. Drug Dev. Ind. Pharm. 27(1): 31-38.
- Baroli, B.; Lopez-Quintela, M. A.; Delgado-Charro, M. B.; Fadda, A. M. and Blanco-Mendez, J. 2000. Microemulsions for topical delivery of 8-methoxsalen. J. Control. Rel. 69: 209-218.
- Chaiyakul, P. 1998. Interactive effects of lidocaine and dextromethorphan in animal analgesia models. Doctoral dissertation, Department of Pharmacology, Massachusetts College of Pharmacy and Allied Health Sciences.
- Changez, M. and Varshney, M. 2000. Aerosol-OT microemulsions as transdermal carriers of tetracaine hydrochloride. Drug Dev. Ind. Pharm. 26(5): 507-512.
- Chien, Y. W. 1987. Developmental concepts and practice in transdermal therapeutic systems. In Y. W. Chien (ed.), Transdermal controlled systemic medications, pp. 25-81. New York: Marcel Dekker.

- Gasco, M.R. 1997. Microemulsions in the pharmaceutical field: Perspectives and applications. In C. Solan and H. Kunieda (eds.), Industrial applications of microemulsions, pp. 97-110. New York: Marcel Dekker.
- Haddox, J. D. and Baumann, P. L. 1997. Local anesthetics. In C. R. Craig and E. Stitzel (eds.), Modern pharmacology with clinical applications (5 th ed.), pp. 347-353. New York: Little Brown and Company.
- Ho, H.; Hsiao, C. and Sheu, M. 1996. Preparation of microemulsions using polyglycerol fatty acid esters as surfactant for the delivery of protein drugs. J. Pharm. Sci. 85 (2): 138-143.
- Itoh, T.; Xia, J.; Magavi, R.; Nishihata, T. and Rytting, J. H. 1990. Use of shed snake skin as a model membrane for *in vitro* percutaneous penetration studies: Comparison with human skin. Pharm. Res. 7(10): 1042-1047.
- Kale, N. J. and Allen, Jr. L. V. 1989. Studies on microemulsions using Brij 96 as surfactant and glycerin, ethylene glycol and propylene glycol as cosurfactants. Int. J. Pharm. 57: 87-93.
- Kemken, J.; Ziegler, A. and Muller, B. W. 1992. Influence of supersaturation on the pharmacodynamic effect of bupranolol after dermal administration using microemulsions as vehicle. Pharm. Res. 9(4): 554-558.
- Kolesnikov, Y. A.; Chereshevnev, I. and Pasternak, G. W. 2000. Analgesic synergy between topical lidocaine and topical opioids. J. Pharmacol. Exp. Ther. 295(2): 546-551.
- Kolesnikov, Y. and Pasternak, G. W. 1999. Topical opioids in mice: Analgesia and reversal of tolerance by a topical *N*-methyl-D-aspartate antagonist. J. Pharmacol. Exp. Ther. 290(1): 247-290.
- Ktistis, G. and Niopas, I. 1998. A study on the in-vitro percutaneous absorption of propranolol from disperse systems. J. Pharm. Pharmacol. 50: 413-418.
- Lalor, C. B.; Flynn, G. L. and Weiner, N. 1994. Formulation factors affecting release of drug from topical formulations. 1. Effect of emulsion type upon *in vitro* delivery of ethyl-*p*-aminobenzoate. 1994. J. Pharm. Sci. 83(11): 1525-1528.
- Lawrence, M. J. and Rees, G. D. 2000. Microemulsion-based media as novel drug delivery systems. Adv. Drug Del. Rev. 45: 89-121.

- Linn, E. E.; Pohland, R. C. and Byrd, T. K. 1990. Microemulsion for intradermal delivery of cetyl alcohol and octyl dimethyl PABA. Drug Dev. Ind. Pharm. 16: 899-920.
- Malcolmson, C.; Satra, C.; Kantaria, S.; Sidhu, A. and Lawrence, M. J. 1998. Effect of oil on the level of solubilization of testosterone propionate into nonionic oil-in-water microemulsions. J. Pharm. Sci. 87(1): 109-116.
- Martin, A.; Bustamante, P. and Chun, A. H. C. 1993. Diffusion and dissolution. In Physical pharmacy: Physical chemical principles in the pharmaceutical sciences, pp. 324-328. London: Lea&Febiger.
- Neubert, R. H. H. and Schmalfub, U. 1999. Microemulsions. In R. L. Bronaugh and H. I. Maibach (eds.), Percutaneous Absorption: Drugs-cosmetics-mechanisms-methodology (3 rd ed. revised and expanded), pp. 879-886. New York: Marcel Dekker.
- Osborn, D. W.; Ward, A. J. I. and O'Neill, K. J. 1991. Microemulsions as topical drug delivery vehicles: in-vitro transdermal studies of a model hydrophilic drug. J. Pharm. Pharmacol. 43: 451-454.
- Pongjanyakul, T.; Prakongpan, S. and Priprem, A. 2000. Permeation studies comparing cobra skin with human skin using nicotine transdermal patches. Drug Dev. Ind. Pharm. 26(6): 635-642.
- Renolds, J. E. F., ed. 1989. Martindale: The extra pharmacopoeia (29 th ed.). London: The Pharmaceutical Press.
- Solans, C.; Pons, R. and Kunieda, H. 1997. Overview of basic aspects of microemulsions. In C. Solan and H. Kunieda (eds.), Industrial applications of microemulsions, pp. 1-16. New York: Marcel Dekker.
- Trotta, M.; Pattarino, F. and Grosa, G. 1998. Formation of lecithin-based microemulsions containing *n*-alkanol phosphocholines. Int. J. Pharm. 174: 253-259.
- United States Pharmacopeial Convention. 2000. USP 24: NF 19 (U.S. Pharmacopeia & National Formulary). Philadelphia: National Publishing.
- Vogel, H. G. and Volgel, W. H., eds. 1997. Drug discovery and evaluation: Pharmacological assays. Germany: Springer-Verlag Berlin Heidelberg.

Walters, K. A. 1989. Penetration enhancers and their use in transdermal therapeutic systems. In J. Hadgraft and R.H. Guy (eds.), Transdermal drug delivery: Development issues and research initiatives, pp. 197-233. New York: Marcel Dekker.

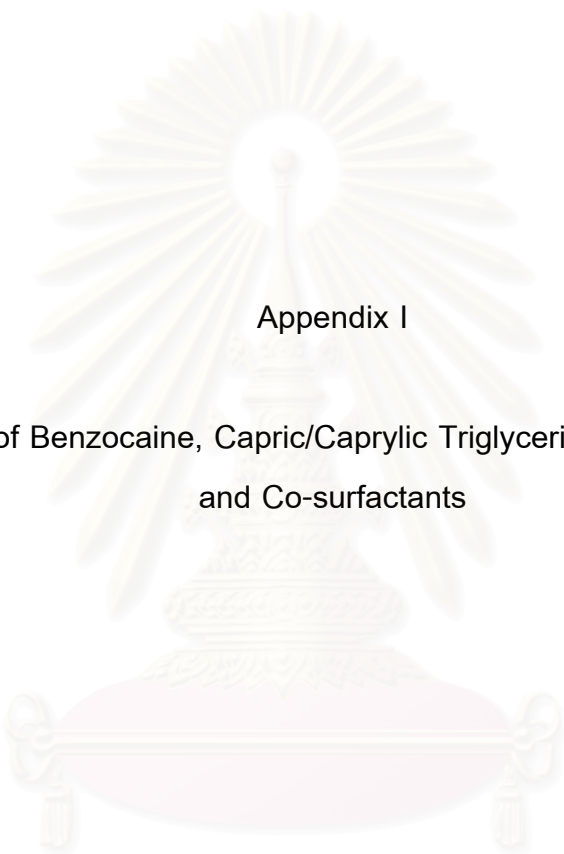


สถาบันวิทยบริการ
จุฬาลงกรณ์มหาวิทยาลัย



APPENDICES

สถาบันวิทยบริการ
จุฬาลงกรณ์มหาวิทยาลัย



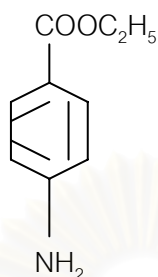
Appendix I

Details of Benzocaine, Capric/Caprylic Triglyceride, Surfactants
and Co-surfactants

สถาบันวิทยบริการ
จุฬาลงกรณ์มหาวิทยาลัย

Benzocaine

Formular



Molecular Formular $C_9H_{11}NO_2$

Molecular Weight 165.19

Appearance

White or colorless crystals or crystalline powder with a bitter taste, followed by local anesthesia of the tongue, almost odourless.

Melting Range

Benzocaine melting range is between $88-92^{\circ}C$, but the range between beginning and end of melting does not exceed 2°

Solubility

Solubility of benzocaine in various solvents at $20^{\circ}C$ as one part per specified parts-solvent are shown table 8.

Table 8 Solubility of benzocaine at $20^{\circ}C$

Solvent	Solubility(parts)
Water	2500
Alcohol	5
Chloroform	2
Ether	4
Almond oil or olive oil	30-50
Mineral acids	Soluble under salt formation

Dissociation Constant

Acid dissociation constant of benzocaine has been given as pKa 2.5. Estimation of microequilibrium constant of ethyl p-aminobenzoate was done spectrophotometrically and a K value of 4.17×10^{-3} was obtained.

Spectrophotometric method applied for estimating microequilibrium constants is simpler, faster and more accurate than the conventional method employing the dissociation constant of an alkylated derivative.

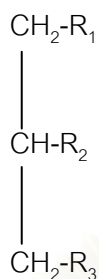
Degradation and Stability

Ester hydrolysis of benzocaine in aqueous media is well known. Attempts have been made to decrease its degradation through the use of complexing agents and surfactants. Stability characteristics of benzocaine, including the effects of pH and ions have been investigated. Benzocaine degradation is both acid and base catalyzed but is much slower in the presence of phosphate ion. Extrapolation of the elevated temperature data to room temperature resulted in a predicted first-order rate constant of 0.0057 hr^{-1} , which compares favorably with the rate constant of 0.0051 hr^{-1} observed at room temperature. p-Aminobenzoic acid was found to be the only decomposition product. Essentially all the benzocaine lost due to degradation was accounted for by the appearance of p-aminobenzoic acid.

สถาบันวิทยบริการ
จุฬาลงกรณ์มหาวิทยาลัย

Capric/Caprylic Triglyceride

Formula



$\text{R}_1, \text{R}_2, \text{R}_3 = \text{CH}_3(\text{CH}_2)_8\text{COO}$ for Capric

$= \text{CH}_3(\text{CH}_2)_6\text{COO}$ for Caprylic

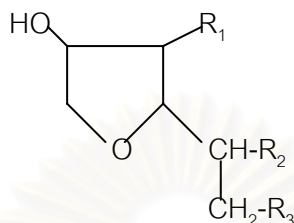
Appearance	Liquid at 25°C
Cloud Point	<-5°C
Viscosity	24-30 mPas at 20°C
Saponification Value	335-350
Acid Value	0.1
Iodine Value	0.5

สถาบันวิทยบริการ
จุฬาลงกรณ์มหาวิทยาลัย

Surfactants

1. Sorbitan Stearate (and) Methylglucose Sesquistearate

Formula



$R_1 = C_8O_5H_{13}$ for Methylglucose

$R_2 = C_{17}H_{35}COO$ for Stearate

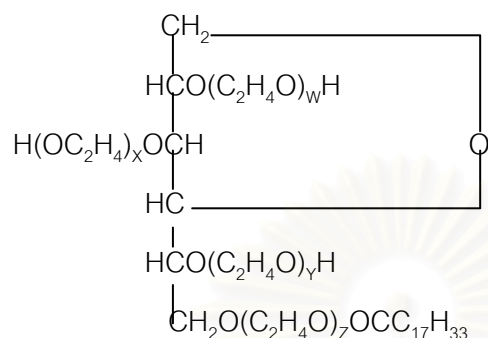
$R_3 = C_{33}H_{63}O_{6.5}$ for Sesquistearate

Origin	Vegetable
Appearance	Pellets at 25° C
Viscosity	Approximately 300 mPas at 60° C
Saponification Value	135-149
Acid Value	Maximum 18
Water Content	Maximum 1.5%
HLB-Value	Approximately 6
Biological Degradability	Approximately 97%

สถาบันวิทยบริการ
จุฬาลงกรณ์มหาวิทยาลัย

2. Polyoxyethylene Sorbitan Monooleate

Formula



$$W+X+Y+Z = 20$$

Molecular Formula	$\text{C}_{64}\text{H}_{125}\text{O}_{26}$
Molecular Weight	1309
Appearance	Yellow oily liquid at 25° C
Viscosity	425 mPas
Saponification Value	45-55
Acid Value	2.0
Water Content	3.0%
Iodine Value	18-24
HLB Value	15
Stability	

Polysorbates are stable to electrolytes as well as to weak acids and bases. There is gradual saponification by strong acids and bases. The oleic acid esters are sensitive to oxidation.

Incompatibility

Discoloration and/or precipitation occurs with various substances, especially with phenols, tannins, tars and/or tar-like compounds.

Safety

Polysorbates are tolerated, practically non-irritating and of very low toxicity.

3. Polyoxyethylene (10) oleyl ether

Formula



Appearance Pale yellow liquid with some solids at 25° C

Viscosity Approximately 100 mPas at 25° C

Saponification Value 75-95

Acid Value Maximum 1.0

Water Content Maximum 3.0%

HLB Value 12.4

Stability

Stable in strongly acidic or alkaline conditions. The surfactants can undergo autooxidation on storage, resulting in the formation of peroxides and a continual increase in acidity.

Solubility

Solubility of polyoxyethylene (10) oleyl ether in various solvents are shown in table 9

Table 9 Solubility of polyoxyethylene (10) oleyl ether

Ethanol	Soluble
Water	Soluble
Cottonseed oil	Insoluble
Mineral oil	Insoluble
Propylene glycol	Insoluble

Co-surfactant

1. *n*-Butanol

Formula



Molecular Formula

C₄H₁₀O

Molecular Weight

74.12

Appearance

Clear, colorless with a characteristic odor

Boiling Point

Approximately 118° C

Soluble

In water; miscible with alcohol, ether and many other organic solvents.

Adverse Effect

Butyl alcohol may cause irritation of the eyes, skin and mucous membranes and mild CNS depression with headache, dizziness and drowsiness.

In Great Britain the recommended exposure limit if butyl alcohol is 50 ppm; suitable precautions should be taken to prevent absorption through the skin

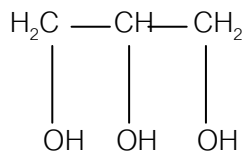
Uses and Administration

Butyl alcohol is used as an industrial and pharmaceutical solvent.

สถาบันวิทยบริการ
จุฬาลงกรณ์มหาวิทยาลัย

2. Glycerin

Formula



Molecular Formula

$\text{C}_3\text{H}_8\text{O}_3$

Molecular Weight

92.09

Appearance

A clear, colorless, odorless, syrupy and hygroscopic liquid

Melting Point

17.9° C

Hygroscopicity

Medium-high

Viscosity

1490 mPas at 20° C; 954 mPas at 25° C

Solubility

Miscible with water, alcohol and methanol. One part of glycerin dissolves in 11 parts of ethyl acetate and in about 500 parts of ethyl ether. Insoluble in benzene, chloroform ether, mineral oil, fixed and volatile oils, halogenated hydrocarbons and aromatic hydrocarbons.

Stability

Pure glycerin decomposes on heating, with the evolution of toxic acrolein.

Mixtures of glycerin with water, ethyl alcohol and propylene glycol are chemically stable.

Incompatibility

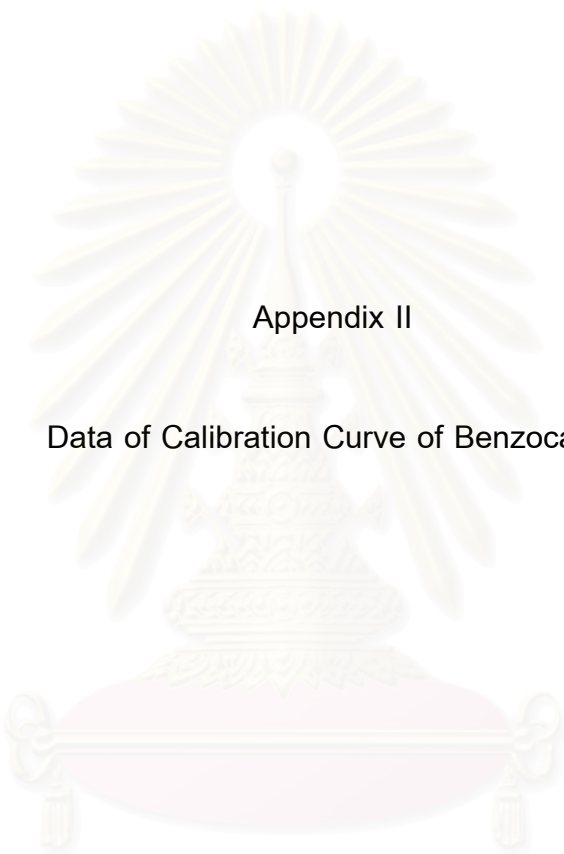
An explosion may occur if glycerin is triturated with strong oxidizing agents, such as chromium trioxide, potassium chlorate and potassium permanganate. In dilute solution, the reaction proceeds at a slower rate, with several oxidation products forming. Black coloration occurs in contact with zinc oxide and basic bismuth nitrate in the presence of light. An iron contaminant in glycerin is responsible for the darkening of the color in mixtures containing phenols, salicylates, tannin, etc. Glycerin forms a complex with boric acid as glyceroboric acid, which is a stronger acid than boric acid.

Safety

Very large oral doses can exert systemic effects, such as headache, thirst and nausea. Injection of large doses may induce convulsions, paralysis and hemolysis. Oral LD₅₀ (mice) = 31.5 g/kg; IV (mice) = 7.45 g/kg.



สถาบันวิทยบริการ
จุฬาลงกรณ์มหาวิทยาลัย



Appendix II

Data of Calibration Curve of Benzocaine

สถาบันวิทยบริการ
จุฬาลงกรณ์มหาวิทยาลัย

Table 10 Data of calibration curve of benzocaine, detecting by UV/vis spectrophotometer at 286 nm

Conc (mcg/ml)	Abs ₁	Abs ₂	Abs ₃	Ave.
2.0	0.194	0.194	0.192	0.193
3.0	0.285	0.286	0.284	0.285
4.0	0.385	0.381	0.381	0.382
5.0	0.473	0.476	0.476	0.475
6.0	0.563	0.565	0.564	0.564
7.0	0.655	0.650	0.650	0.652

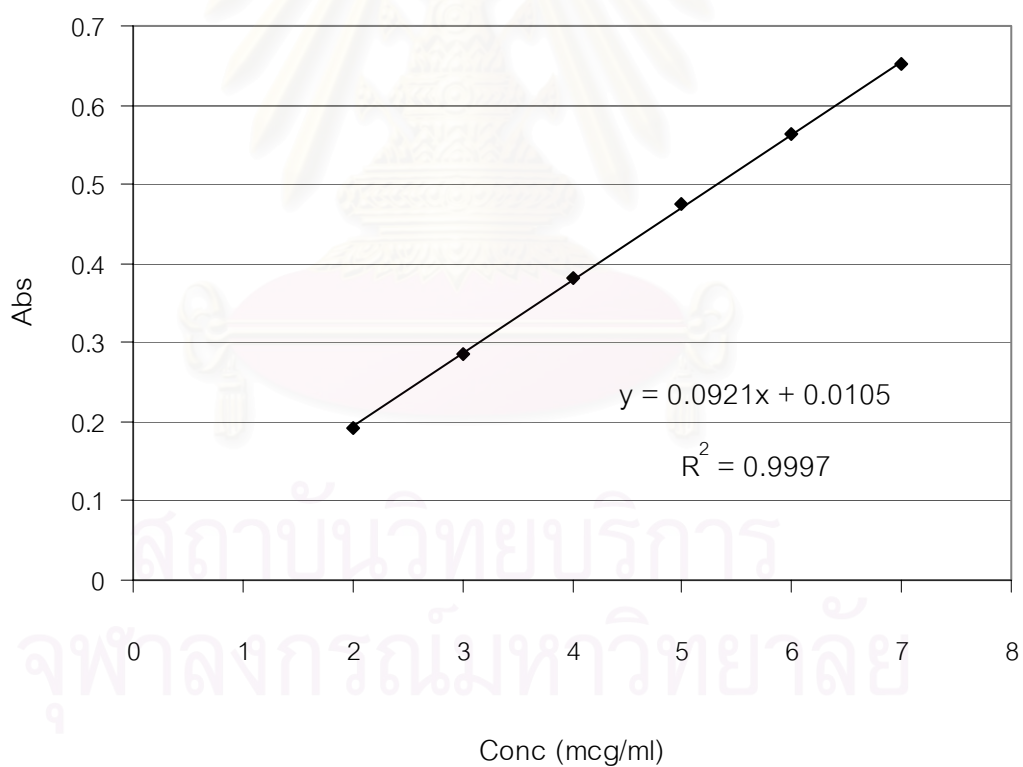


Figure 30 Calibration curve of benzocaine in phosphate buffer pH 7.4 with 30% methanol solution.

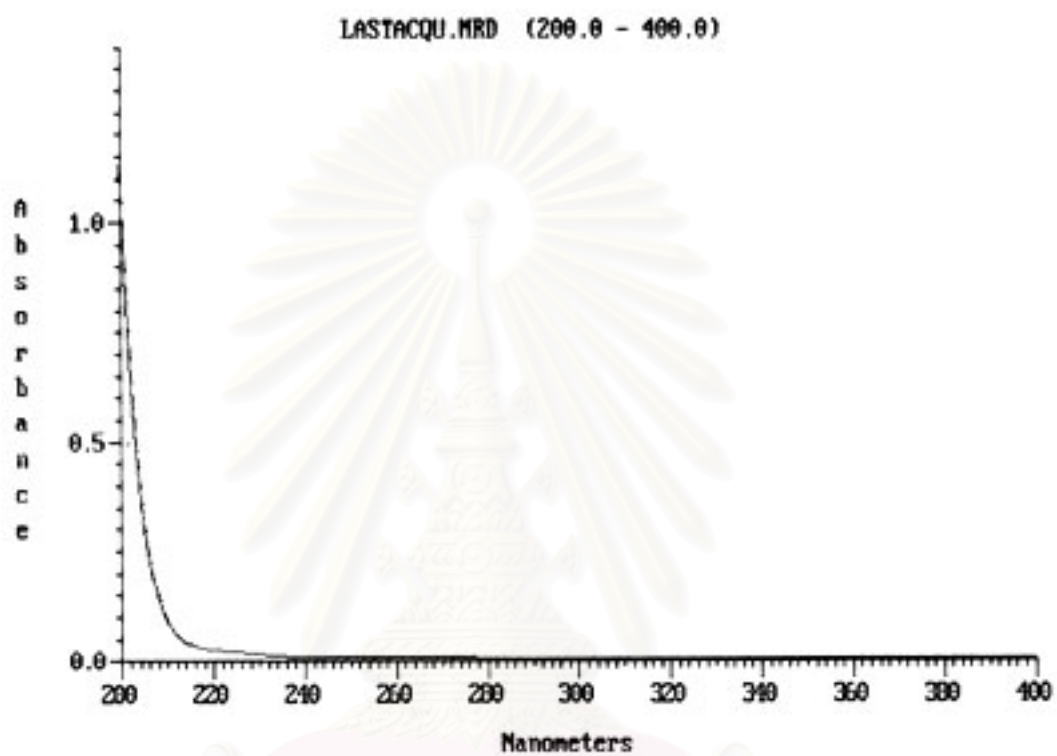


Figure 31 UV spectrum of phosphate buffer pH 7.4 with 30% methanol solution.

สถาบันวิทยบริการ
จุฬาลงกรณ์มหาวิทยาลัย

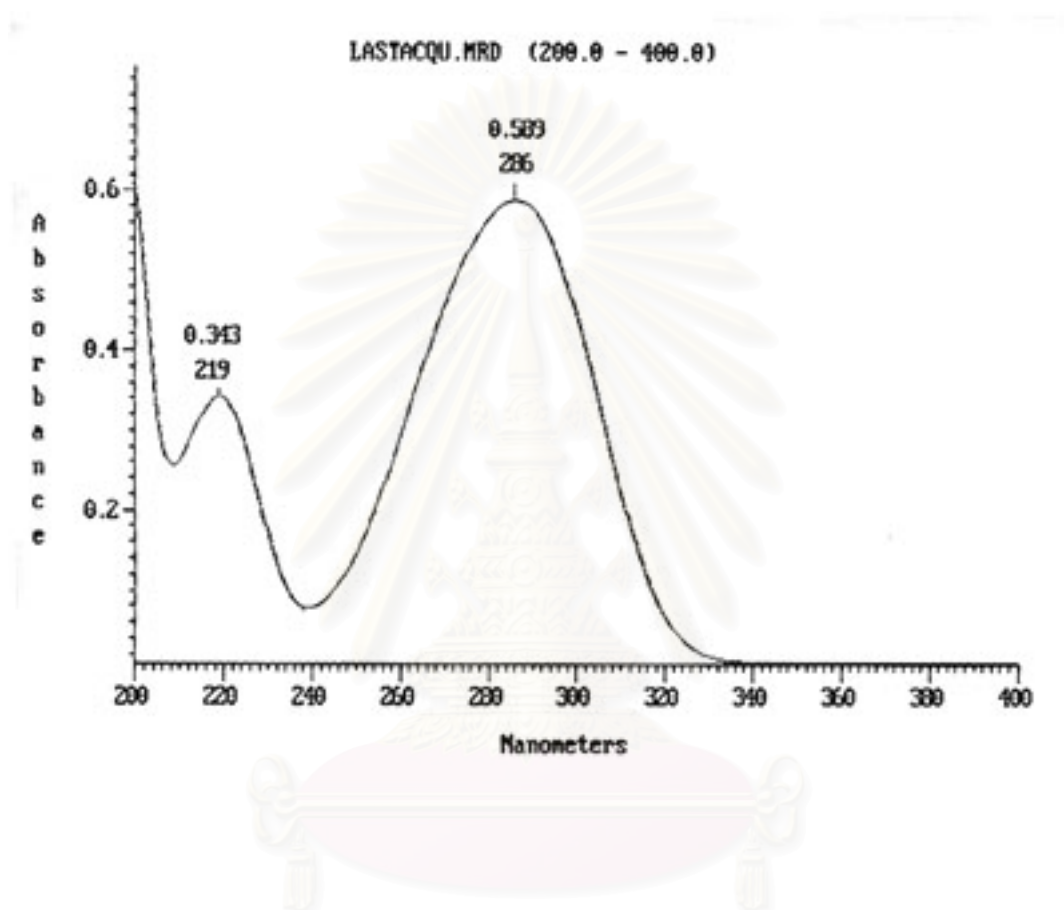


Figure 32 UV spectrum of benzocaine in phosphate buffer pH 7.4 with 30% methanol solution.

สถาบันวิทยบริการ
จุฬาลงกรณ์มหาวิทยาลัย

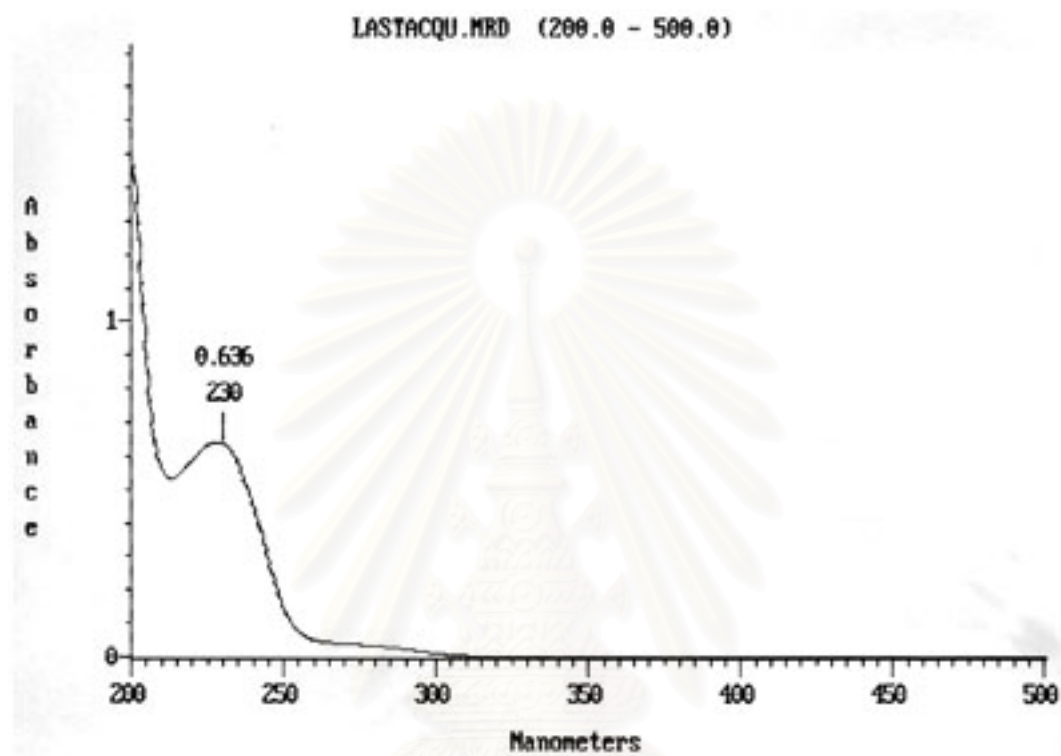


Figure 33 UV spectrum of microemulsion base in phosphate buffer pH 7.4 with 30% methanol solution.

สถาบันวิทยบริการ
จุฬาลงกรณ์มหาวิทยาลัย

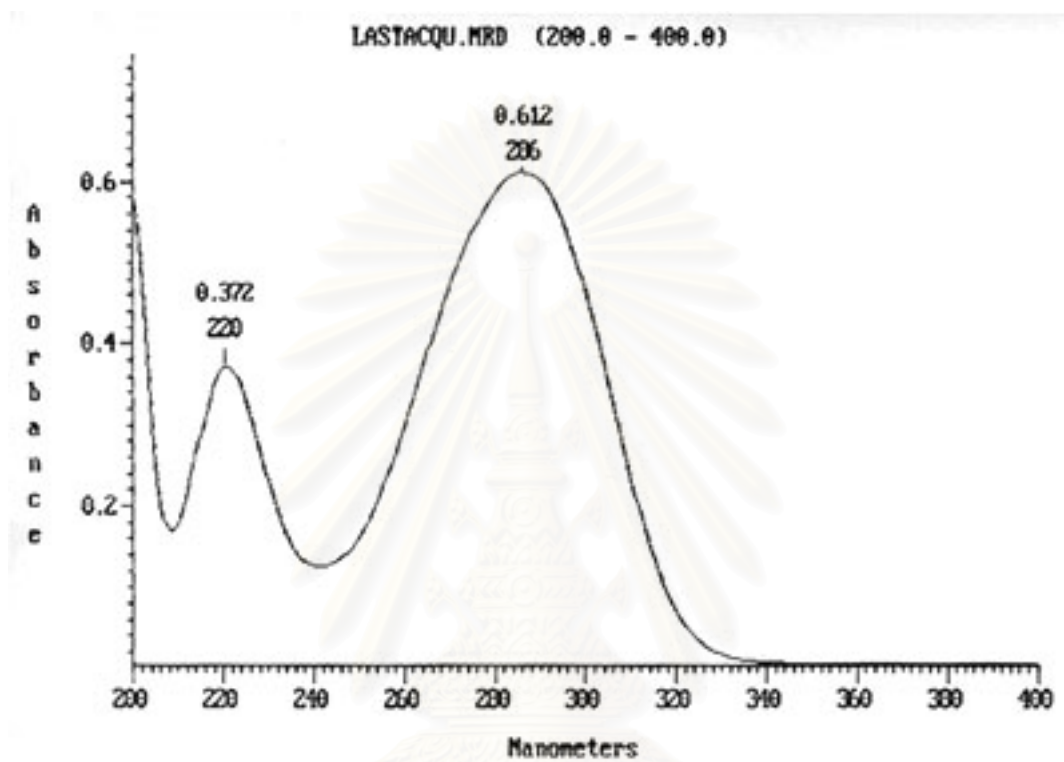
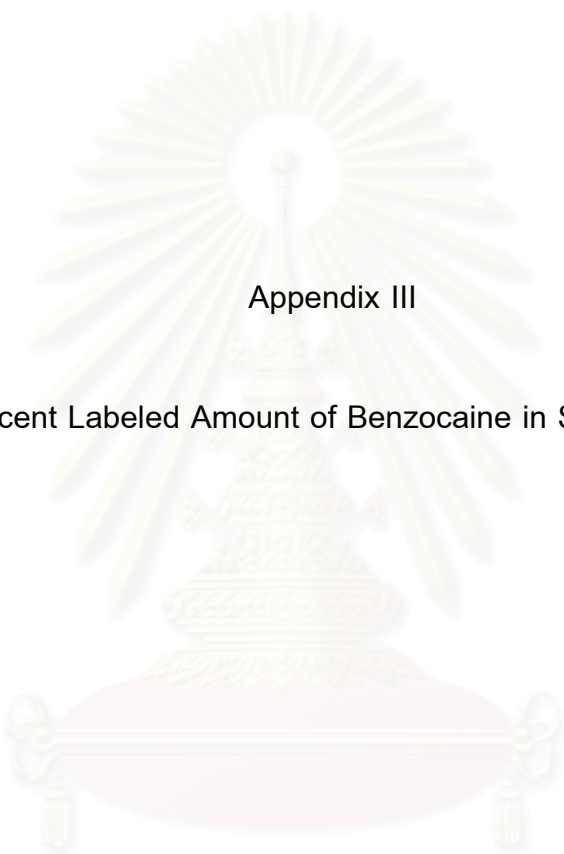


Figure 34 UV spectrum of benzocaine microemulsion in phosphate buffer pH 7.4 with 30% methanol solution.

สถาบันวิทยบริการ
จุฬาลงกรณ์มหาวิทยาลัย



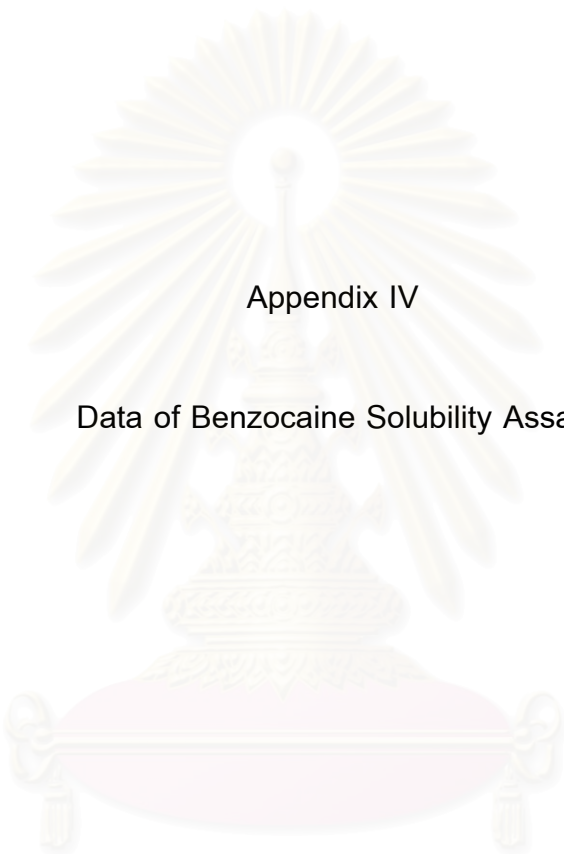
Appendix III

Data of Percent Labeled Amount of Benzocaine in Six Microemulsions

สถาบันวิทยบริการ
จุฬาลงกรณ์มหาวิทยาลัย

Table 11 Data of percent labeled amount of benzocaine in microemulsions, detecting by UV/vis spectrophotometer at 286 nm

Sample	Sample Weight(gm)	Conc from Weight (mg/ml)	Abs	Conc from Assay(mg/ml)	% LA	Ave
A ₁	0.101	7.575	0.691	7.389	97.54	98.14
A ₂	0.103	7.725	0.713	7.628	98.74	
B ₁	0.100	7.500	0.686	7.334	97.79	96.86
B ₂	0.103	7.725	0.693	7.410	95.92	
C ₁	0.098	7.350	0.672	7.182	97.71	96.12
C ₂	0.101	7.575	0.670	7.161	94.53	
D ₁	0.102	7.650	0.686	7.334	95.87	97.30
D ₂	0.102	7.650	0.706	7.552	98.72	
E ₁	0.100	7.500	0.662	7.074	94.32	95.10
E ₂	0.102	7.650	0.686	7.334	95.87	
F ₁	0.103	7.725	0.712	7.617	98.60	97.38
F ₂	0.099	7.425	0.668	7.139	96.15	



Appendix IV

Data of Benzocaine Solubility Assay

สถาบันวิทยบริการ
จุฬาลงกรณ์มหาวิทยาลัย

Table 12 Data of benzocaine solubility in phosphate buffer pH 7.4, detecting by UV/vis spectrophotometer at 286 nm

Sample	Abs [*]	Conc (mcg/ml)
1	0.291	1015.20
2	0.293	1022.44
3	0.294	1026.06
Ave	0.293	1021.23

* dilution factor = 333.33, SD = 5.53

สถาบันวิทยบริการ
จุฬาลงกรณ์มหาวิทยาลัย



Appendix V

Data of the Permeation of Benzocaine Microemulsions Through Shed Snake
Skin

สถาบันวิทยบริการ
จุฬาลงกรณ์มหาวิทยาลัย

Table 13 Permeation data of benzocaine through shed snake skin from microemulsion formula A (surfactant: water: oil; 60: 15: 25 by weight)

Permeation Run Data

Permeation Run	Run I	Run II	Run III
Time (hr)	Cumulative Amount (mcg)	Cumulative Amount (mcg)	Cumulative Amount (mcg)
1.0	51.48	47.24	48.64
2.0	94.80	88.09	96.37
3.0	131.65	118.49	131.81
4.0	162.66	154.82	163.62
5.0	201.49	190.84	202.37
6.0	234.24	222.69	238.49
7.0	268.84	257.29	270.43
8.0	303.58	291.64	305.39
(3.0-8.0 hr) Steady-State Slope (mcg/hr)	34.39	34.63	34.72
S (cm ²)	2.09	2.17	2.19
Jss (mcg/hr/cm ²)	16.45	15.96	15.85
r ²	0.9998	0.9998	0.9997

$$\text{Average flux (Jss)} = 16.09 \pm 0.32$$

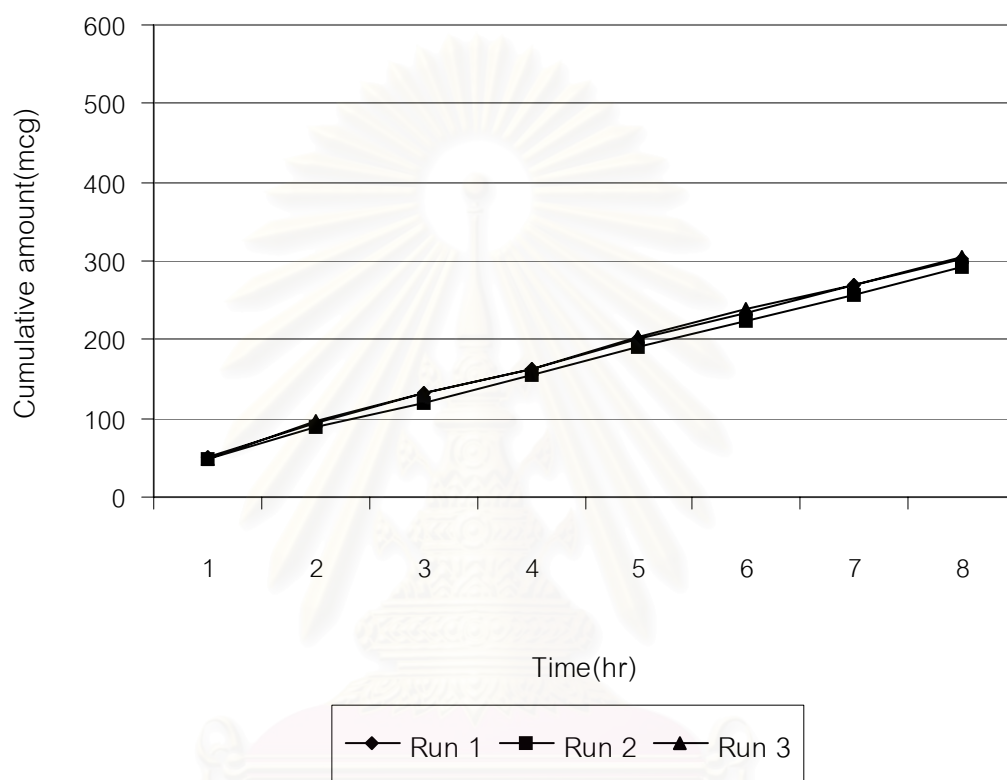


Figure 35 Permeation profile of benzocaine through shed snake skin from microemulsion formula A.

Table 14 Permeation data of benzocaine through shed snake skin from microemulsion formula B (surfactant: water: oil; 60: 10: 30 by weight)

Permeation Run Data

Permeation Run	Run I	Run II	Run III
Time (hr)	Cumulative Amount (mcg)	Cumulative Amount (mcg)	Cumulative Amount (mcg)
1.0	30.15	29.54	29.24
2.0	58.76	78.25	62.50
3.0	87.74	98.95	91.86
4.0	121.11	121.36	120.38
5.0	151.90	149.20	148.01
6.0	174.10	174.40	172.74
7.0	202.68	203.10	200.81
8.0	238.63	233.13	234.55
(3.0-8.0 hr) Steady-State Slope (mcg/hr)	30.18	26.84	28.54
S (cm ²)	2.09	2.17	2.19
Jss (mcg/hr/cm ²)	14.44	12.37	13.03
r ²	0.9981	0.9991	0.9991

$$\text{Average flux (Jss)} = 13.28 \pm 1.06$$

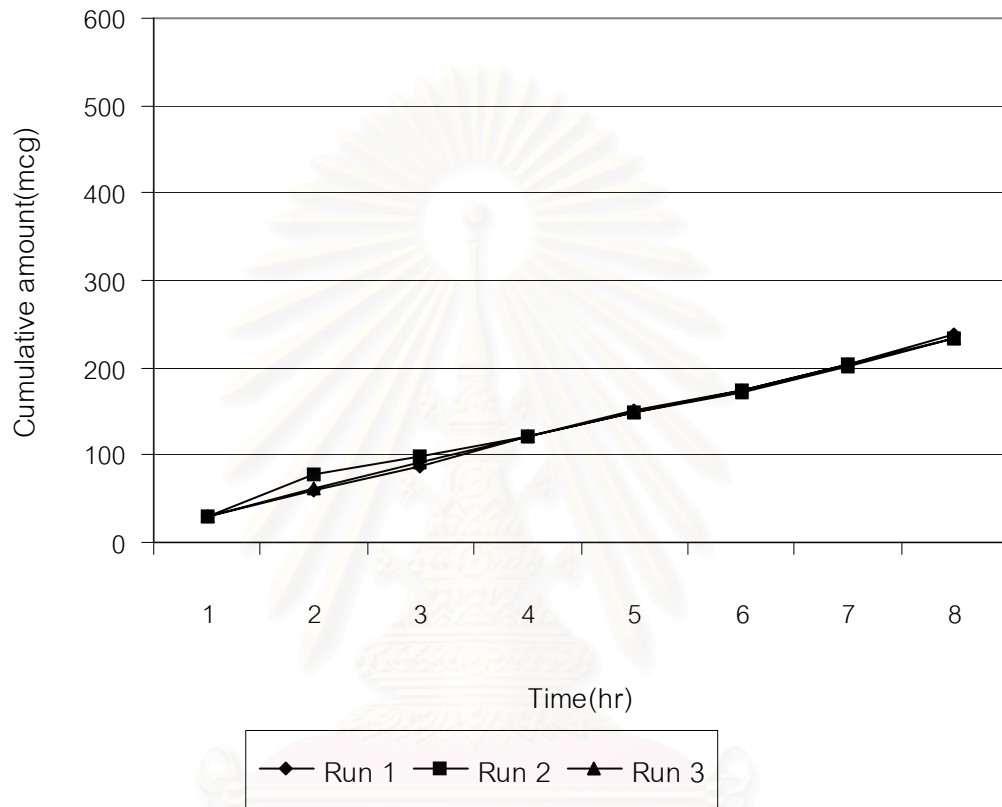


Figure 36 Permeation profile of benzocaine through shed snake skin from microemulsion formula B

สถาบันวิทยบริการ
จุฬาลงกรณ์มหาวิทยาลัย

Table 15 Permeation data of benzocaine through shed snake skin from microemulsion formula C (surfactant: water: oil; 60: 5: 35 by weight)

Permeation Run Data

Permeation Run	Run I	Run II	Run III
Time (hr)	Cumulative Amount (mcg)	Cumulative Amount (mcg)	Cumulative Amount (mcg)
1.0	31.69	31.37	30.15
2.0	47.96	49.88	48.45
3.0	65.00	72.14	67.78
4.0	88.75	99.30	92.65
5.0	109.74	121.01	114.10
6.0	130.50	143.79	137.10
7.0	152.50	163.37	156.22
8.0	176.36	187.17	181.18
(3.0-8.0 hr) Steady-State Slope (mcg/hr)	22.27	23.01	22.68
S (cm ²)	2.09	2.17	2.19
Jss (mcg/hr/cm ²)	10.66	10.60	10.36
r ²	0.9997	0.9991	0.9995

$$\text{Average flux (Jss)} = 10.54 \pm 0.16$$

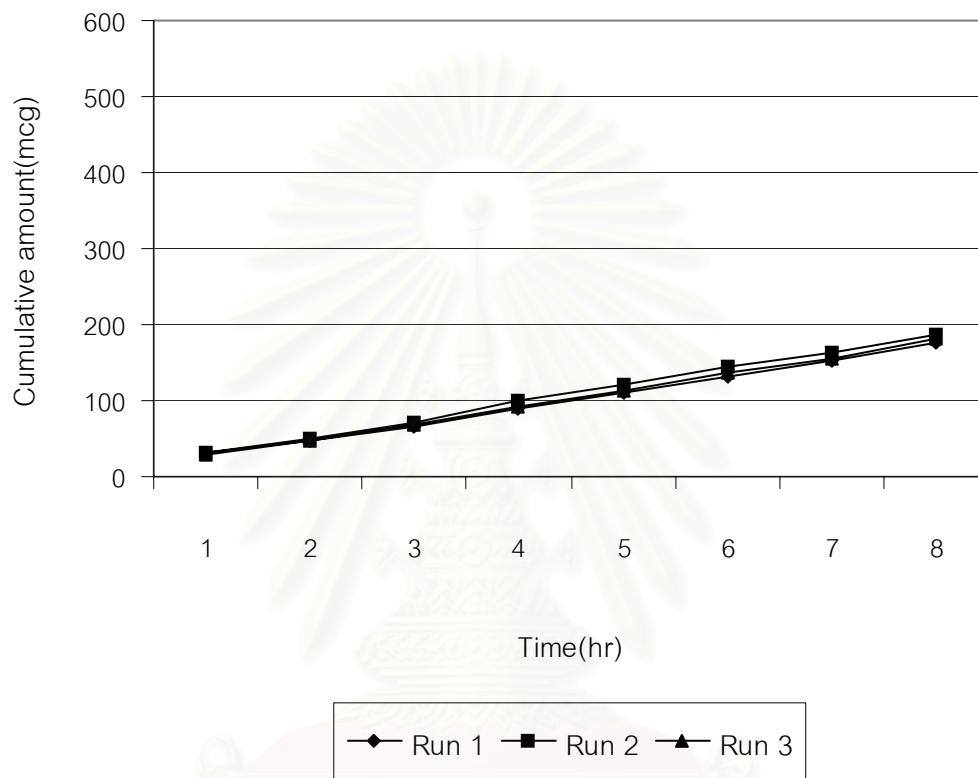


Figure 37 Permeation profile of benzocaine through shed snake skin from microemulsion formula C.

สถาบันวิทยบริการ
จุฬาลงกรณ์มหาวิทยาลัย

Table 16 Permeation data of benzocaine through shed snake skin from microemulsion formula D (surfactant: water: oil; 40: 10: 50 by weight)

Permeation Run Data

Permeation Run	Run I	Run II	Run III
Time (hr)	Cumulative Amount (mcg)	Cumulative Amount (mcg)	Cumulative Amount (mcg)
1.0	50.56	46.04	47.12
2.0	109.75	103.12	103.62
3.0	178.25	162.64	162.81
4.0	241.63	230.99	230.10
5.0	314.32	299.24	298.76
6.0	392.21	373.91	372.44
7.0	468.35	448.62	448.63
8.0	545.55	531.84	535.27
(3.0-8.0 hr) Steady-State Slope (mcg/hr)	73.46	73.84	74.49
S (cm ²)	2.09	2.17	2.19
Jss (mcg/hr/cm ²)	35.15	34.03	34.01
r ²	0.9995	0.9993	0.9990

$$\text{Average flux (Jss)} = 34.40 \pm 0.65$$

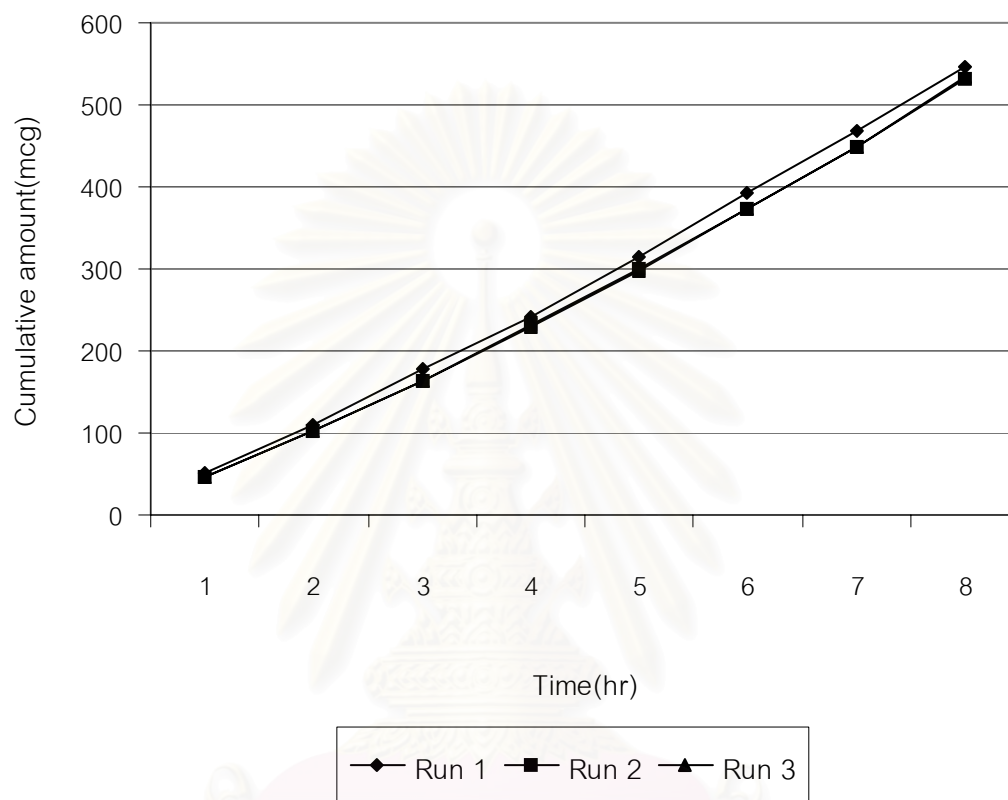


Figure 38 Permeation profile of benzocaine through shed snake skin from microemulsion formula D.

สถาบันวิทยบริการ
จุฬาลงกรณ์มหาวิทยาลัย

Table 17 Permeation data of benzocaine through shed snake skin from microemulsion formula E (surfactant: water: oil; 50: 10: 40 by weight)

Permeation Run Data

Permeation Run	Run I	Run II	Run III
Time (hr)	Cumulative Amount (mcg)	Cumulative Amount (mcg)	Cumulative Amount (mcg)
1.0	40.66	45.74	44.09
2.0	79.53	82.96	80.85
3.0	143.34	136.92	137.40
4.0	188.37	183.55	183.12
5.0	230.46	224.57	225.89
6.0	276.15	267.89	267.71
7.0	329.65	320.65	322.90
8.0	378.41	371.76	371.42
(3.0-8.0 hr) Steady-State Slope (mcg/hr)	47.01	46.97	46.81
S (cm ²)	2.09	2.17	2.19
Jss (mcg/hr/cm ²)	22.49	21.64	21.37
r ²	0.9992	0.9989	0.9990

$$\text{Average flux (Jss)} = 21.83 \pm 0.58$$

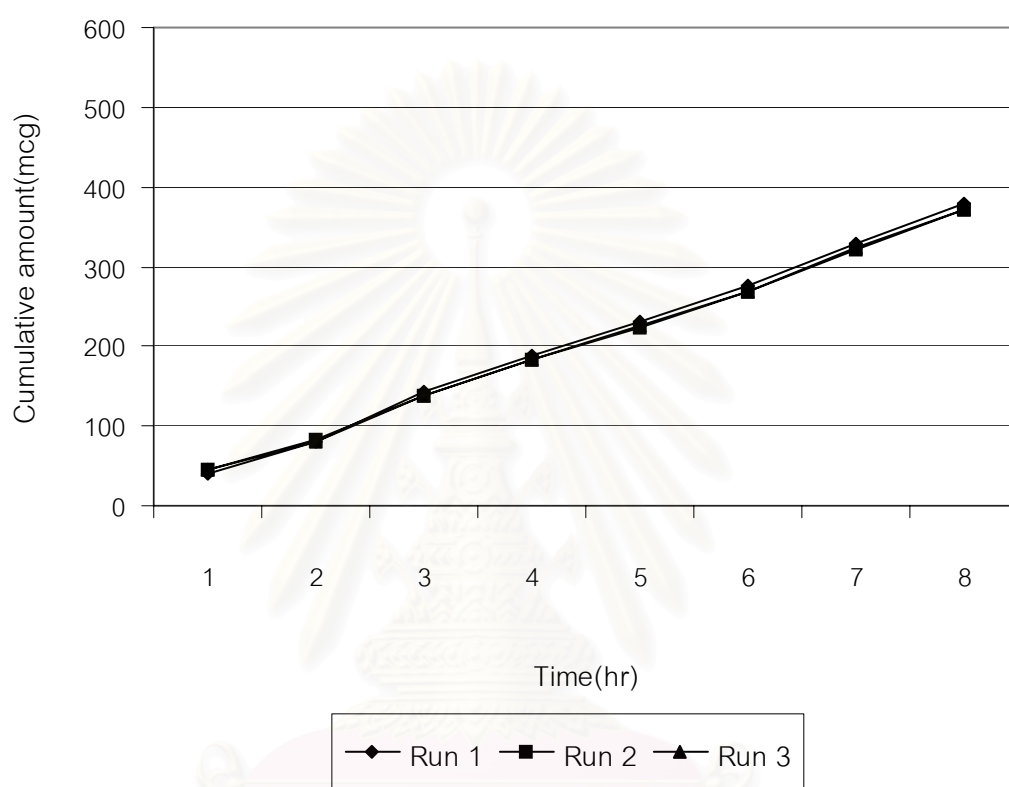


Figure 39 Permeation profile of benzocaine through shed snake skin from microemulsion formula E.

สถาบันวิทยบริการ
จุฬาลงกรณ์มหาวิทยาลัย

Table 18 Permeation data of benzocaine through shed snake skin from microemulsion formula F (surfactant: water: oil; 70: 10: 20 by weight)

Permeation Run Data

Permeation Run	Run I	Run II	Run III
Time (hr)	Cumulative Amount (mcg)	Cumulative Amount (mcg)	Cumulative Amount (mcg)
1.0	41.90	34.37	38.64
2.0	53.82	48.73	49.37
3.0	68.86	63.39	65.47
4.0	87.24	78.69	80.71
5.0	107.87	99.00	102.44
6.0	127.17	115.56	119.43
7.0	146.33	135.24	139.55
8.0	160.47	157.35	158.48
(3.0-8.0 hr) Steady-State Slope (mcg/hr)	18.32	18.79	18.60
S (cm ²)	2.09	2.17	2.19
J _{ss} (mcg/hr/cm ²)	8.77	8.66	8.49
r ²	0.9988	0.9986	0.9993

$$\text{Average flux (J}_{ss}) = 8.64 \pm 0.14$$

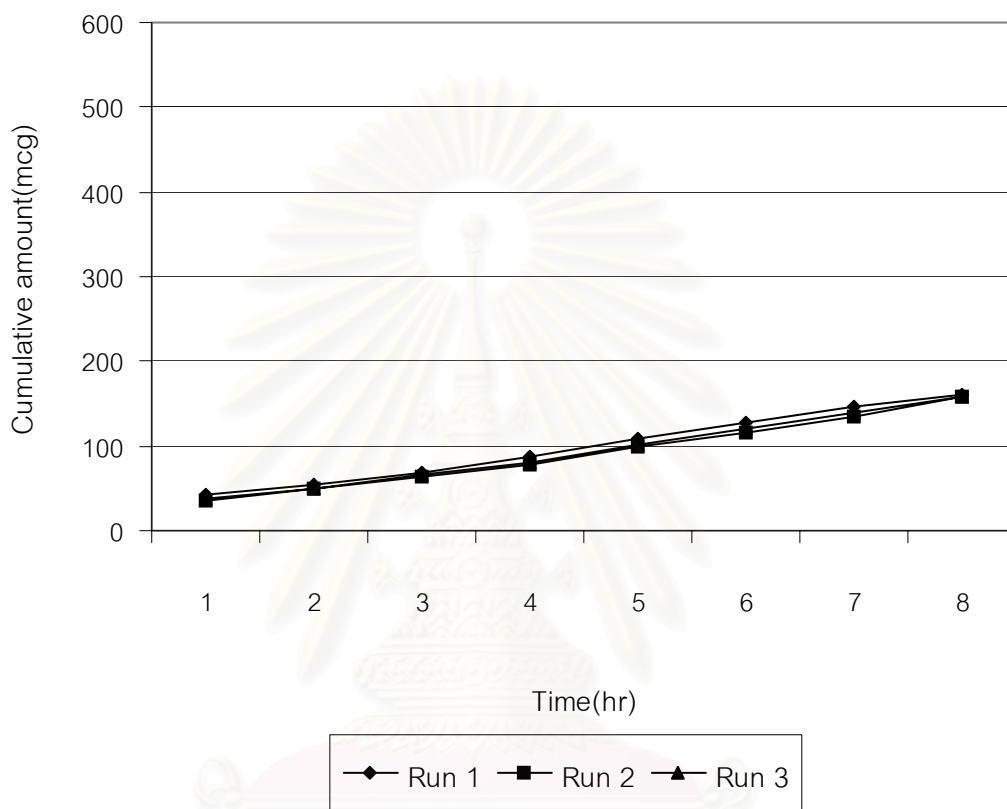
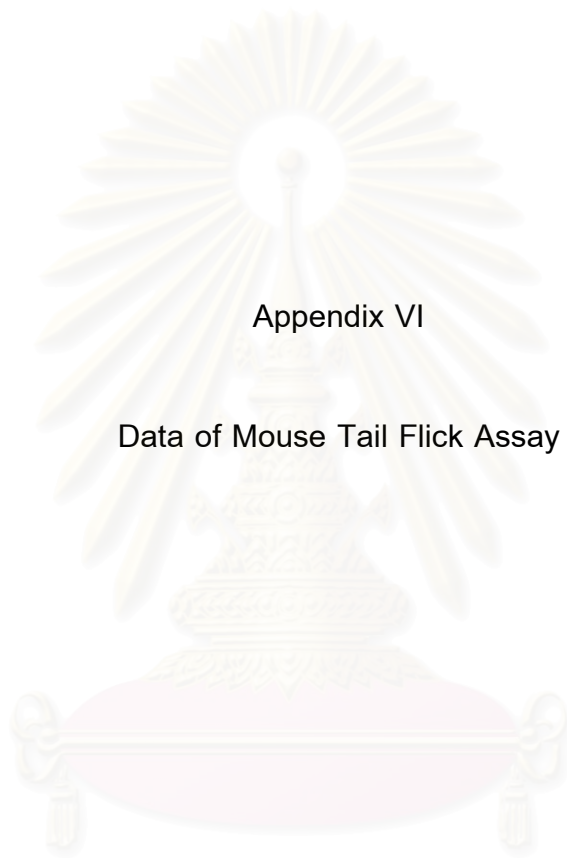


Figure 40 Permeation profile of benzocaine through shed snake skin from microemulsion formula F.

สถาบันวิทยบริการ
จุฬาลงกรณ์มหาวิทยาลัย



Appendix VI

Data of Mouse Tail Flick Assay

สถาบันวิทยบริการ
จุฬาลงกรณ์มหาวิทยาลัย

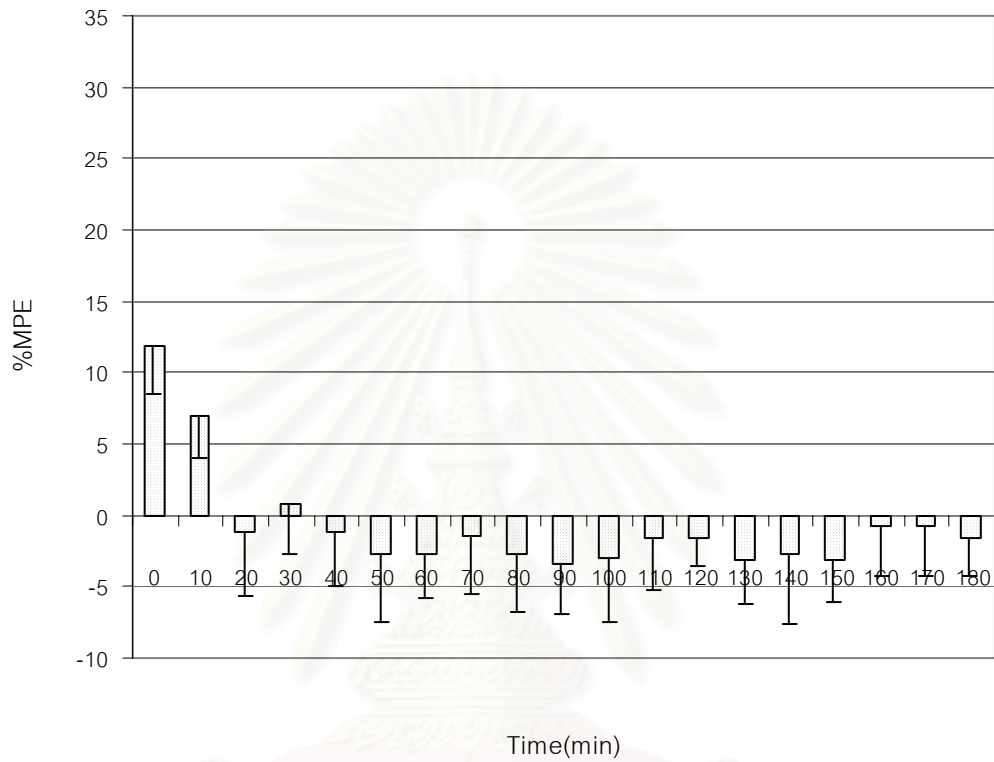


Figure 41 Profile of the analgesic responses provided by microemulsion base formula A. (n = 10)

สถาบันวิทยบริการ
จุฬาลงกรณ์มหาวิทยาลัย

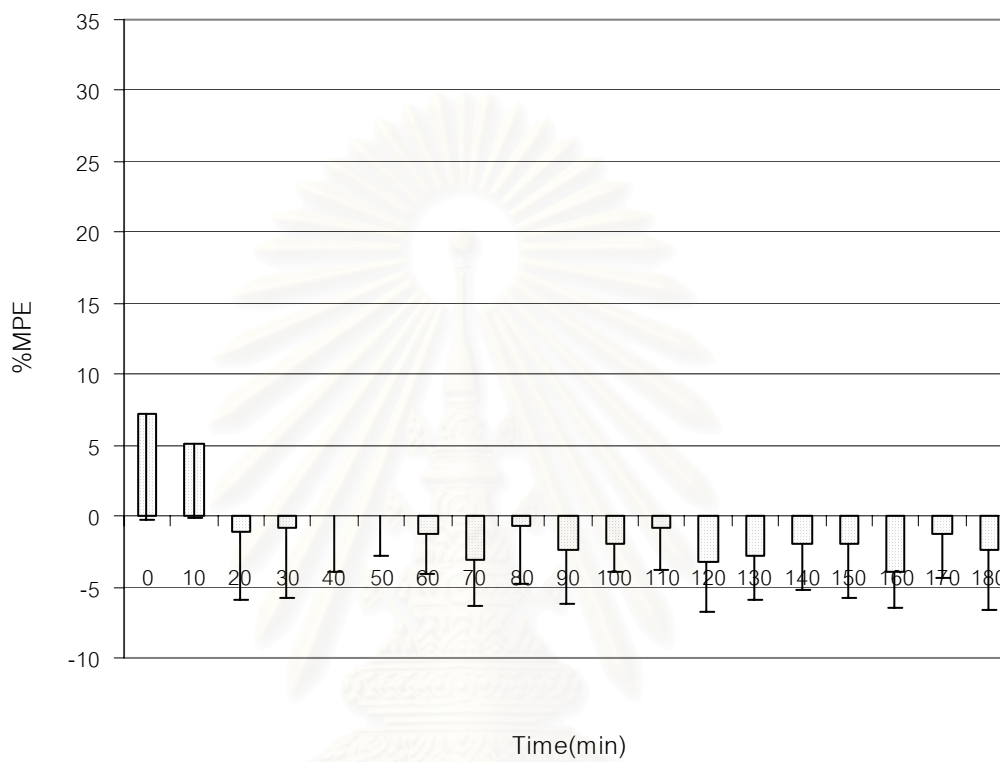


Figure 42 Profile of the analgesic responses provided by microemulsion base formula B. (n = 10)

สถาบันวิทยบริการ
จุฬาลงกรณ์มหาวิทยาลัย

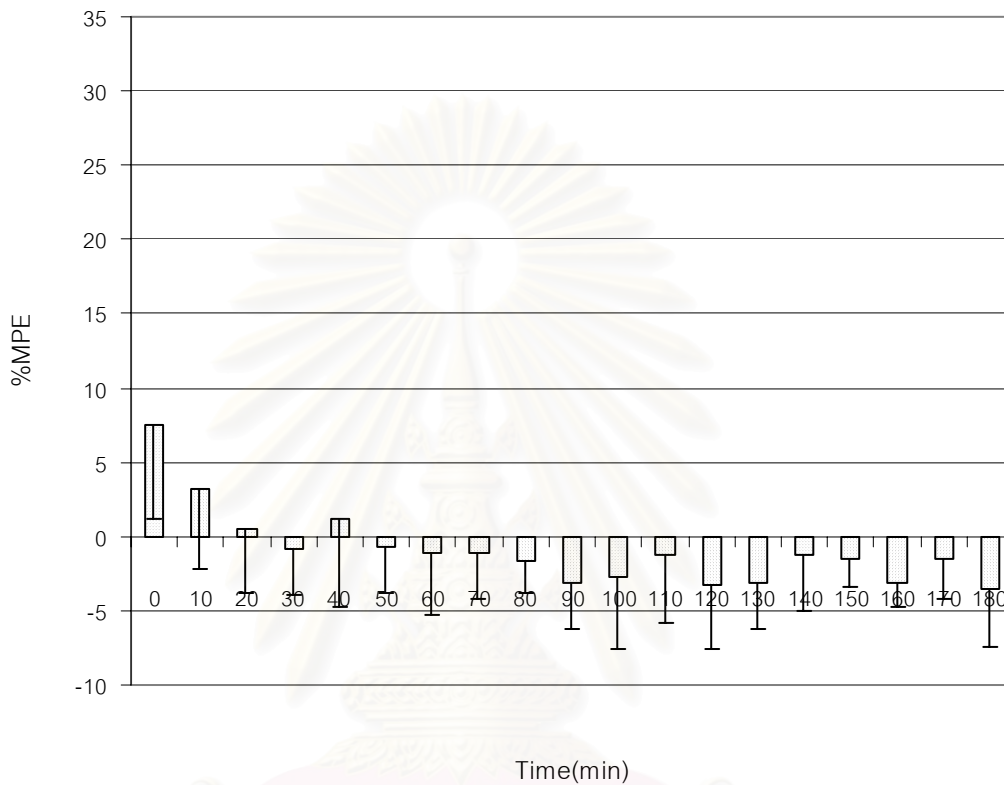


Figure 43 Profile of the analgesic responses provided by microemulsion base formula C. (n = 10)

สถาบันวิทยบริการ
จุฬาลงกรณ์มหาวิทยาลัย

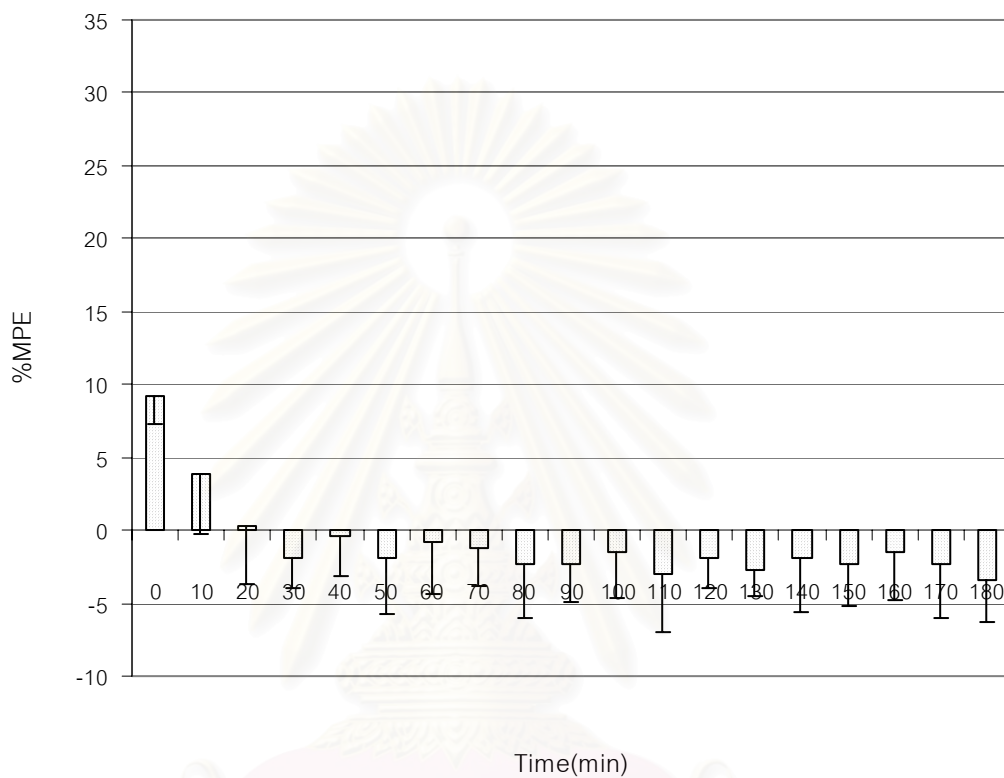


Figure 44 Profile of the analgesic responses provided by microemulsion base formula D. (n = 10)

สถาบันวิทยบริการ
จุฬาลงกรณ์มหาวิทยาลัย

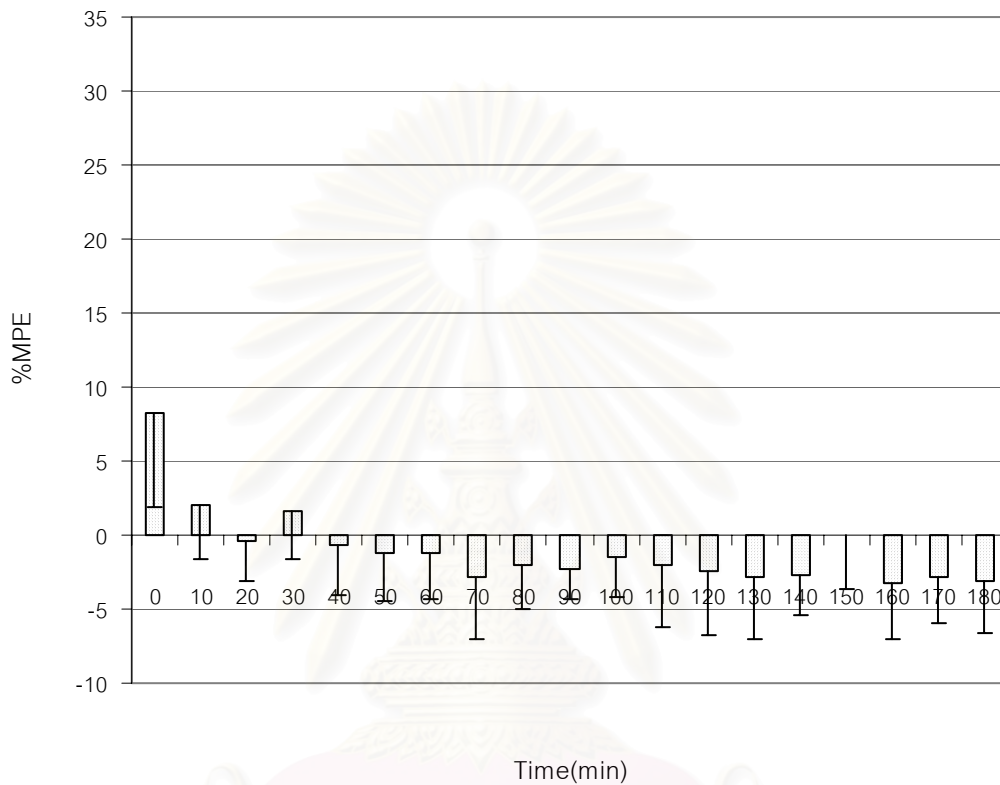


Figure 45 Profile of the analgesic responses provided by microemulsion base formula E. (n = 10)

สถาบันวิทยบริการ
จุฬาลงกรณ์มหาวิทยาลัย

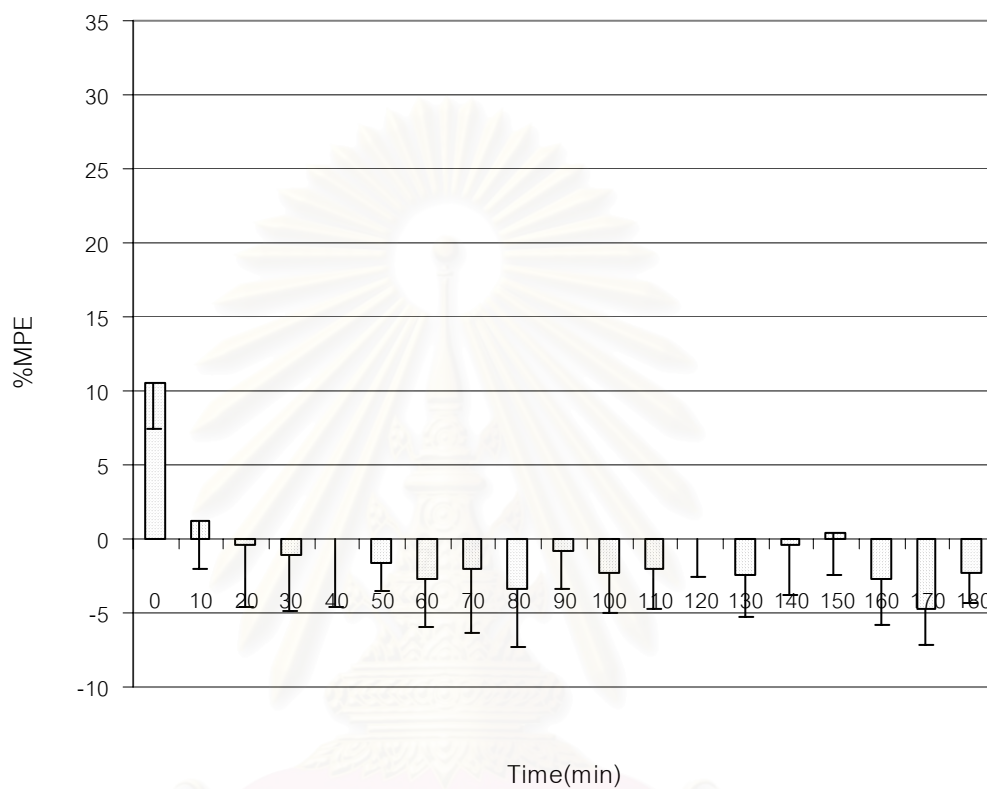


Figure 46 Profile of the analgesic responses provided by microemulsion base formula F. (n = 10)

สถาบันวิทยบริการ
จุฬาลงกรณ์มหาวิทยาลัย

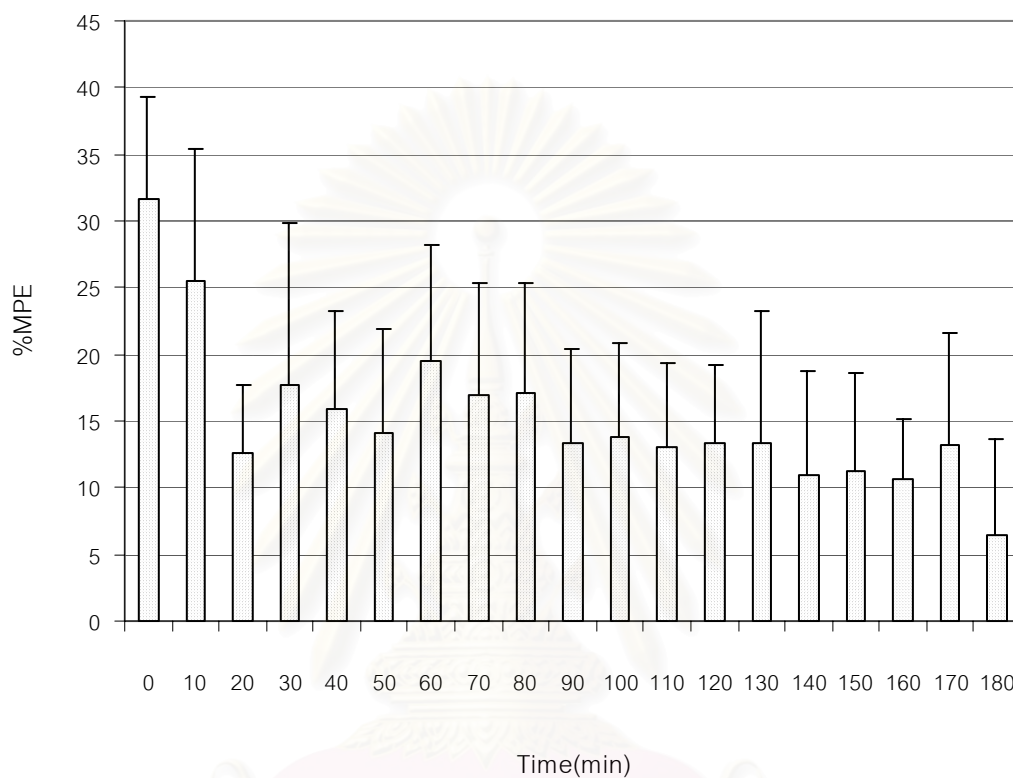


Figure 47 Profile of the analgesic responses provided by benzocaine microemulsion formula A. (n = 10)

สถาบันวิทยบริการ
จุฬาลงกรณ์มหาวิทยาลัย

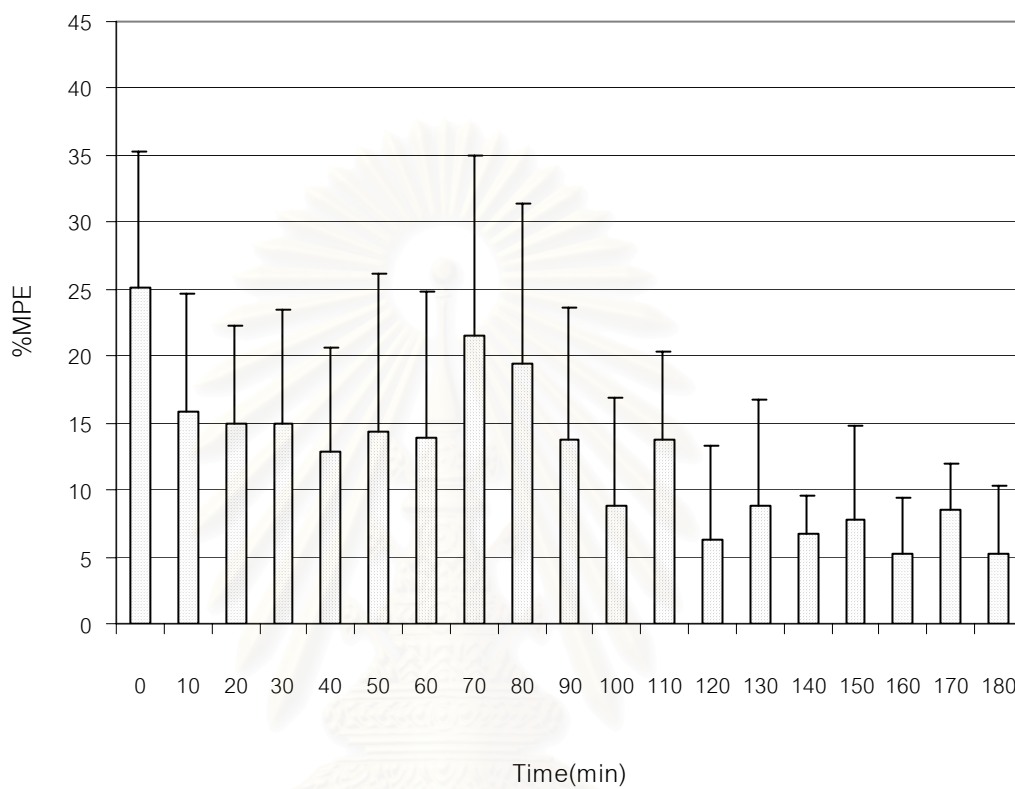


Figure 48 Profile of the analgesic responses provided by benzocaine microemulsion formula B. (n = 10)

สถาบันวิทยบริการ
จุฬาลงกรณ์มหาวิทยาลัย

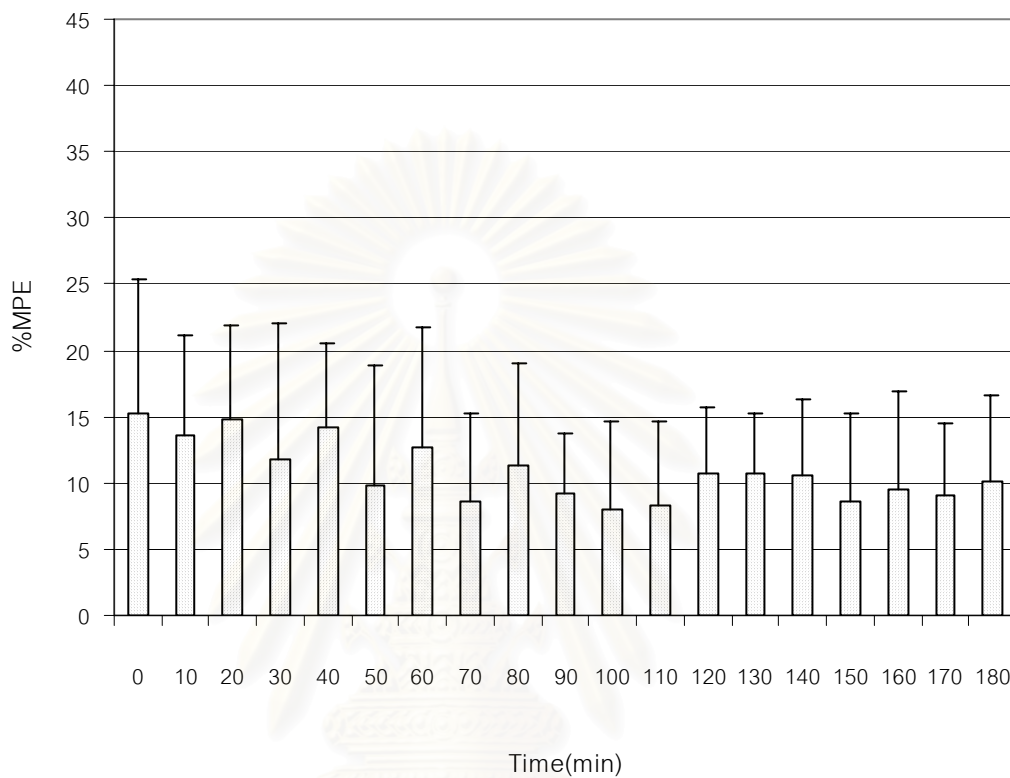


Figure 49 Profile of the analgesic responses provided by benzocaine microemulsion formula C. (n = 10)

สถาบันวิทยบริการ
จุฬาลงกรณ์มหาวิทยาลัย

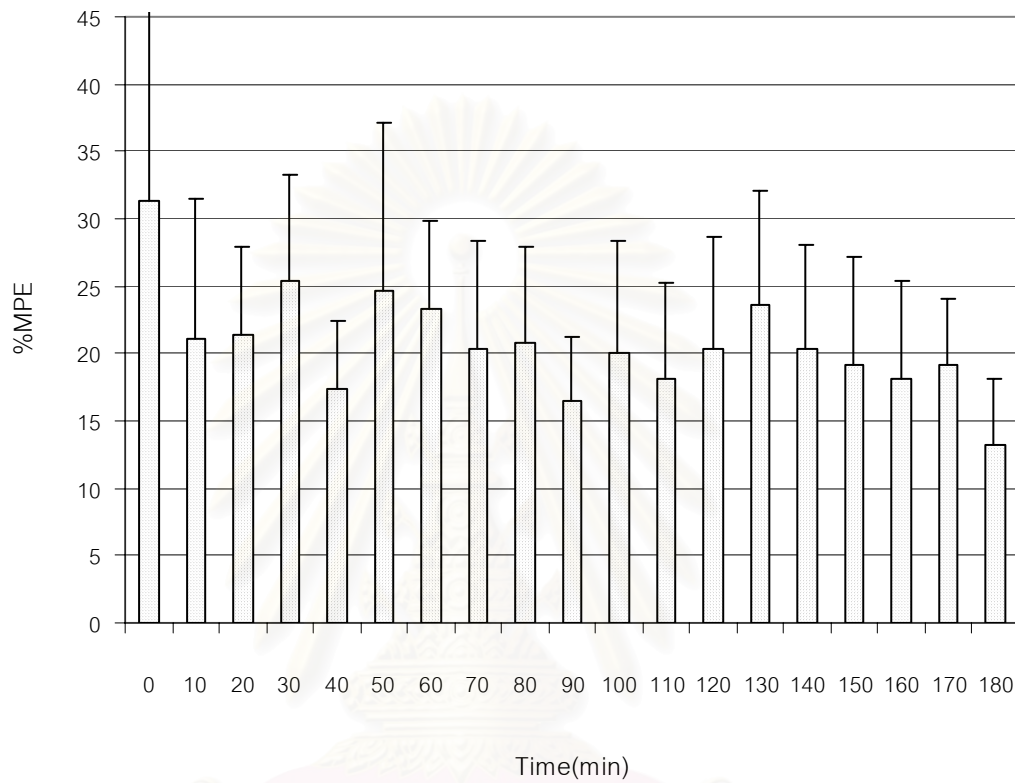


Figure 50 Profile of the analgesic responses provided by benzocaine microemulsion formula D. (n = 10)

สถาบันวิทยบริการ
จุฬาลงกรณ์มหาวิทยาลัย

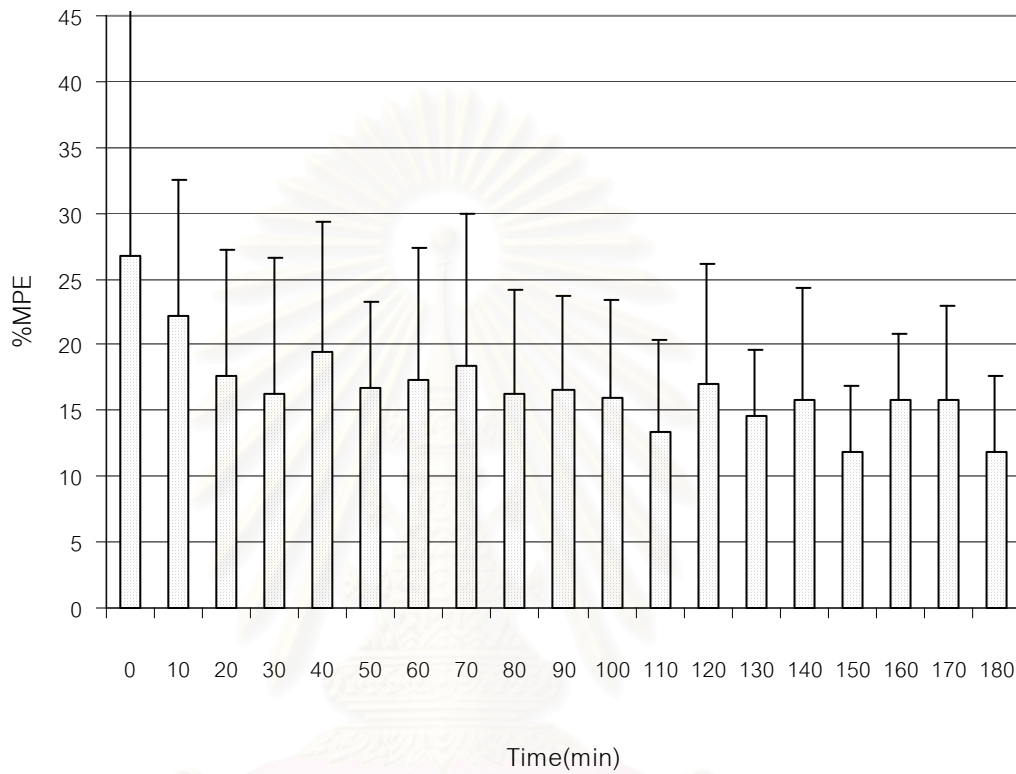


Figure 51 Profile of the analgesic responses provided by benzocaine microemulsion formula E. (n = 10)

สงวนลิขสิทธิ์
จุฬาลงกรณ์มหาวิทยาลัย

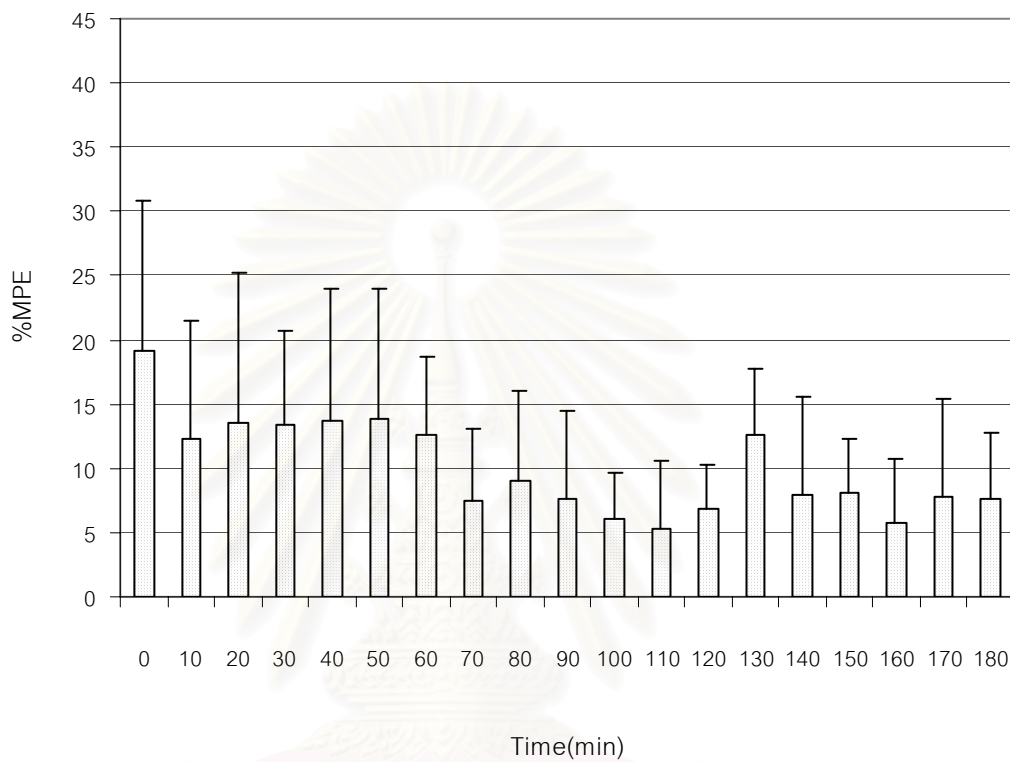
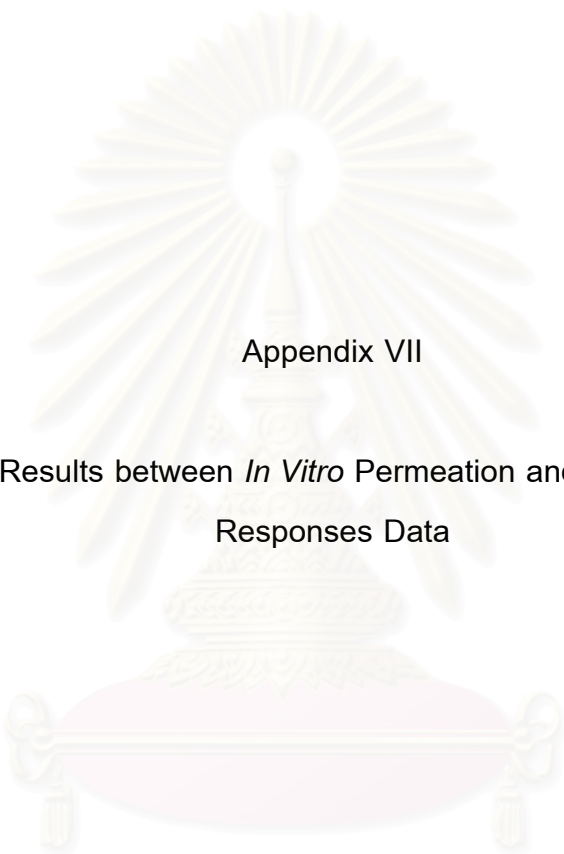


Figure 52 Profile of the analgesic responses provided by benzocaine microemulsion formula F. (n = 10)

สงวนลิขสิทธิ์
จุฬาลงกรณ์มหาวิทยาลัย



Appendix VII

Correlation Results between *In Vitro* Permeation and *In Vivo* Analgesic
Responses Data

สถาบันวิทยบริการ
จุฬาลงกรณ์มหาวิทยาลัย

Table 19 Correlation data of steady state flux of benzocaine permeate through shed snake skin from six microemulsions and area of analgesia measured by mouse tail flick assay

Formula	Steady State Flux (mcg/hr/cm ²)	Area of Analgesia (%MPE-min)
A	16.09	2709.59
B	13.28	2229.86
C	10.54	1942.63
D	34.40	3719.25
E	21.83	3003.24
F	8.64	1774.03

Correlation coefficient test

$$H_0 : \rho = 0, \quad H_a : \rho \neq 0$$

Where ρ is the true correlation coefficient, estimate by r

$$t_{n-2} = \frac{|r(N-2)^{1/2}|}{(1-r^2)^{1/2}}$$

when r = 0.9783

$$\therefore t_{6-2} = \frac{|0.9783(6-2)^{1/2}|}{(1-0.9783^2)^{1/2}}$$

$$= 9.443$$

A value of $t_{0.01}$, df4 equal to 4.604 is needed for significance correlation. Therefore, there is correlation between steady state flux of benzocaine through shed snake skin and area of analgesia measured by mouse tail flick test ($p < 0.01$).

Table 20 Correlation data of cumulative amount of benzocaine permeate through shed snake skin from six microemulsions and area of analgesia measured by mouse tail flick assay

Formula	Cumulative Amount (mcg)	Area of Analgesia (%MPE-min)
A	300.20	2709.59
B	235.44	2229.86
C	181.57	1942.63
D	537.55	3719.25
E	373.87	3003.24
F	158.77	1774.03

Correlation coefficient test

$$H_0 : \rho = 0, \quad H_a : \rho \neq 0$$

Where ρ is the true correlation coefficient, estimate by r

$$t_{n-2} = \frac{|r(N-2)^{1/2}|}{(1-r^2)^{1/2}}$$

when r = 0.9939

$$\therefore t_{6-2} = \frac{|0.9939(6-2)^{1/2}|}{(1-0.9939^2)^{1/2}}$$

$$= 18.024$$

A value of $t_{0.01}$, df4 equal to 4.604 is needed for significance correlation. Therefore, there is correlation between cumulative amount of benzocaine through shed snake skin and area of analgesia measured by mouse tail flick test ($p < 0.01$).

VITA

Lieutenant Junior Grade Orawadee Pongvutitham was born on 9th May 1975 in Bangkok, Thailand. She has graduated Bachelor of science in Pharmacy from Faculty of Pharmaceutical science, Chulalongkorn University, Bangkok, Thailand since 1996. She works at Pharmacy department of Queen Sirikit Hospital, Royal Thai Navy, Chonburi, Thailand.



สถาบันวิทยบริการ
จุฬาลงกรณ์มหาวิทยาลัย